Role of VHL in DNA double-strand break repair and genomic instability in renal cell carcinoma

by

Julie Lynn Metcalf

A thesis submitted in conformity with the requirements
for the degree of Doctor of Philosophy

Laboratory Medicine and Pathobiology
University of Toronto

Role of VHL in DNA double-strand break repair and genomic instability in renal cell carcinoma

Julie Lynn Metcalf

Doctor of Philosophy

Laboratory Medicine and Pathobiology
University of Toronto

2013

Abstract

DNA repair is essential for maintaining genomic stability and defects in this process significantly increase the risk of cancer. Clear-cell renal cell carcinoma (CCRCC) caused by inactivation of the von Hippel-Lindau (*VHL*) tumour suppressor gene is characterized by high genomic instability. However, the molecular mechanisms underlying the association between loss of VHL and genomic instability remain unclear. Here, we show that suppressor of cytokine signalling 1 (SOCS1) promotes nuclear redistribution and K63-ubiquitylation of VHL in response to DNA double-strand breaks (DSBs). Loss of VHL or VHL mutations that compromise its K63-ubiquitylation attenuates the DNA-damage response (DDR), resulting in decreased homologous recombination repair and persistence of DSBs. We further demonstrate that the 30kDa and 19kDa isoforms of VHL have opposing roles in the DDR. Upon induction of DSBs, VHL30 activates the DDR, while VHL19 attenuates this response and is actively degraded through the proteasome to alleviate its inhibitory effect. Finally, we show that VHL30 binds heterochromatin protein 1 alpha (HP1α) in the presence of DSBs and this interaction is required for the full activation of the DDR. VHL binding to HP1α transiently releases it from chromatin to induce chromatin relaxation, which is predicted to allow for the access of DNA

repair proteins. Remarkably, the DDR defect in VHL-null and VHL mutant cells deficient for HP1α binding could be rescued in the presence of a histone deacetylase inhibitor (HDACI), suggesting that VHL activates the DDR by inducing chromatin decondensation to promote the recruitment of DNA repair factors to the lesion. Collectively, these results identify VHL as a component of the DDR network, inactivation of which contributes to the genomic instability associated with CCRCC.

Acknowledgements

First and foremost, I would like to thank my supervisor, Prof Michael Ohh for challenging and molding me into the scientist I am today. Thank you for giving me the independence I needed to mature as a scientist and the resources, support, and guidance to succeed. I would also like to extend my sincere gratitude to the members of my advisory committee, Dr. Rod Bremner and Dr. Lori Frappier, who graciously offered their time and provided valuable advice and support throughout my graduate studies. In addition, I would like to acknowledge Dr. Stephen Meyn, Dr. Paul Bradshaw, and Martin Komosa for their critical contributions to the work presented in Chapter 2 and their expertise and advice. A big thank you to my extended family in the Ohh lab, both past and present. Your continued encouragement, support, advice (both scientific and life in general), and comic relief has been essential to my success and pulled me through the tough times. I am grateful to have worked with such a talented group of people and I will miss you all very much. In particular, I would like to thank Dr. Ryan Russell for taking the time to teach me the ways of the lab and for sharing his diverse knowledge and skills with me; Pardeep Heir for the critical reading and revising of this thesis, many fruitful scientific discussions, advice and support, and willingness to help in any way possible; Dr. Severa Bunda for taking the time to listen, encourage and support me during my studies; and technicians Nadine Burry, Stephanie Sybingco, and Betty Poon for keeping the lab in order so I could focus on experiments unhindered. Finally, I would like to extend a big thank you to all of my friends and family for your love, support, and encouragement throughout this journey. I could not have done it without you!

Table of Contents

List of Abbreviations

53BP1	53 binding protein-1
Ad-Cre	adenovirus Cre-recombinase
APLF	aprataxin and PNK-like factor
ARF	ADP ribosylation factor
ARNT	aryl hydrocarbon receptor nuclear translocator
ATLD	ataxia telangiectasia-like disorder
ATM	ataxia-telangiectasia mutated
ATR	ataxia-telangiectasia and Rad3 related
BLM	Bloom syndrome helicase
BRCA	breast and ovarian cancer susceptibility protein
BRCC36	BRCA1-BRCA2-containing complex subunit 36
CARD9	caspase recruitment domain-containing protein 9
CBP	creb-binding protein
CCRCC	clear-cell renal cell carcinoma
CD	chromodomain
Cdc25	cell division cycle 25
CDK1	cyclin-dependent kinase 1
c-FLIP	cellular FLICE-like inhibitory protein
c-IAP1/2	cellular inhibitor of apoptosis protein-1/2
CHD3/4	chromodomain helicase DNA binding protein 3/4
ChIP	chromatin immunoprecipitation
Chk1/2	checkpoint kinase 1/2
CK2	casein kinase 2
CSD	chromoshadow domain
CQ	chloroquine
Cul2	cullin 2
Cyto	cytoplasmic
DAPI	4′,6-diamidino-2-phenylindole
DDR	DNA-damage response

DNA-PK$_{cs}$	DNA-dependent protein kinase catalytic subunit
DMEM	Dulbecco's modified Eagle's medium
DR-GFP	direct repeat-green fluorescent protein
DSB	DNA double-strand break
dsDNA	double-stranded DNA
DUB	de-ubiquitinating enzyme
ECM	extracellular matrix
ECV	ElonginsBC/Cul2/VHL
EPO	erythropoietin
ERCC1	excision repair cross-complementing rodent repair deficiency, complementation group 1
GLUT1	glucose transporter 1
H3K9me3	trimethylation on lysine 9 of histone 3
HA	haemagluttinin
HDAC1/2	histone deacetylase 1/2
HDACI	histone deacetylase inhibitors
HIF	hypoxia-inducible factor
HP1	heterochromatin protein 1
HR	homologous recombination
HRE	hypoxia responsive element
IB	immunoblotted
IL-2	interleukin-2
IP	immunoprecipitated
IR	ionizing radiation
IRIF	ionizing radiation-induced foci
ISN	insoluble nuclear
JAK2	*Janus* kinase 2
KAP-1	KRAB-domain associated protein 1
LE	long exposure
LET	linear energy transfer
MDC1	mediator of the DNA damage checkpoint 1
MDM2	murine double minute 2

MMS21	methyl methanesulfonate-sensitivity protein 21
MNase	micrococcal nuclease
MOI	multiplicity of infection
MRN	Mre11-Rad50-Nbs1
mTOR	mammalian target of rapamycin
NEDD8	neural precursor cell expressed developmentally down-regulated protein 8
NES	nuclear export sequence
NFκB	nuclear factor kappa-light-chain-enhancer of activated B cells
NHEJ	non-homologous end joining
NLS	nuclear localization signal
Nucl	nuclear
OIS	oncogene-induced senescence
Opti-MEM	opti-minimum essential media
OTUB1	otubain-1
PAGE	polyacrylamide gel electrophoresis
PARP	poly(ADP-ribose) polymerase
PBS	phosphate-buffered saline
PDGFRβ	platelet-derived growth factor receptor β
PEI	polyethyleneimine
PHD	prolyl hydroxylase domain
PIAS	protein inhibitors of activated STAT
PIKK	phosphatidylinositol 3-kinase-like kinase
PNK	polynucleotide kinase
POH1	pad one homolog-1
PRMT3	protein arginine N-methyltransferase 3
PTM	post-translational modification
PVDF	polyvinylidene difluoride
REGM	renal epithelial growth medium
RNF	RING finger protein
ROS	reactive oxygen species
RPA	replication protein A
RPTEC	renal proximal tubule epithelial cells

SAHF	senescence-associated heterochromatin foci
SCF	Skp1/Cdc25/F-Box
SDS	sodium dodecyl sulphate
SE	short exposure
SENP	SUMO1/sentrin specific peptidase
SETDB1	SET domain bifurcated 1
SN	soluble nuclear
SOCS1	suppressor of cytokine signalling 1
SSB	single-strand break
ssDNA	single-stranded DNA
STAT5	signal transducer and activator of transcription 5
SUMO	small ubiquitin-like modifier
Suv39H1	suppressor of variegation 3-9 homolog 1
Suv39H2	suppressor of variegation 3-9 homolog 2
TBE	tris-borate-EDTA
TBST	tris-buffered saline-Tween 20
TNFα	tumour necrosis factor-alpha
TRITC	tetramethyl rhodamine isothiocyanate
UBL	poly-ubiquitin-like
UCP	ubiquitin carrier protein
USP	ubiquitin-specific protease
UTR	untranslated region
VEGF	vascular endothelial growth factor
VEGFR	vascular endothelial growth factor receptor
VHL	von Hippel-Lindau
VPA	valproic acid
WCE	whole cell extract
WT	wild-type

List of Figures

Chapter 1

List of Appendices

Chapter 1

1 Introduction

1.1 DNA-Damage Response

1.1.1 Sources of DNA double-strand breaks

The genomic integrity of cells is under constant attack by highly toxic DNA lesions. Of the many types of DNA damage that exist, DNA double-strand breaks (DSBs) are the most dangerous because no intact DNA strand remains to be used as a template for repair. These DNA lesions may arise from both exogenous and endogenous sources[1].

Ionizing radiation (IR) is a well-known exogenous source of DSBs that is frequently used in diagnostic X-ray imaging and cancer radiotherapy, but is also produced from the natural decay of environmental radioactive compounds such as uranium[1]. Chemotherapeutic drugs such as etoposide and doxorubicin are also potent inducers of DSBs which act by inhibiting topoisomerase II to prevent the re-ligation of DNA breaks induced by topoisomerase II activity[2].

In addition to exogenous sources, many normal cellular processes give rise to endogenous DSBs. One of the major endogenous sources of DSBs is reactive oxygen species (ROS) generated from oxidative respiration, cell injury, or inflammation[3, 4]. DSBs can also occur during replication when replication forks encounter a single-strand break (SSB), causing replication fork collapse. Although DSBs are generally considered undesirable, they are also introduced as intermediates during normal developmentally regulated processes such as V(D)J recombination, immunoglobulin class switching, and meiotic recombination in germ cells, which generates essential genetic and phenotypic variability[5]. Finally, naturally-occurring DNA ends may become exposed when telomeres become critically short during replicative senescence, which are then recognized by the cell as DSBs[6].

1.1.2 Detection and signalling of DNA double-strand breaks

To minimize the deleterious effects of DSBs, multicellular organisms utilize a complex signalling network known as the DNA damage response (DDR) to detect the presence of DNA damage and activate appropriate cellular defences. The DDR is transduced by three members of

the phosphatidylinositol 3-kinase-like kinase (PIKK) protein family: ataxia-telangiectasia mutated (ATM), ataxia-telangiectasia and Rad3 related (ATR), and DNA-dependent protein kinase catalytic subunit (DNA-PK_{cs})[7]. ATM and DNA-PK_{cs} are primarily activated in response to DSBs, while ATR is activated response to single-stranded DNA (ssDNA) ends generated by DNA adducts, replication fork collapse, or during the processing of DSBs (discussed in section 1.1.3)[8-10]. These serine-threonine kinases phosphorylate substrates which contain the consensus motif (SQ/TQ) to initiate a complex downstream signalling cascade[10-13].

In response to DSBs, ATM rapidly dissociates from its inactive dimer, is autophosphorylated, and recruited to the DNA lesion by the Mre11-Rad50-Nbs1 (MRN) sensor complex[14, 15]. Alternatively, during nonhomologous end joining (NHEJ; discussed in section 1.1.3), the Ku70/Ku80 heterodimer binds DNA ends and recruits DNA-PK to form an active holoenzyme[16]. Activated ATM and DNA-PK_{cs} then phosphorylate the H2A histone variant, H2AX, on Ser139 in its C-terminal tail (referred to a γH2AX when phosphorylated), which promotes the recruitment of DNA repair proteins to the lesion[17] (**Fig 1.1)**. The DDR is further amplified by mediator of the DNA damage checkpoint 1 (MDC1), which binds to γH2AX and through interactions with ATM and the MRN complex, promotes the retention and spreading of DDR proteins along the damaged chromatin[18, 19]. The ability of MDC1 to amplify the DDR is accomplished through several mechanisms. First, MDC1 appears to shield the C-terminus of γH2AX from dephosphorylation to allow for the completion of DNA repair[18]. Secondly, its interaction with ATM leads to the phosphorylation of adjacent H2AX and additional MDC1 and ATM recruitment to form a positive feedback loop. Finally, MDC1 itself is phosphorylated by ATM, triggering binding to the E3 ligase RING finger protein (RNF)8, which together with RNF168, mediates K63-linked ubiquitylation (discussed in section 1.2.1) of histones H2A and H2AX to promote the recruitment of DNA repair factors such as 53 binding protein-1 (53BP1) and BRCA1[20-22]. The accumulation of γH2AX and other DDR proteins extends for megabases around the DSB, forming ionizing-radiation induced foci (IRIF) that can be visualized by immunofluorescence microscopy.

The activation of ATM also triggers the phosphorylation of the effector kinases checkpoint kinase 1 and 2 (Chk1 and Chk2), which initiates a downstream signalling network that results in the phosphorylation of hundreds of DDR proteins[23]. Some substrates, such as γH2AX and p53,

are likely direct targets of ATM, while others such as cell division cycle 25 (Cdc25), breast and ovarian cancer susceptibility protein (BRCA)1, and replication protein A (RPA), may be phosphorylated by Chk1 and Chk2[24] (**Fig 1.1)**. It was previously thought that ATM signalled through Chk2 in response to DSBs, and its related protein kinase, ataxia-telangiectasia and Rad3 related (ATR) acted in a separate parallel pathway to target Chk1 in response to single-strand breaks (SSBs) and replication fork stalls[25, 26]. However, recent studies have demonstrated that ATR can be activated in an ATM-dependent manner when DNA ends are resected into single-stranded DNA (ssDNA) during homologous recombination (HR) repair (discussed in section 1.1.3), suggesting that ATM and ATR signalling pathways may have a cooperative role in DSB repair[27].

Through these and other molecular events, the DDR promotes survival and genome stability by activating cell cycle checkpoints, initiating DNA repair, and triggering stress responses. Alternatively, if the damage is too extensive or the DNA break irreparable, the DDR can induce apoptosis or senescence[28, 29] (**Fig. 1.1)**. These ATM-dependent cellular responses will be discussed in more detail in the following sections.

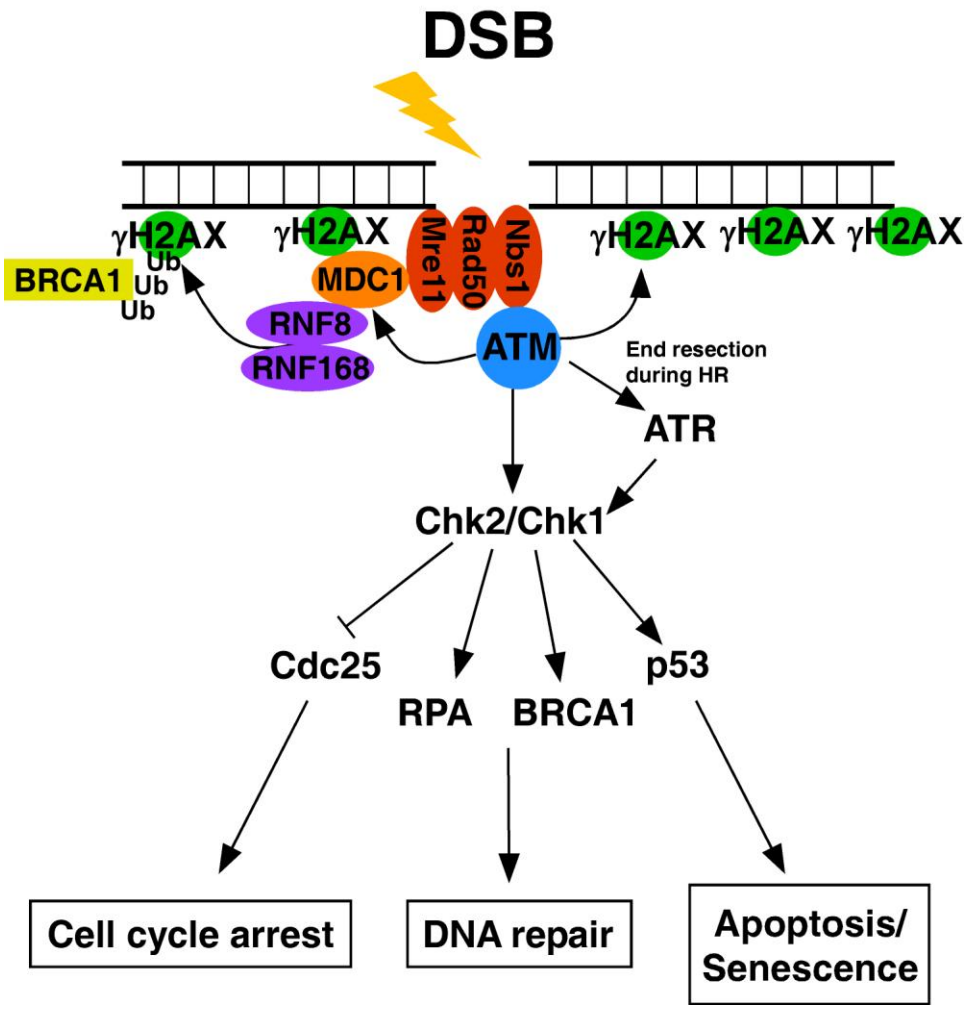

Figure 1.1. DNA-damage response. In response to a DNA double-strand break (DSB), ATM is autophosphorylated and recruited to the DNA lesion by the Mre11-Rad50-Nbs1 (MRN) complex. Activated ATM then phosphorylates the histone variant H2AX (known as γH2AX when phosphorylated). Mediator of the DNA damage checkpoint 1 (MDC1) binds to γH2AX and phosphorylation of MDC1 by ATM recruits RING finger protein (RNF)8 and RNF168 to K63-ubiquitylate γH2AX for the recruitment of additional DDR proteins such as breast and ovarian cancer susceptibility protein 1 (BRCA1). ATM activates Chk2 and end resection during HR activates Chk1 through ATR to initiate an extensive phosphorylation cascade, promoting the phosphorylation of hundreds of proteins, including Cdc25, replication protein A (RPA), BRCA1, and p53, which serves to arrest the cell cycle, initiate DNA repair, or activate apoptosis/senescence if the DNA damage is too extensive (see text for more detail, section 1.1.2).

1.1.3 DSB Repair

Non-homologous end joining (NHEJ) and homologous recombination (HR) are the two major DSB repair pathways in eukaryotic cells (**Fig. 1.2**). NHEJ directly ligates the DNA ends and is inherently error-prone, frequently resulting in small deletions and translocations due to non-compatible end joining. In contrast, HR uses homologous DNA on a sister chromatid as a template for accurate repair and is therefore restricted to the S/G_2 phases of the cell cycle. These mechanistically distinct pathways play both competitive and compensatory roles in DNA repair in an attempt to maintain genomic stability[30-35].

In NHEJ, the Ku70/Ku80 heterodimer binds DNA ends and recruits DNA-PK_{cs} to form the active holoenzyme[36]. Non-ligatable ends are minimally processed by factors such as Artemis, polynucleotide kinase (PNK), Aprataxin, and Aprataxin and PNK-like factor (APLF) to produce compatible DNA ends[16]. Finally, adjacent DNA ends are ligated by the XLF-XRCC4-Ligase IV complex[16] (**Fig. 1.2**).

During HR, the MRN complex binds to DNA ends and activates 5′ to 3′ exonuclease activity to resect the double-stranded DNA (dsDNA). The exonucleases Mre11, CtIP, and Exo1, as well as the Bloom syndrome helicase (BML), are thought to play a role in this critical end resection step[37-39]. As a result, long 3′ single-stranded DNA (ssDNA) overhangs are generated and coated with replication protein A (RPA). Notably, the generation of ssDNA during resection activates ATR and its effector kinase Chk1 to phosphorylate a number of HR proteins including BRCA1, BML, and XRCC3[40-44]. Thus, both ATM and ATR signalling pathways contribute to the repair of DSBs by HR. RPA is exchanged for Rad51 and other associated HR proteins (eg. BRCA1, BRCA2, Rad52, Rad54) to form a nucleoprotein filament, which mediates a homology search in the sister chromatid and initiates strand invasion. A complementary strand of DNA is synthesized by DNA polymerases using the homologous strand as a template. Finally, the DNA ends are ligated by DNA ligase I, followed by cleavage and resolution of the HR intermediates to yield intact DNA strands[45] (**Fig. 1.2**).

HR requires extensive 5′ to 3′ DNA end resection to allow for strand invasion and recent reports suggest that this critical step may play a significant role in regulating the choice between HR and NHEJ. Two key DDR proteins, 53BP1 and BRCA1 have been shown to be recruited to DSBs in

a mutually exclusive manner to regulate DNA end resection[46]. 53BP1 cooperates with Rif1 to inhibit 5′ end resection and restrict the recruitment of BRCA1 to DBSs to promote NHEJ[47]. During the S/G_2 phase of the cell cycle, cyclin-dependent kinase 1 (CDK1) phosphorylates CtIP to promote its interaction with BRCA1 and recruitment to DSBs[48, 49]. The BRCA1-CtIP complex at DSBs blocks the recruitment of Rif1 and promotes HR[47]. Thus, the critical end resection step which determines whether cells utilize the NHEJ or HR repair pathway is tightly regulated by cell cycle.

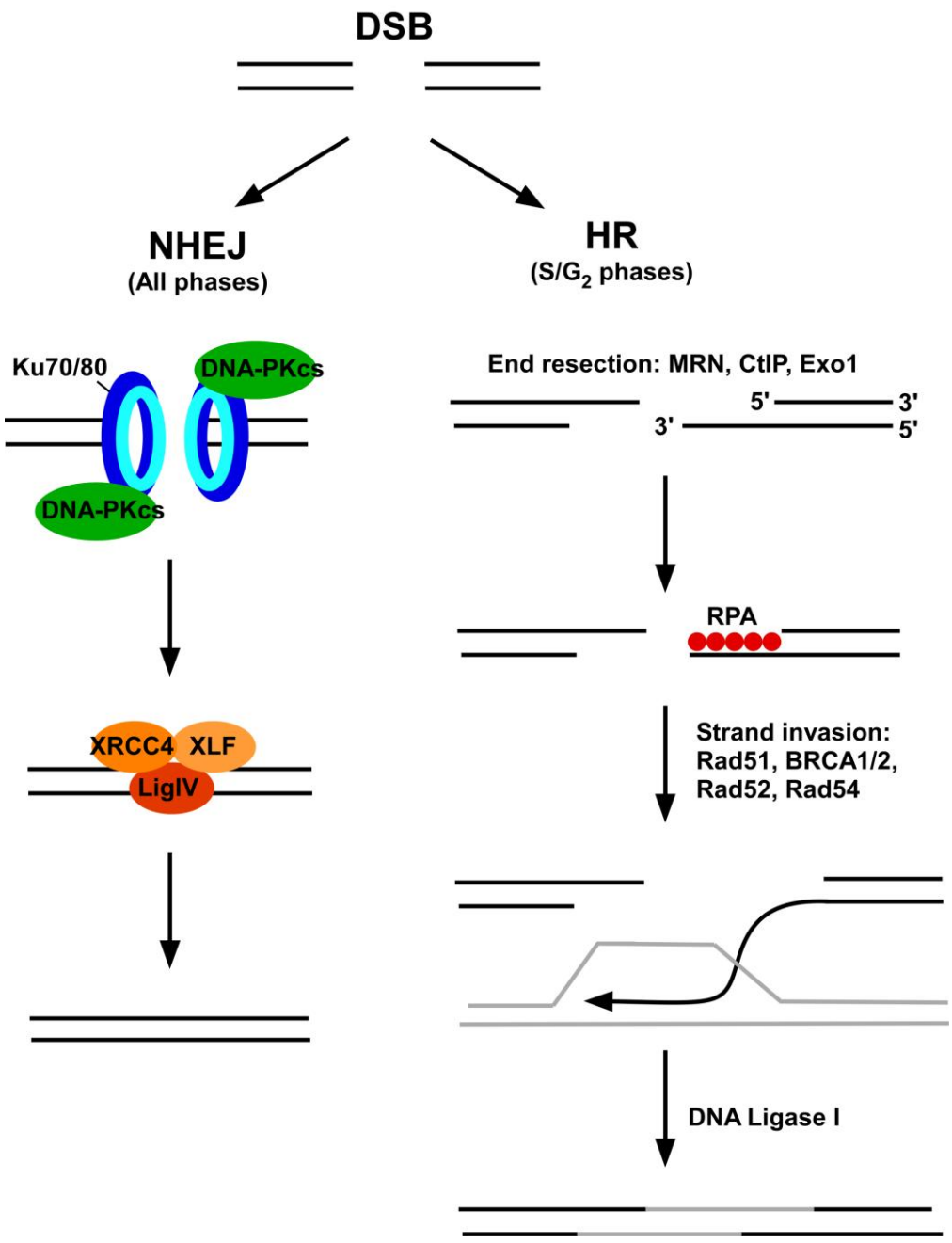

Figure 1.2. DSB repair pathways in mammalian cells. In mammalian cells DNA double-strand breaks (DSBs) are repaired by non-homologous end joining (NHEJ) or homologous recombination (HR). During NHEJ, the DNA ends are bound by Ku70/80 complex which recruits DNA-PK_{cs} to form an active holoenzyme. The DNA ends are minimally processed and directly ligated by LigIV/XRCC4/XLF complex. HR, which occurs during S/G_2 phases of the cell cycle, uses a template for accurate repair. DNA ends are resected 5′ to 3′ by MRN, CtIP, and ExoI to generate long ssDNA which is coated by replication protein A (RPA). RPA is then exchanged for Rad51 and other HR proteins, undergoes a homology search, and invades the sister chromatid. DNA polymerase extends the DNA using the homologous strand as a template and intermediates are then resolved to generate intact DNA.

1.1.4 Cell cycle checkpoints

One of the critical functions of the DDR is to arrest the cell cycle, allowing the cell time to repair the lesion and prevent the replication of mutations. Activated ATM mediates cell cycle arrest at G_1/S and intra-S checkpoints to inhibit DNA replication, as well as the G_2/M checkpoint to prevent the segregation of damaged chromosomes.

ATM regulates the G_1/S checkpoint primarily through the activation and stabilization of p53. p53 is phosphorylated on Ser15 directly by ATM and Ser20 by Chk1 and Chk2[50-53]. Although phosphorylation of Ser15 does not seem to contribute to the stabilization of p53, it has been reported to increase its transcriptional activity through increased binding to the co-activator Creb-binding protein (CBP)/p300[54, 55]. Several reports suggest that stabilization of p53 is likely mediated through the downstream effector kinases, Chk1 and Chk2. Chk1 and Chk2 phosphorylate p53 on Ser20, disrupting the interaction with its negative regulator, murine double minute 2 (MDM2), to promote its stabilization and transcriptional activity[53, 54, 56, 57]. In addition, phosphorylation of MDM2 by ATM may also promote p53 stabilization[58]. Transcriptionally activated p53 then induces expression of p21/WAF1, which inhibits Cdk2/CyclinE activity, resulting in G_1 arrest[28] (**Fig. 1.3**).

The intra-S phase checkpoint is mediated by two parallel ATM-dependent pathways: Nbs1-Mre11-MDC1 and Chk2-Cdc25A-Cdc2[59]. Nbs1 is phosphorylated by ATM, which activates the Mre11-Nbs1-Rad50 complex and interactions between Nbs1 and MDC1 promote the retention of the MRN complex at DSBs[60]. Loss of Nbs1, Mre11, or disruption of the Nbs1-MDC1 interaction has been shown to impair intra-S phase checkpoint activation in cells; however the molecular mechanisms underlying this pathway remain unknown[60-63]. In the parallel Chk2-Cdc25-Cdc2 pathway, ATM activates Chk2, which phosphorylates Cdc25A and targets it for degradation[64]. Degradation of Cdc25A prevents it from activating Cdc2, which is required to initiate Cdc45 loading onto pre-initiation complexes at the origins of DNA replication[65-67]. A failure to recruit Cdc45 therefore results in a replication block (**Fig. 1.3**).

Progression through the G_2/M checkpoint is mediated by the Cdc2-Cyclin B complex. Under normal conditions, the phosphatase Cdc25C removes the inhibitory Tyr-15 phosphorylation on Cdc2 to activate the Cdc2-Cyclin B complex and facilitate mitotic entry. In response to DSBs,

ATM activates Chk1 and Chk2, which phosphorylate Ser216 on Cdc25C[68]. Phosphorylation of Cdc25C promotes its binding to 14-3-3, sequestering it in the cytoplasm to prevent dephosphorylation of Cdc2 and entry into mitosis[69]. p53 may also play a role in the maintenance of the G_2/M checkpoint through transcriptional repression of Cdc2 and Cyclin B[70] (**Fig. 1.3**).

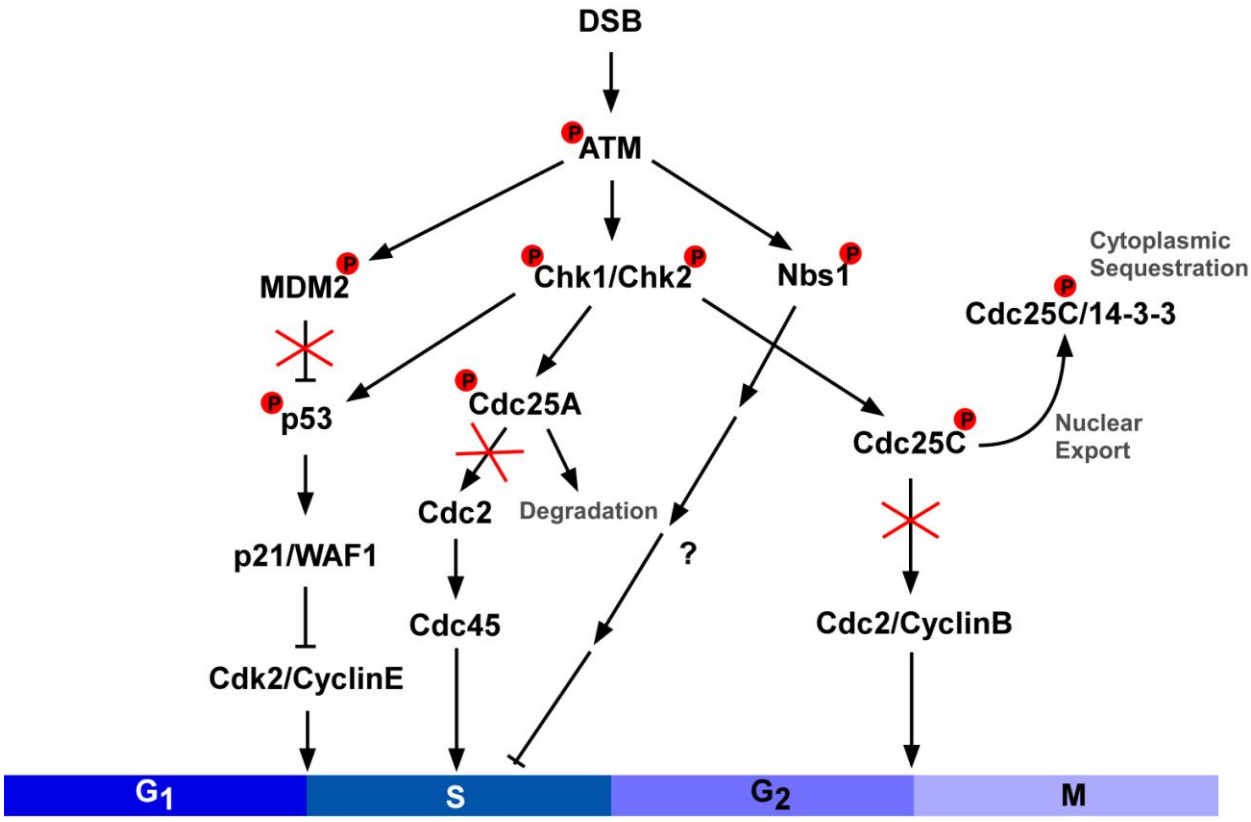

Figure 1.3. Cell cycle checkpoint response to DSBs. In response to DSBs, cell cycle is arrested at G_1/S, intra-S, and G_2/M phases in an ATM-dependent manner. The G_1/S phase is controlled primarily by p53. Phosphorylation of p53 by Chk1/2 activates the transcription of p21/WAF1 to inhibit Cdk2/CyclinE. Activation of Chk2 also phosphorylates Cdc25A promoting its degradation to block Cdc2/Cdc45-mediated progression through intra-S phase. Intra-S phase is blocked by a second unknown mechanism mediated through ATM phosphorylation of Nbs1. Finally, Chk1/Chk2-mediated phosphorylation of Cdc25C promotes binding to 14-3-3 and sequesters it in the cytoplasm to inhibit Cdc2/Cyclin B-dependent progression through the G_2/M checkpoint.

1.1.5 Apoptosis and Cellular Senescence: Secondary defence mechanisms

Inappropriate progression of damaged cells through the cell cycle generally leads to mitotic catastrophe, apoptosis and cell death, which acts as a secondary defence mechanism to prevent the persistence or replication of DNA damage that would compromise the genomic integrity of the cell. Apoptosis is primarily regulated by p53 and DDR-induced stabilization and activation of p53 induces the expression of several pro-apoptotic factors including, Bax, Puma, and Noxa[71-73]. Activation of p53-mediated apoptotic signalling promotes mitochondrial permeability, release of cytochrome c, and activation of downstream caspases to induce cell death[74, 75]. However, since p53 also regulates cell cycle checkpoints, it remains unclear how cells differentially control these two distinct pathways.

Cell cycle checkpoints are generally temporary pauses in the cell cycle which can be overcome if the cell is properly repaired. However, the persistence of DSB may result in permanent cell cycle arrest known as senescence[76]. Cellular senescence has been speculated to act as a "back-up" pathway when apoptosis is inhibited. In support of this hypothesis, Rebbaa *et al*. have shown that inhibition of caspase-3 and apoptosis can promote cellular senescence[77]. Therefore, senescence may act as a final barrier to transformation. Both replicative and oncogene-induced senescence (OIS) are similarly activated by the DDR[78]. In replicative senescence, telomeres become critically short and uncapping of the chromosome end reveals a free DNA end that is recognized by the DDR as a DSB[6, 79]. During OIS, replicative stress caused by uncontrolled proliferation leads to the generation of single- and double-stranded breaks[80]. While the mechanisms that regulate DSB-induced senescence have remained elusive, ATM/ATR-dependent activation of Chk1/2 and p53, as well as p21, p16, and retinoblastoma protein (Rb), have been shown to be involved this response[81-86].

Recently, epigenetic silencing of growth-promoting E2F genes has been proposed as a mechanism to induce permanent cell cycle arrest. Narita *et al.* have demonstrated that Rb and heterochromatin proteins are recruited to E2F promoters in senescent cells and are associated with the stable repression of E2F target genes[87]. In addition, senescent cells have been observed to contain H3K9 trimethylation foci, known as senescence-associated heterochromatin foci (SAHF)[87]. Methylation of gene promoters is strongly associated with H3K9me3 and

methylation-induced silencing of genes may represent a general mechanism by which cells stabilize the senescent phenotype[88, 89].

1.2 Post-translational modifications and the DDR

Undoubtedly, phosphorylation is a major regulator of the DDR. However, a number of other post-translational modifications (PTMs) including acetylation, methylation, ubiquitylation, and small ubiquitin-like modifier (SUMO)ylation play critical roles in DNA damage signalling. Acetylation and methylation are key regulators of chromatin organization and will be discussed in the following section 1.3.

1.2.1 Ubiquitylation

Ubiquitin is a small 76-amino acid protein that is highly conserved in eukaryotic cells, with only three amino acid changes between yeast and humans[90, 91]. Ubiquitin regulates a number of protein functions via covalent attachment to its substrates through a process known as ubiquitylation. Ubiquitylation is a multi-step enzymatic reaction that involves the sequential activation of an E1 ubiquitin activating enzyme, an E2 ubiquitin-conjugating enzyme and an E3 ubiquitin ligase[90, 91]. Ubiquitin first forms a thioester bond between its carboxy-terminus and the cysteine residue of the E1 in an ATP-dependent reaction[90, 91]. Subsequently, ubiquitin is transferred from the E1 to the active site cysteine of the E2-conjugating enzyme through a thioester bond[90, 91]. In the final step, the E3 ubiquitin ligase catalyzes the transfer of ubiquitin from the E2 enzyme to the target protein, generating a stable isopeptide bond between a lysine on the target protein and the C-terminal glycine of ubiquitin[90, 91]. Mammalian cells have 2 E1 enzymes, over 35 E2s and over 600 E3s[92]. Thus, the number of possible protein interactions increases dramatically with each step, increasing the specificity of the reaction. Ultimately, the substrate specificity is conferred by the E3 ubiquitin ligase, necessitating a large diversity of these enzymes[91].

Polyubiquitylation of proteins involves sequential reactions to covalently attach additional ubiquitin proteins onto the lysine residue of a previously conjugated ubiquitin. The ubiquitin protein contains seven lysine residues that can act as acceptor sites for polyubiquitin chains: K6, K11, K27, K29, K33, K48, and K63. The lysine residue used for the attachment of ubiquitin chains determines the functional outcome. For example, ubiquitin K48-linked chains typically

target proteins for proteasomal degradation, while K63-linked chains often act as regulatory signals for cellular pathways such as endocytosis, vesicular trafficking, NFκB-mediated transcription, and DNA repair[93].

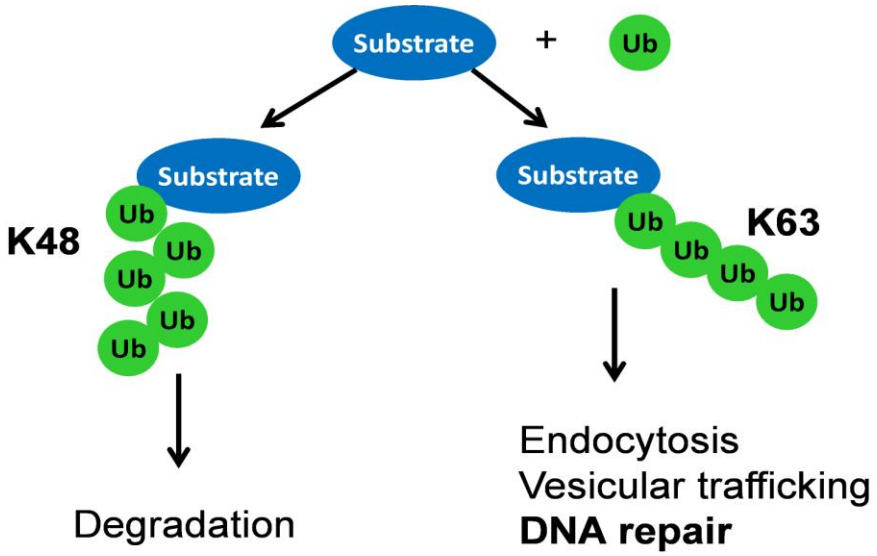

Figure 1.4. Cellular outcomes of polyubiquitylation. The ubiquitin protein contains 7 lysine residues that can act as acceptor sites for polyubiquitylation. K48-linked ubiquitylation generally targets proteins for degradation through the proteasome. K63-linked ubiquitylation acts as a regulatory signal for cellular pathways such as endocytosis, vesicular trafficking, and DNA repair.

K63-ubiquitylation plays a critical role in the recruitment of DNA repair proteins to the DNA lesion. As previously discussed, ATM-dependent phosphorylation of H2AX and MDC1 promotes the recruitment of the E3 ubiquitin ligase RNF8, which cooperates with another E3 ligase, RNF168 and the E2 conjugating enzyme, Ubc13, to mediate K63-ubiquitylation of substrates in the vicinity of the break[20, 22]. This coordinated ubiquitylation cascade is required for the recruitment of BRCA1 and 53BP1[22]. BRCA1 itself is also an E3 ligase, which cooperates with its constitutive binding partner, BARD1, for optimal enzymatic activity[94-96]. Following DNA damage, CtIP is ubiquitylated by BRCA1, which promotes its chromatin association[97]. Chromatin-bound CtIP has been proposed to stimulate resection of DSBs to regulate HR and the G_2/M checkpoint[97].

Ubiquitylation is a reversible process that is catalyzed by de-ubiquitinating enzymes (DUBs). As such, DUBs play an essential role in the regulation of the DDR. The DUBs ubiquitin-specific protease (USP)3, USP13, BRCA1-BRCA2-containing complex subunit 36 (BRCC36), pad one homolog-1 (POH1), and otubain-1 (OTUB1) have all been associated with the negative regulation of the RNF8-mediated K63-ubiquitylation pathway[20, 98-101]. In addition, USP7 has been shown to regulate the stability of multiple DDR proteins, including p53 and excision repair cross-complementing rodent repair deficiency, complementation group 1 (ERCC1)[102].

1.2.2 SUMOylation

SUMO is structurally related to ubiquitin and requires a similar reaction cascade involving E1, E2, and E3 enzymes. In contrast to ubiquitylation, there is only one heterodimeric SUMO E1, one E2 (Ubc9), and ten E3s[92]. There are three SUMO isoforms: SUMO1, SUMO2, and SUMO3, however SUMO2/3 are highly similar and appear to be functionally redundant[92, 103]. In addition, only SUMO2/3 can form poly-SUMO chains because SUMO1 contains no lysine residues to act as acceptor sites[92].

SUMOylation has only recently been linked to the DSB response. SUMO1, SUMO2/3, Ubc9, and the E3 SUMO ligases, protein inhibitors of activated STAT (PIAS) and methyl methanesulfonate-sensitivity protein 21 (MMS21), have all been shown to associate with sites of DBSs or replication stalling[104, 105]. PIAS1 or PIAS4 were shown to be required for ubiquitylation mediated by RNF8, RNF168, and BRCA1 to promote DSB repair[104]. These results suggest that the DDR is orchestrated by coordinated SUMOylation and ubiquitylation pathways.

Analogous to DUBs, protein SUMOylation is reversed by a unique family of peptidases (SUMO1/sentrin specific peptidase (SENP)1-3 and SENP5-7). SENP6 has been shown to regulate HR through its interaction with RPA70. SENP6 interacts with RPA70 during S-phase to keep it in a hypo-SUMOylated state[106]. In response to replicative stress, SENP6 dissociates from RPA70 and SUMO2/3 promotes its SUMOylation[106]. SUMO2/3-modified RPA70 then promotes HR by recruiting Rad51 to DNA lesions[106].

1.3 Chromatin Accessibility and DNA Repair

DSBs do not occur on naked DNA, but on complex, compacted, DNA-protein structures known as chromatin. Recent evidence suggests that the chromatin environment in which a DSB arises has a significant effect on DNA repair.

1.3.1 Chromatin organization in eukaryotes

Human cells contain about 2m of DNA that must be compacted into the cell nucleus. To achieve this high level of compaction, 146 base pairs of double-stranded DNA is wound around a core histone octamer composed of two copies of histone H2A, H2B, H3 and H4[107]. These protein-DNA subunits, called nucleosomes, are connected together by short linker DNA. Notably, the N-terminal tails of histones extend out from the nucleosome and contain critical lysine residues that can be modified by acetylation, methylation, or ubiquitylation to regulate chromatin structure. These nucleosomes pack together into 30nm fibers composed of 6-11 nucleosomes, which are stabilized by the associated linker histone H1[108-110]. The 30nm fibers are then folded into loops to produce 200-300nm chromatid fibers and higher-order chromatin associated with metaphase chromosomes[111, 112].

In eukaryotic cells, chromatin can be divided into two functional subtypes: euchromatin and heterochromatin. Euchromatin has a relatively decondensed structure, is highly acetylated, gene rich, and predominantly transcriptionally active. By contrast, heterochromatin, which represents about 10-25% of the DNA in the cell, is highly condensed, gene poor, and transcriptionally silent. Heterochromatin is characterized by hypoacetylation and trimethylation on lysine 9 of histone 3 (H3K9me3). In mouse cells, heterochromatin forms spatially distinct regions that are easily identified by their intense staining with the DNA dye, 4′,6-diamidino-2-phenylindole (DAPI)[113]. These DAPI-dense regions of heterochromatin are referred to as chromocenters[113]. Heterochromatin can be further classified as constitutive and facultative heterochromatin. Constitutive heterochromatin is composed of highly repetitive sequences and is enriched at centromeres and telomeres, while facultative heterochromatin contains genes that were originally transcriptionally active, but are silenced during development or aging[114]. A classic example of facultative heterochromatin is the mammalian female X chromosome, which is silenced early during embryogenesis[114].

Nonetheless, euchromatin and heterochromatin represent extremes of a spectrum as chromatin is a highly dynamic structure that is constantly transitioning from condensed to more relaxed structures during cellular processes such as transcription, replication, and DSB repair.

1.3.2 Heterochromatin proteins

Several proteins are involved in heterochromatin building and play key roles in stabilizing nucleosome compaction. First sequence-specific repressors bind to target DNA and recruit co-repressors such as KRAB-domain associated protein 1 (KAP-1) to activate heterochromatin-forming activities[115]. Generally, histone acetylation promotes chromatin relaxation and methylation induces chromatin compaction. Thus, histone deacetylases such as histone deacetylase 1 (HDAC1) and histone deacetylase 2 (HDAC2) remove acetyl groups from histone tails and histone methyltransferases such as suppressor of variegation 3-9 homolog 1 (Suv39H1), suppressor of variegation 3-9 homolog 2 (Suv39H2), and SET domain bifurcated 1 (SETDB1), add methyl groups to promote chromatin condensation[115]. In addition, ATP-dependent chromatin remodelling enzymes, such as chromodomain helicase DNA binding protein 3 (CHD3)/Mi-2α and chromodomain helicase DNA binding protein 4 (CHD4)/Mi-2β, adjust the spacing between nucleosomes to facilitate compaction[116]. Finally, chromodomain containing adaptors such as heterochromatin protein 1 (HP1) bind to the methylated histone tails to stabilize the densely packed nucleosomes[117]. Each of these components plays an integral part of the self-reinforcing heterochromatin structure and loss of any step may compromise its stability.

1.3.3 Heterochromatin as a barrier to DSB repair

The compact nature of heterochromatin poses a considerable barrier for DSB repair. Following exposure to IR, γH2AX foci form preferentially in euchromatic regions, suggesting that the decondensed chromatin may be more accessible to repair[118]. In support of this hypothesis, several studies have shown that γH2AX expansion within heterochromatin is inhibited[119, 120]. While γH2AX foci occur within minutes of IR exposure in euchromatin, they do not form in heterochromatin regions until much later and are localized to the periphery of these DAPI-dense regions[121, 122]. Based on this data it is unclear whether the compact nature of heterochromatin protects the DNA from DSBs or prevents the recruitment of DNA repair proteins. However, in *Drosophila melanogaster* and murine cells, γH2AX foci have been observed in heterochromatin regions at very early times after DSBs, but rapidly relocalize to the periphery[121, 123]. These

studies suggest that DSBs can arise in heterochromatin but are rarely observed in these regions because they are rapidly relocalized to more decondensed regions at the periphery of heterochromatin domains. Consistent with this notion, a recent study using high linear energy transfer (LET) radiation, which generates DSBs along the linear path of the ion particles, has shown that the γH2AX foci do not follow the DSB track, but bend around the DAPI-rich or H3K9me3-rich regions[124]. Collectively, these studies suggest that heterochromatin is not refractory to DSB, but the condensed structure restricts the access of DNA repair proteins to the lesion. In support of this theory, γH2AX foci in heterochromatin have been shown to be enhanced by histone deacetylase inhibitors (HDACIs)[119].

1.3.4 ATM signalling is required for repair of DSBs in heterochromatin

Heterochromatic breaks are generally repaired with slower kinetics than euchromatic breaks, reflecting the increased chromatin complexity surrounding these lesions[122]. Interestingly, ATM is dispensable for the repair of the majority of DSBs (~85%), but is specifically required for the repair of the slow-repairing DSBs within heterochromatin[122]. ATM and DNA-PK_{cs} function redundantly to phosphorylate H2AX, so in the absence of ATM the majority of DSBs are repaired by NHEJ through the activation of DNA-PK[17]. Despite these compensatory mechanisms, loss of ATM results in the persistence of DSBs at the periphery of DAPI-dense heterochromatic regions[122, 125]. However, knockdown of heterochromatin proteins such as HP1 (α + β + γ), KAP-1, or HDAC1/2, alleviates the need for ATM in DSB repair[122]. These results suggest that the requirement for ATM in the repair of heterochromatic DSBs relies on its ability to modulate heterochromatin structure.

1.3.5 Dynamic DSB-induced heterochromatin response

The general integrity of heterochromatin remains relatively unperturbed except for brief periods during replication and mitosis. However, following DSB induction, heterochromatin undergoes dynamic, localized relaxation to facilitate DNA repair[126-128]. Recently, the histone acetyltransferase Tip60 and the heterochromatin proteins, KAP-1 and HP1, have been shown to be critical mediators of heterochromatin relaxation following DSBs.

While earlier studies have demonstrated the requirement of ATM for heterochromatic DSB repair, the mechanism underlying this process has remained elusive until recently. It is well-

established that upon induction of a DSB, ATM dissociates from its inactive dimer and is autophosphorylated[14, 15]. However, more recent studies have revealed that the autophosphorylation of ATM is activated by the histone acetyltransferase Tip60[129]. ATM and Tip60 form a stable complex that is recruited to DSBs by the MRN complex[129]. Sun *et al.* have recently shown that in response to a DSB, Tip60 binds to the heterochromatin mark H3K9me3, which activates its acetyltransferase activity[130]. Acetylation of ATM by Tip60 then promotes the autophosphorylation of ATM, providing a key link between heterochromatin associated DSBs and ATM activation. In addition, Tip60 can acetylate histones H2A and H4 surrounding the DSB to promote a more open chromatin configuration[131, 132].

Since binding of Tip60 to H3K9me3 activates ATM, understanding how this histone modification is specifically recognized during DSB induction is critical. Two potential mechanisms for H3K9me3 recognition could be envisioned: *de novo* H3K9me3 modifications could be produced at sites of DSBs or a previously occupied H3K9me3 site could be unmasked to recruit and activate Tip60. Recent evidence supports the latter hypothesis. HP1 binds to H3K9me3 groups to stabilize nucleosome compaction within heterochromatin[117]. Upon induction of a DSB, casein kinase 2 (CK2) has been shown to phosphorylate the heterochromatin protein HP1β, dissociating it from heterochromatin to expose H3K9me3[133]. Although conflicting reports have shown that HP1 may be recruited to DSBs, this is thought to be a later event that is independent of its H3K9me3 interaction[134]. Thus, H3K9me3 unmasking by HP1 dissociation may provide a mechanism for the early activation of the Tip60/ATM complex at heterochromatic breaks to initiate repair.

Finally, understanding how ATM activation promotes heterochromatin remodelling and DNA repair has been the focus of recent studies. In response to DSB, the heterochromatin building protein, KAP-1, is phosphorylated by ATM on Ser824 within its C-terminus[135, 136]. KAP-1 is phosphorylated exclusively at sites of DNA damage and spreads rapidly throughout the chromatin[135]. A study by Goodarzi *et al.* has provided evidence to suggest that this ATM target may be essential for the repair of heterochromatic DSBs[122]. They have demonstrated that cells expressing a KAP-1 mutant that cannot be phosphorylated have a constitutive defect in the repair of heterochromatic DSBs, while a phospho-mimic mutant of KAP-1 bypasses the need for ATM[122]. The phosphorylation of KAP-1 has previously been shown to correlate with global chromatin relaxation[135]. Furthermore, the association of KAP-1 with nuclease-resistant

heterochromatin is reduced in an ATM-dependent manner upon induction of DSBs and siRNA-mediated knockdown of KAP-1 alleviates the need for ATM in the repair of heterochromatic breaks[122, 135]. Collectively, these results suggest that the role of ATM in the repair of heterochromatic DSBs is to regulate the chromatin association of KAP-1 via its phosphorylation status. Upon induction of a DSB within heterochromatin, ATM phosphorylates KAP-1 to promote its dissociation from chromatin to facilitate chromatin relaxation and the recruitment of DNA repair factors[122].

While the dynamic reorganization of heterochromatin proteins following DSBs has not been fully elucidated, these recent studies support the following model. In response to DSBs, HP1β is phosphorylated by CK2 and released from H3K9me3[133]. The MRN complex binds the DNA end and recruits the ATM/Tip60 complex to the exposed H3K9me3. Binding of Tip60 to H3K9me3 activates its acetyltransferase activity to promote the acetylation and subsequent phosphorylation/activation of ATM[129, 137]. Together, the phosphorylation of KAP-1 by ATM and the acetylation of H2A and H4 by Tip60, promotes chromatin decondensation to allow for the recruitment of repair factors[122, 138] (**Fig. 1.5**).

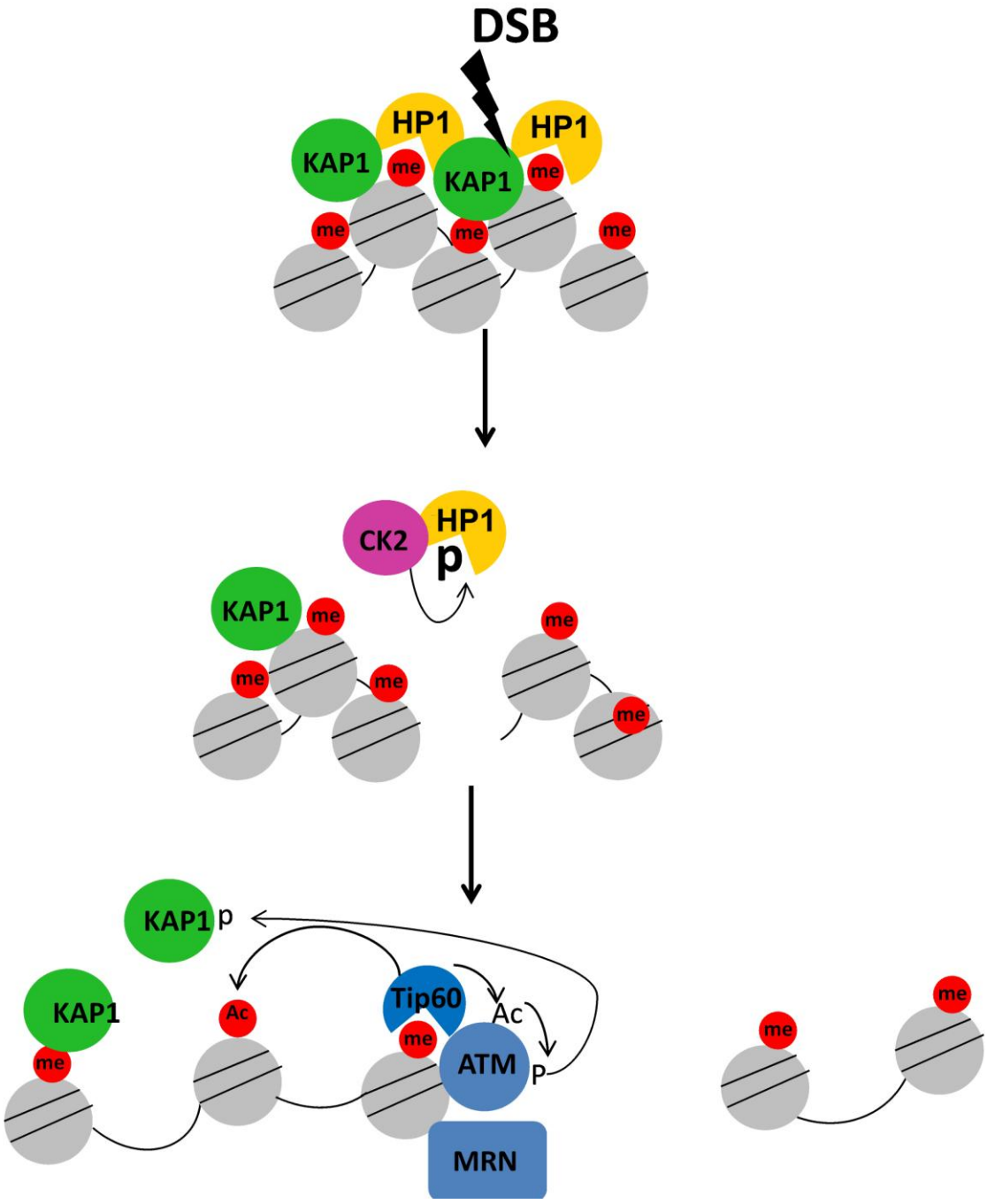

Figure 1.5. Dynamic DSB-induced heterochromatin decondensation. Upon induction of a DSB, casein kinase 2 (CK2) phosphorylates HP1β, releasing it from H3K9me3. MRN binds the DNA end and recruits Tip60/ATM to the exposed H3K9me3, activating the acetyltransferase activity of Tip60. Tip60 acetylates ATM to promote its autophosphorylation and activation. Phosphorylation of KAP-1 by ATM and acetylation of H2A and H4 by Tip60 then promotes chromatin decondensation.

1.4 Cancer and Genomic Instability

1.4.1 Genomic instability as a hallmark of cancer

In order for normal cells to become cancerous, they must acquire unique characteristics that confer a selective proliferative advantage over normal cells, while evading several cellular surveillance mechanisms. Cancer cells must be able to divide indefinitely by sustaining proliferative signals, inhibiting growth suppressors, and evading apoptosis and senescence[139]. In addition, cancer cells must create a self-sustaining environment by inducing angiogenesis to ensure a steady supply of oxygen and nutrients and acquire the ability to invade other tissues and metastasize[139]. Therefore, for normal cells to become cancerous, they must acquire a series of mutations in key regulatory pathways such as cell cycle, apoptosis, and growth factor signalling.

However, the normal mutation rate of cells cannot account for the multiple mutations found in human cancers[140]. To reconcile this apparent conundrum, the mutator phenotype hypothesis has been proposed[141]. The basis of this hypothesis is that cells acquire mutations in genes which regulate genome stability to increase mutation rates and promote tumourigenesis[141]. Genomic instability is a hallmark of almost all human cancers and is present in precancerous lesions to advanced cancers, providing additional evidence that this may be an early initiating event[142, 143].

1.4.2 DNA repair, genomic instability, and cancer

DNA repair is essential for maintaining genomic stability and mutations in DDR genes have been linked to many sporadic and inherited forms of cancer[144]. For example, homozygous mutations in ATM cause a childhood disease called ataxia telangiectasia, which is characterized by genomic instability, immunodeficiency, neurodegeneration, radiation hypersensitivity, and a predisposition to cancer[145]. Similarly, mutations in the core MRN sensor complex proteins, Mre11 and Nbs1, lead to ataxia telangiectasia-like disorder (ATLD) and Nijmegen breakage syndrome, respectively, which share the radio-sensitivity and genomic instability associated with ataxia telangiectasia[62]. Finally, BRCA1 and BRCA2 have been shown to play essential roles in HR and individuals with mutations in these genes are at increased risk of developing breast and ovarian cancer[146].

1.5 Clear-cell renal cell carcinoma (CCRCC)

1.5.1 Clinical features, treatments, and outcomes

Clear-cell renal cell carcinoma (CCRCC) is the most common form of kidney cancer, accounting for approximately 3% of all adult malignancies[147]. CCRCC is thought to originate from the proximal convoluted tubule of the nephron and, as its name suggests, is characterized by cells with distinctive clear cytoplasm and prominent uniform nuclei[147-150]. These tumours have a characteristic hypoxic profile and are highly vascularized (discussed further in section 1.6.3). CCRCC is arguably one of the most aggressive cancers and is notoriously resistant to radiation and chemotherapy[147]. The 5-year survival rate for localized disease is 75-90%, however up to one third of patients present with metastatic disease at diagnosis and the survival rate for these patients is reduced to less than 10%[147].

The main treatment option for CCRCC is partial or total nephrectomy. Although nephrectomy is only curative for localized disease, it is often performed in metastatic disease for its beneficial effects on symptom control and survival[151]. Given the low response rates to traditional radiation and chemotherapies, alternative treatments for metastatic CCRCC are being explored. In the early 1980s, the rare spontaneous remission of CCRCC observed in some patients led to the search for immunomodulatory agents that could heighten the host immune function and eliminate malignant cells. These efforts led to the use of interleukin-2 (IL-2) and interferon-α for advanced CCRCC, which are associated with modest response rates of 13-21% and 14%, respectively[147]. While this is significantly better than traditional chemotherapies (4-6%), better treatment options are warranted[152]. Recently, significant progress has been made in the development of receptor tyrosine kinase inhibitors and humanized antibodies, which target key signalling pathways known to be upregulated in CCRCC (discussed in Section 1.6.3). Bevacizumab, a vascular endothelial growth factor (VEGF) antibody, and the VEGF receptor 2 (VEGFR2) and platelet-derived growth factor receptor β (PDGFRβ) inhibitors, sorafenib and sunitinib, have all been shown to prolong progression-free survival[151]. In addition, an inhibitor of mammalian target of rapamycin (mTOR), temsirolimus, increased the progression-free survival of metastatic CCRCC in clinical trials[151]. Despite these promising advances, bevacizumab has no effect on overall survival rate, sorafenib and sunitinib have serious clinical toxicities, and temsirolimus, although well tolerated, has a very low response rate[151].

Evidently, new treatments for advanced stage CCRCC need to be explored to improve the overall survival rate for these patients. Further elucidating the signalling pathways deregulated in CCRCC may aid in development of novel targeted therapies to selectively sensitize malignant cells.

1.5.2 Mutations and Genomic Instability

CCRCC is characterized by high genomic instability, with frequent chromosomal translocations and deletions. Aberrations of chromosome 3 with loss of 3p or translocations of different chromosome sections to the deleted chromosome 3 regions are most common[153]. Gain of chromosomes 5q and 7 are also frequent and additional loss of 1p, 4, 9, 13q, and 14q has been associated with a more aggressive disease[153]. While the molecular mechanisms underlying this genomic instability have remained unclear, mutations in the SWI/SNF chromatin remodelling complex gene, *PBRM1*, were recently identified in approximately 41% of CCRCC cases[154]. In addition, mutations in the histone modifying genes *UTX*, *JARID1C*, and *SETD2* have been identified in a small number of cases[154]. These recent findings suggest that changes in chromatin structure play an important role in CCRCC tumourigenesis and may underlie some of the genomic instability.

The vast majority of hereditary and sporadic CCRCC are associated with loss of function of the von Hippel-Lindau (*VHL*) tumour suppressor gene, located on chromosome 3p[155]. Most CCRCC occur sporadically from biallelic inactivation of VHL through somatic mutation(s) (40-80% of cases) or hypermethylation (10-20% of cases) of the *VHL* gene[155, 156]. However, a predisposition to CCRCC may also be inherited through germline mutations in *VHL* in a rare cancer syndrome called VHL disease[157]. VHL patients inherit one mutated *VHL* allele and somatic mutation of the remaining wild-type (WT) allele gives rise to the clinical manifestations of the disease, which include retinal and cerebral haemangioblastomas (vascular tumours of the eye and brain), phaeochromocytomas (neuroendocrine tumours of the adrenal medulla), and CCRCC[158, 159]. Notably, CCRCC remains the primary cause of morbidity and mortality in VHL patients[158, 159].

1.6 Structure and Functions of VHL

1.6.1 *VHL* gene and tumour suppressor protein

In 1993, Latif *et al*. identified and cloned *VHL* from chromosome 3p25, a region frequently mutated in sporadic CCRCC[157, 160]. *VHL* is highly conserved in worms, flies, and rodents[157]. It contains three exons encoding a 4.5kB mRNA that is ubiquitously expressed in mammalian cells. Alternative splicing gives rise to a second *VHL* transcript missing exon 2 and some tumours exclusively produce this exon 2 deletion transcript, suggesting that this region may be important for its tumour suppressor activity (**Fig 1.6**).

VHL mRNA encodes two protein isoforms: a 213 amino acid protein with a molecular weight of 30-kilodaltons (VHL30) and a shorter 160 amino acid, 19-kilodalton protein (VHL19) produced from an internal translational start site at methionine 54[161] (**Fig. 1.6**). The function of the N-terminal acidic domain (aa1-53), lacking in VHL19, remains poorly defined. Both proteins have been shown to independently suppress tumour growth in nude mouse xenograft assays and were originally thought to have overlapping tumour suppressor functions[162-164]. However, several disease-causing mutations have been found in the N-terminal domain of VHL (aa1-53), which would presumably allow for the translation of a functional VHL19 protein[165-167]. This suggests that VHL30 may have some unique tumour suppressor functions associated with its N-terminal acidic domain. In addition, Lolkema *et al*. have demonstrated that phosphorylation of the N-terminal domain is necessary for deposition of a fibronectin extracellular matrix, which is essential for tumour suppression (Discussed in Section 1.7.1)[168].

VHL is predominantly cytoplasmic, but can shuttle between the nucleus and cytoplasm[169, 170]. Several cellular triggers have been shown to promote accumulation of VHL in the nucleus, including transcriptional arrest, low cell density, or low pH[169-171]. VHL contains a putative bipartite nuclear localization signal (NLS) between aa1-60 and an ATP-dependent nuclear export signal (NES) in exon 2 (aa114-154), which regulates its shuttling[169, 170, 172] (**Fig 1.6**). Nuclear-cytoplasmic shuttling of VHL has been shown to be essential for its tumour suppressor activity, which is exemplified by the occurrence of cancer-causing mutations in the nuclear export motif[170, 172]. Although VHL is primarily cytoplasmic, Lewis and Roberts demonstrated that exclusively nuclear or shuttling forms of VHL are sufficient to inhibit tumour invasion, promote fibronectin deposition, and downregulate integrin expression[173]. This study suggests that several

key tumour suppressor activities of VHL are dependent upon its nuclear localization and cellular trafficking.

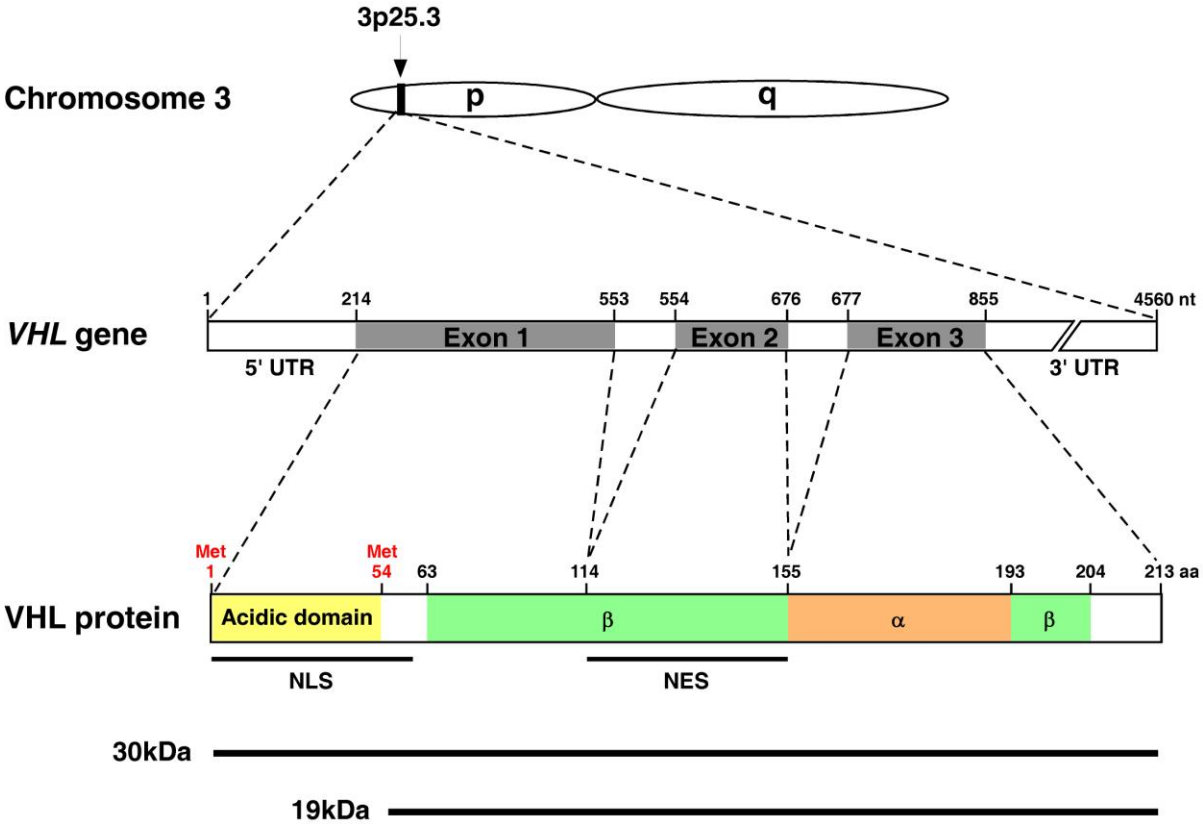

Figure 1.6. VHL gene and protein structure. The *VHL* gene (accession NM_000551.3) located on chromosome 3p25.3 is 4560 nucleotides (nt) in length and contains 3 exons. The VHL mRNA codes for two proteins, a 213 amino acid (aa), 30kDa protein and a 160aa, 19kDa protein that results from internal translation initiation from Met 54. The α and β domains of VHL are coloured in orange and green, respectively and the N-terminal acidic domain is shown in yellow. VHL contains a bipartite nuclear localization signal (NLS) between aa1-60 and a nuclear export sequence (NES) between aa114-154.

1.6.2 ECV complex

Unfortunately, isolation of the *VHL* gene revealed no nucleotide or amino acid sequence homology to any known proteins that would provide insight into its function. Therefore, in an effort to identify its cellular function, VHL-associated proteins were investigated. As a result of this initial work, it is now known that VHL interacts with Elongin B, Elongin C, Cullin 2 (Cul2), and Rbx1 in a multiprotein complex referred to as ECV (Elongins BC/ Cul2/ VHL)[161, 174-176]. Insight into the function of VHL came from the observation that Elongin C and Cul2 were structurally similar to two *Saccharomyces cerevisiae* yeast proteins Skp1 and Cdc53[177]. Skp1 and Cdc53 bind to F-box proteins in a multiprotein SCF(Skp1/Cdc25/F-box) complex, which targets proteins for ubiquitin-mediated destruction via recruitment by the F-box protein [178-180]. Analogous to the SCF complex, the ECV complex was found to act as an E3 ubiquitin ligase[181, 182] (See section 1.6.3 for further discussion). The crystal structure of VHL revealed two distinct domains: α and β[183] (**Fig. 1.6**). The α domain of VHL mediates binding to Elongin C and its associated proteins (Cul2/Rbx1), while the β domain acts as the substrate docking site[183]. Notably, disease-causing mutations in VHL patients frequently map to the α or β domain, emphasizing the importance of these domains in the tumour suppressor function of VHL[183].

1.6.3 Oxygen-dependent regulation of HIFα

The clinical manifestations of VHL patients provided significant clues for the identification a biological substrate for the ECV complex. Loss of VHL is associated with highly vascular tumours such as hemangioblastomas and CCRCCs, which frequently overexpress vascular endothelial growth factor (VEGF) and occasionally erythropoietin (EPO)[184-191]. Interestingly, the mRNA expression of both VEGF and EPO is induced under low oxygen conditions by the transcription factor hypoxia-inducible factor (HIF)[192, 193]. Based on this evidence, HIF was investigated and later revealed to be a bona fide substrate for ECV-mediated ubiquitylation[181, 182, 194, 195].

HIF is a major regulator of the adaptive response to low oxygen levels in the cell[196]. It is a heterodimeric transcription factor composed of an oxygen-labile α subunit and a constitutively expressed β subunit, also known as aryl hydrocarbon receptor nuclear translocator (ARNT)[196]. There are three HIFα isoforms in mammalian cells: HIF1α, HIF2α, and HIF3α[197]. Under

normal oxygen tension, HIFα is hydroxylated on conserved proline residues by a family of prolyl hydroxylase domain enzymes (PHDs, also known as EGLNs)[198, 199]. Hydroxylated HIFα is recruited to the ECV complex through its interaction with the β domain of VHL and is subsequently ubiquitylated and targeted for degradation through the 26S proteasome (**Fig. 1.7**)[196, 200, 201]. Notably, hydroxylation of HIFα is necessary for its recognition by VHL[200-202]. PHD enzymes require oxygen for their catalytic activity and consequently, HIFα hydroxylation is attenuated under hypoxia, escaping recognition by the ECV complex. Stabilized HIFα dimerizes with its β subunit to form an active transcription factor[203]. HIF subsequently translocates into the nucleus where it binds to hypoxia-responsive elements (HRE) in the promoters/enhancers of genes involved in the adaptive response to low oxygen, including VEGF, EPO, and glucose transporter 1 (GLUT1), resulting in their transcriptional upregulation[196, 197].

Inactivation of VHL in CCRCC results in aberrant stabilization of HIFα and upregulation of hypoxia-responsive genes in the presence of normal oxygen tension, generating the classic hypoxic profile of these tumours. Similarly, all CCRCC-causing VHL mutations associated with VHL disease have a defect in ECV complex formation or HIFα binding[183]. Upregulation of HIF activates numerous genes involved in anaerobic metabolism, cell proliferation, survival, angiogenesis, erythropoiesis, invasion, and metastasis, which characterize and promote tumourigenesis[197]. Thus, by exploiting the HIF pathway, tumour cells gain a significant growth advantage. Accordingly, overexpression of HIF is frequently associated with increased tumour aggressiveness and poor prognosis and knockdown of HIF2α is sufficient to suppress the tumourigenic capacity of CCRCC cells devoid of VHL[204-209].

1.7 HIF-independent functions of VHL

In addition to its well-characterized role in the negative regulation of HIFα, several other tumour suppressive functions have been attributed to VHL, including regulation of extracellular matrix (ECM) assembly, ciliogenesis, and apoptosis (**Fig. 1.7)**. These VHL functions are independent of its role in the negative regulation of HIF, but significantly contribute to its tumour suppressive activities.

1.7.1 Extracellular matrix assembly

VHL binds to the extracellular glycoprotein, fibronectin, but unlike HIFα, does not target it for degradation[210]. Instead, the interaction between VHL and fibronectin has been shown to be essential for ECM assembly and tumours devoid of VHL fail to assemble a proper fibronectin matrix[210]. Both phosphorylation and neural precursor cell expressed developmentally down-regulated protein 8 (NEDD8)-modification of VHL have been shown to promote its interaction with fibronectin[168, 211]. Interestingly, NEDD8-conjugation to VHL acts as a molecular switch to dissociate the ECV complex and promote binding to fibronectin, clearly distinguishing this as a HIF-independent function[211]. In addition, VHL has been shown to interact with collagen IV to promote its deposition in the extracellular space[212, 213]. Similar to fibronectin, a number of VHL tumour-causing mutations, including mutants with normal HIF regulation, are associated with defective collagen IV matrix assembly[213]. These findings highlight an important HIF-independent tumour suppressor function of VHL in the maintenance of ECM integrity.

1.7.2 Stabilization of microtubules and assembly of primary cilia

Renal cysts are frequently observed in VHL patients and are thought to be the precursors of CCRCC[214]. The development of renal cysts are commonly associated with a defect in primary cilia, the hair-like structures on the surface of renal epithelial cells which act as flow sensors[215, 216]. The core of these cilia is composed of microtubules, which are anchored to the basal body by the centrosome[217]. Changes in flow trigger bending of the cilia and intracellular calcium fluxes to active downstream signalling pathways[218]. Several studies have shown that inactivation of VHL in CCRCC cells leads to loss of primary cilia and reconstitution of VHL can appropriately restore cilia growth[219-221]. Notably, the ability of VHL to promote ciliogenesis was independent of HIF function, but dependent upon the ability of VHL to bind and stabilize microtubules and orient their growth[220, 221].

1.7.3 Regulation of apoptosis

CCRCC is highly resistant to radiation and chemotherapy, in part due to a suppression of apoptotic pathways. In support of this notion, several studies have reported increased expression and activity of the nuclear factor kappa-light-chain-enhancer of activated B cells (NFκB) transcription factor in CCRCC cells, which correlates with an increased resistance to tumour

necrosis factor-alpha (TNF-α)-induced apoptosis[222-224]. Recent evidence suggests that VHL acts as a negative regulator of NFκB by promoting the inhibitory phosphorylation of the NFκB agonist, caspase recruitment domain-containing protein 9 (CARD9)[225]. Thus, loss of VHL promotes NFκB activity and upregulates the expression of several anti-apoptotic targets including, cellular FLICE-like inhibitory protein (c-FLIP), survivin, and cellular inhibitor of apoptosis protein-1/2 (c-IAP-1/2), which block the activities of caspase 8 and 3 to suppress p53-mediated apoptosis[222]. In addition, VHL has been reported to bind p53 to promote its stability and transactivation in response to genotoxic stress[226]. Phosphorylation of VHL by Chk2 was shown to direct the recruitment of the transcriptional co-activator, p300, and Tip60 to the chromatin of p53 target genes to enhance p53-mediated transcription[227].

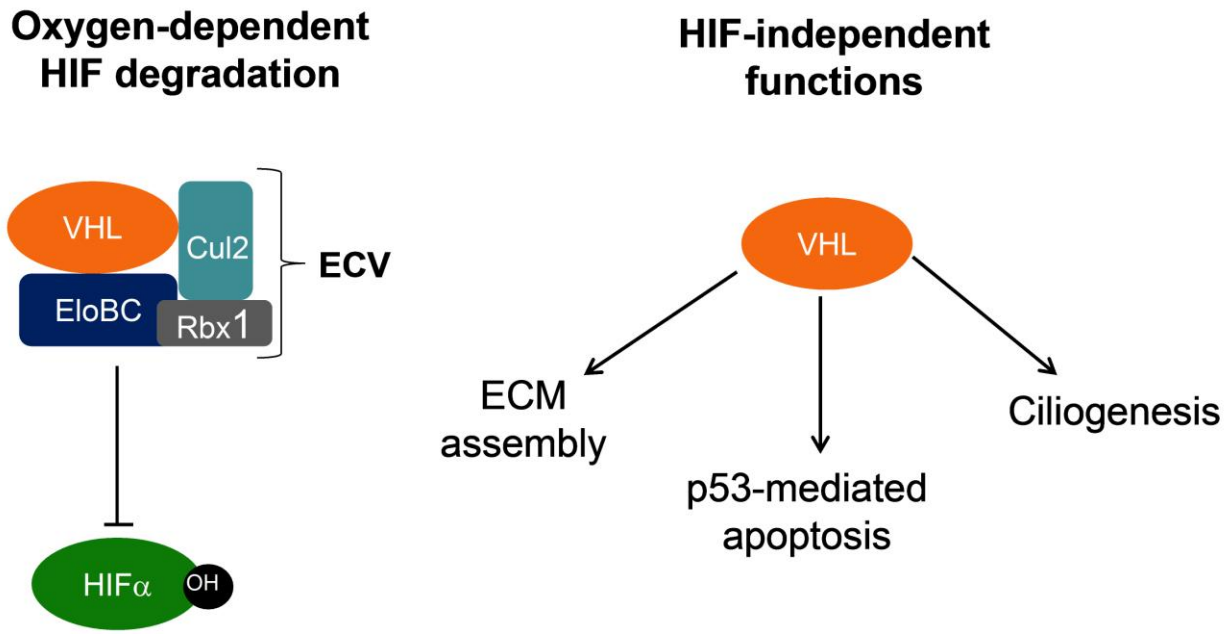

Figure 1.7. Functions of VHL. VHL is the substrate-recognition component of an E3 ubiquitin ligase complex with ElonginsBC, Cul2, and Rbx1 (ECV) which targets hydroxylated hypoxia-inducible factor alpha (HIFα) for oxygen-dependent degradation. In addition, VHL has been shown to regulate extracellular matrix (ECM) assembly, p53-mediated apoptosis, and ciliogenesis in a HIF-independent manner.

1.8 Thesis Rationale

DNA repair is essential for maintaining genomic stability, and defects in this process significantly increase the risk of cancer[144]. CCRCC, caused by inactivation of the *VHL* tumour suppressor gene, is characterized by an elevated hypoxic profile and high genomic instability. While the former is explained by the canonical role of VHL as a negative regulator of HIF which is responsible for numerous adaptive responses to hypoxia, the molecular mechanism underlying the association between the loss of VHL and genomic instability has remained unclear.

Although the best characterized function of VHL is in the negative regulation of HIFα, there is a growing list of HIF-independent functions that have been attributed to VHL and may likewise contribute to its tumour suppressor activity. Recently, our lab has shown that VHL cooperates with suppressor of cytokine signalling 1 (SOCS1) for the ubiquitin-mediated destruction of *Janus* kinase 2 (JAK2) in the negative regulation of erythropoiesis[228]. In addition to its role in cytokine signalling, SOCS1 has previously been shown to be highly expressed and associated with ATM in the nucleus of cells undergoing signal transducer and activator of transcription 5 (STAT5)-mediated oncogene-induced senescence, suggesting that SOCS1 may actively participate in the DDR[229]. Given the high genomic instability in CCRCC, we asked whether VHL cooperates with SOCS1 for a nuclear role in the DDR.

In Chapter 2 we show that SOCS1 promotes nuclear redistribution and K63-ubiquitylation of VHL in response to DNA damage, and VHL mutations that compromise its K63-ubiquitylation attenuates the DDR independent of HIF activity, resulting in decreased repair and persistence of DSBs. In Chapter 3, we further characterized the role VHL in the DDR by examining the 30kDa and 19kDa isoforms of VHL. We show that while VHL30 activates the DDR, VHL19 has an inhibitory effect on the DDR. VHL19 is bound to undamaged chromatin, but is degraded upon induction of DSBs, presumably to alleviate its inhibitory effect on the DDR. Finally, in Chapter 4 we further elucidate the role of VHL in the repair of DSBs. We show that VHL binds HP1α and dissociates it from damaged chromatin to promote chromatin relaxation. We further demonstrate that the interaction between VHL and HP1α is necessary for DNA damage-induced chromatin relaxation and activation of the DDR. Collectively, these results demonstrate for the first time that VHL30 plays a role in DDR and loss of this function promotes the unchecked

accumulation of DNA damage, which likely contributes to the genomic instability that commonly characterizes and drives CCRCC.

Chapter 2

2 K63-Ubiquitylation of VHL by SOCS1 mediates DNA double-strand break repair

This work has been published:

Metcalf JL, Bradshaw PS, Komosa M, Greer SN, Meyn MS, Ohh M. K63-ubiquitylation of VHL by SOCS1 mediates DNA double-strand break repair. (2013). *Oncogene.* doi: 10.1038/onc.2013.22. [Epub ahead of print].

2.1 Introduction

DNA double-strand breaks (DSBs) are highly toxic lesions that if left unrepaired promote genomic instability, one of the hallmarks of cancer. To minimize the deleterious effects of DSBs, multicellular organisms utilize a complex signalling network known as the DNA damage response (DDR) to detect the presence of DNA damage and activate appropriate cellular defences. In response to DSBs, ataxia-telangiectasia mutated (ATM) is rapidly autophosphorylated and recruited to DNA lesions by the Mre11-Rad50-Nbs1 (MRN) sensor complex[14, 15]. Activated ATM phosphorylates histone variant H2AX (known as γH2AX when phosphorylated) surrounding the DSB, which promotes the recruitment of DDR proteins to the DNA lesion[230, 231]. ATM also phosphorylates the effector kinases Chk1/2, which initiate a downstream signalling cascade through the phosphorylation of other DDR proteins, including Cdc25, breast and ovarian cancer susceptibility protein (BRCA) 1, replication protein A (RPA), and p53[232]. Through these and other molecular events, the DDR promotes survival and genome stability by activating cell cycle checkpoints, initiating DNA repair, and triggering stress responses. Alternatively, if the damage is too extensive or the DNA break irreparable, the DDR can induce apoptosis or senescence[28, 29].

Non-homologous end joining (NHEJ) and homologous recombination (HR) are the two major DSB repair pathways in eukaryotic cells. NHEJ directly ligates the DNA ends and is considered error-prone, as it frequently results in small deletions and translocations due to non-compatible end joining. In contrast, HR typically uses homologous DNA on a sister chromatid as a template

for accurate repair and is generally restricted to S and G_2 phases of the cell cycle. These mechanistically distinct pathways play both competitive and compensatory roles in DNA repair in an attempt to maintain genomic stability[30-35].

DNA repair is essential for maintaining genome stability and mutations in DDR genes have been linked to many sporadic and inherited forms of cancer[144]. Clear-cell renal cell carcinoma (CCRCC), the most common form of kidney cancer, is associated with high genomic instability characterized by frequent chromosomal deletions and translocations. Recently, mutations in the SWI/SNF chromatin remodelling complex gene, *PBRM1*, were identified in approximately 41% of CCRCC cases which may underlie some of the genomic instability[154]. However, the majority of CCRCC cases have no reported mutations in chromatin remodelling or DNA repair genes, and the molecular mechanisms underlying genomic instability in CCRCC remains largely unknown.

The vast majority of hereditary and sporadic CCRCC is associated with loss or inactivating mutations of the von Hippel-Lindau (*VHL*) tumour suppressor gene. VHL is best characterized as a substrate-conferring component of an E3 ubiquitin ligase ECV (Elongins BC/Cul2/VHL) that targets hypoxia-inducible factor α (HIFα) for oxygen-dependent ubiquitylation and subsequent proteasome-mediated destruction[200, 233]. Thus, the inactivation of VHL results in the stabilization of HIFα and transcriptional activation of a host of hypoxia-inducible genes involved in various adaptive responses to low oxygen tension, such as anaerobic metabolism, angiogenesis, and erythropoiesis. Moreover, VHL has been implicated in other cellular functions, loss of which may likewise contribute to oncogenesis, including endocytosis, extracellular matrix assembly, ciliogenesis, and senescence[210, 220, 234-236].

Recently, VHL was shown to cooperate with suppressor of cytokine signalling 1 (SOCS1) for the ubiquitin-mediated destruction of *Janus* kinase 2 (JAK2) in the negative regulation of erythropoiesis[228]. Analogous to VHL, SOCS1 forms the substrate recognition component of an E3 ubiquitin ligase complex in association with ElonginsBC, Cul2 or Cul5, and Rbx1 (known as the ECS complex)[237, 238]. In addition to its role in cytokine signalling, SOCS1 has previously been observed to be highly expressed and associated with ATM in the nucleus of cells undergoing signal transducer and activator of transcription 5 (STAT5)-mediated oncogene-induced senescence, suggesting that SOCS1 may actively participate in the DDR[229]. We now show that while VHL is primarily cytoplasmic, co-expression with SOCS1 redistributes VHL to

discrete nuclear foci which colocalize with SOCS1. Therefore, given the high genomic instability in CCRCC, we hypothesized that VHL may cooperate with SOCS1 for a nuclear role in the DDR.

2.2 Materials and Methods

2.2.1 Cells

786-O, HEK293A, HEK293T, ACHN and U2OS cells were obtained from the American Type Culture Collection (Rockville, MD). Renal proximal tubule epithelial cells were purchased from Lonza (Basel, Switzerland). 786-O subclones ectopically expressing haemagluttin (HA) tagged-VHL wild-type(WT), HA-VHL(F119S), HA-VHL(RRR) or empty plasmid (Mock) were previously described[228, 239, 240]. 786-VHL(L118R) was generated as previously described[239]. RCC10 parentals and HA-VHL(WT) reconstituted subclones were a kind gift from Dr Karl Plate (Goethe University Medical School, Frankfurt, Germany). 786-O and RCC10 stable subclones were selected under 1 mg/ml G418 in culture medium. U2OS DR-GFP cells were a generous gift from Dr. Maria Jasin (Memorial Sloan-Kettering Cancer Center, New York, NY, USA). Renal proximal tubule epithelial cells were maintained in renal epithelial growth medium (REGM) (Lonza) and all other cell lines were maintained in Dulbecco's modified Eagle's medium (DMEM) supplemented with 10% heat-inactivated fetal bovine serum (Wisent, St-Bruno, QC, Canada) at 37 °C in a humidified 5% CO_2 atmosphere.

2.2.2 Plasmids

HA-SOCS1(WT) was generously provided by Dr Robert Rottapel (Ontario Cancer Institute, Toronto, ON, Canada). Triple-FLAG-tagged SOCS1 (FLAG-SOCS1) was gene synthesized (Mr. Gene, Regensburg, Germany) and subcloned into pcDNA3. HA-VHL(WT, RRR and F119S) and T7-VHL were previously described[202, 239]. HA-VHL(L118R) was generated using QuikChange site-directed mutagenesis kit (Stratagene, La Jolla, CA, USA) and verified by direct DNA sequencing. HA-Ub(WT), HA-Ub(K48) and HA-Ub(K63) were kind gifts from Dr Zhijian Chen (UTSW Medical Center, Dallas, TX, USA). pGL3 was purchased from Promega (Madison, WI, USA)

2.2.3 Chemicals

Doxorubicin was obtained from Santa Cruz Biotechnology (Santa Cruz, CA, USA) and MG132 was obtained from Peptides International (Louisville, KY, USA).

2.2.4 Antibodies

The following antibodies were used: monoclonal anti-FLAG(M2) (Sigma-Aldrich, Oakville, ON, Canada), monoclonal rabbit anti-HA (Cell Signaling, Danvers, MA, USA), monoclonal mouse anti-HA(12CA5) (Roche Applied Science, Laval, QC, Canada), anti-hnRNP C1/C2 (AbCam, Cambridge, MA, USA), anti-vinculin (Sigma-Aldrich), polyclonal anti-FLAG (Novus Biologicals, Oakville, ON, Canada), anti-α-tubulin (Sigma-Aldrich), anti-VHL (BD Biosciences, Mississauga, ON, Canada), anti-ubiquitin (Dako, Burlington, ON, Canada), anti-T7 (Novagen, Madison, WI, USA), anti-γH2AX (immunoblotting; Cell Signaling), anti-γH2AX (immunofluorescence; Millipore, Billerica, MA, USA), anti-SOCS1 (Invitrogen, Burlington, ON, Canada), anti-Ubc13 (Cell Signaling), anti-pChk1 (Cell Signaling), anti-pATM(Ser1981) (Cell Signaling), anti-ATM (Cell Signaling), anti-Mre11 (Genetex, Irvine, CA, USA), anti-HIF2α (Novus Biologicals), anti-β-actin (AbCam), and anti-DNA ligase IV (AbCam). Horseradish peroxidase or rhodamine-conjugated goat anti-rabbit and goat anti-mouse secondary antibodies were obtained from Thermo Scientific (Billerica, MA, USA). Alex Fluor-488-conjugated goat anti-rabbit or anti-mouse secondaries were obtained from Invitrogen and tetramethyl rhodamine isothiocyanate (TRITC)-conjugated secondary antibody was obtained from Jackson ImmunoResearch (West Grove, PA, USA).

2.2.5 Transfection

Cells were transfected with a 1μg/uL solution of polyethyleneimine (PEI). 3-5μg of DNA was resuspended in 400μL of serum-free opti-minimum essential media (Opti-MEM)(Gibco, Burlington, ON, Canada). PEI was added at a ratio of 4:1 PEI to DNA and incubated at room temperature for 15min. Cells were trypsinized and resuspended in serum-free Opti-MEM (Gibco) at a concentration of 1×10^7 cells/mL. Cells were added to DNA complexes and incubated for 10min at room temperature before plating into 100mm plates. Cells were

harvested 48hrs post-transfection for immunoprecipitation and/or immunoblotting (see Section 2.2.7).

2.2.6 RNA Interference

ON-TARGETplus SMART pool siRNA targeted to *SOCS1, VHL, RAD51, UBC13, HIF2α* (Thermo Scientific) or non-targeting scrambled siRNA (Thermo Scientific) were transfected with X-Treme Gene siRNA transfection reagent (Roche, Mississauga, ON, Canada), according to the manufacturer's instructions.

2.2.7 Immunoprecipitation and Immunoblotting

Immunoprecipitation and immunoblotting were performed as previously described[210]. In brief, cells were washed with phosphate-buffered saline (PBS) and lysed in EBC buffer (50 mM Tris [pH 8.0], 120 mM NaCl, 0.5% NP-40) supplemented with a cocktail of protease and phosphatase inhibitors (Roche, Laval, Canada). Cell lysates were sonicated for 5sec followed by centrifugation at 14,000 rpm for 10min to remove cell debris. Protein concentrations were determined by Bradford method. A fraction of cleared lysates were prepared for whole cell extracts (WCE) by combining with sodium dodecyl sulfate (SDS)-containing sample buffer and remaining lysate was used for immunoprecipitation. Immunoprecipitation was performed by incubating appropriate antibody (1μg per mg of lysate) and protein-A agarose (RepliGen, Waltham, MA, USA) with cleared lysate for 1.5hrs at 4°C with rocking. Immunoprecipitates were washed five times with NETN buffer (20 mM Tris [pH 8.0], 100 mM NaCl, 1 mM EDTA [pH 8.0], 0.5% NP-40), eluted by boiling in SDS-containing buffer, and separated by SDS-polyacrylamide gel electrophoresis (PAGE). Proteins were transferred to polyvinylidene difluoride (PVDF) (Bio-Rad Laboratories, Hercules, CA) for immunoblotting. The membrane was subsequently blocked in tris-buffered saline-Tween 20 (TBST) (10 mM Tris pH 8.0, 150 mM NaCl, 0.05% Tween-20) containing 4% skim milk powder for 1 hr at room temperature and incubated with primary antibody diluted in TBST for 16hrs at 4°C. Five washes with TBST were followed by 1hr incubation at room temperature with horseradish peroxidase-conjugated secondary antibodies (Pierce Chemical, Rockford, IL, USA) diluted in TBST containing 2% skim milk. The membrane was washed five times in TBST and proteins were detected using a chemiluminescence reagent (Lumi-light, Roche, Laval, Canada).

2.2.8 Cellular Fractionation

Cellular fractionation was performed as previously described[241]. Briefly, cells were trypsinized, washed twice with cold PBS, and pelleted by centrifugation at 1100 rpm at 4°C for 4 min. Cells were resuspended in Buffer A (10 mM HEPES [pH 7.9], 10 mM KCl, 1.5 mM MgCl2, 0.34 M sucrose, 10% glycerol, 1 mM DTT) containing 0.1% Triton X-100 and supplemented with complete protease inhibitors (Roche; Indianapolis, IN) and incubated on ice for 7 min. The nuclear fraction was pelleted by centrifugation at 3500 rpm for 5 min at 4°C, and the cytoplasmic cell fraction was transferred to a fresh tube. The cytoplasmic fraction was further clarified by centrifugation at 14,000 rpm for 10min. The nuclear pellet was washed once with Buffer A without Triton X-100 and centrifuged at 3500 rpm for 5min. The nuclear pellet was then resuspended in Buffer B (0.2 mM EGTA [pH 8], 3 mM EDTA [pH 8], 1 mM DTT) and incubated on ice for 30 min while undergoing periodic vortexing. The nuclear fraction was collected following centrifugation at 4000 rpm for 5 min at 4°C. Protein concentrations were determined by Bradford method, and immunoprecipitations were performed as described in section 2.2.7.

2.2.9 Generation of 786-VHL-shScr and –shSOCS1 cells

pGIPZ shSOCS1 and non-silencing control (shScr) plasmids were obtained from Open Biosystems (Huntsville, AL, USA). HEK293T cells were co-transfected with pMDG1.vsvg and psPAX2 (a gift from Dr Linda Penn, Ontario Cancer Institute, Toronto, ON, Canada). The medium was replaced with fresh medium the next day. Viral supernatant was collected 2 days after transfection, passed through a 0.45-μm filter. 786-VHL(WT) cells stably expressing HA-VHL(WT) were infected with the viral supernatant and incubated at 37 °C for 24 h. Polyclonal populations of cells stably expressing shSOCS1 and shScr were selected with 2 μg/ml puromycin (Wisent).

2.2.10 RNA Purification and Quantitative Real-Time PCR (qRT-PCR)

Total RNA was extracted using a Qiagen RNeasy extraction kit (Qiagen, Hilden, Germany) according to the manufacturer's instructions. For the synthesis of cDNA, 1 μL of random hexamer primer (Thermo Scientific) was mixed with 5 μg of RNA in a total reaction volume of 20 μL and incubated for 10 min at 70°C in a PTC-200 Peltier Thermal Cycler (MJ Research, Boston, MA). The mixture was cooled to 4°C and the following components were added to the

reaction: 4 µL of 5x 1st strand reaction buffer, 2 µL of 0.1 M DTT, 1 µL of 10 mM dNTPs, and 1 µL Superscript II reverse transcriptase (all obtained from Invitrogen). cDNA synthesis was performed for 1.5 h at 42°C, followed by 15 min at 70°C. Human genomic DNA standards (Roche, Mannheim, Germany) or cDNA equivalent to 20 ng of total RNA were added to the qPCR reaction in a final volume of 10 µL containing 1x PCR buffer (without MgCl2), 3 mM MgCl2, 0.25 units of Platinum Taq DNA polymerase, 0.2 mM dNTPs, 0.3 µL SYBR Green I, 0.2 µL ROX reference dye, and 0.5 µM each primer (Invitrogen). The following primer sets were used: *β-Actin* (5′-AAAGCCACCCCACTTCTCTCTAA-3' and 5′-ACCTCCCCTGTGTGGACTTG-3′), *SOCS1* (5′-CCTTCTGTAGGATGGTAGCACA-3′ and 5′-CTCTGCTGCTGTGGAGACTG-3′). All reactions were performed in triplicate. Values were normalized to *β-Actin* mRNA and expressed relative to scrambled siRNA samples (arbitrarily set to 1.0).

2.2.11 Immunofluorescence microscopy

Cells were grown on glass coverslips, transfected and fixed 48 h later for 10 min in 4% paraformaldehyde in PBS, followed by permeabilization in 0.1% Triton X-100 in PBS for 3 min. Cells were washed several times in PBS and blocked for 2 h at room temperature in block buffer (5% bovine serum albumin (BSA, w/v), 50 mM Tris-HCl (pH 7.4), 150 mM NaCl, 0.5% NP-40 (v/v)). After several washes in wash buffer (1% BSA (w/v), 50 mM Tris–HCl (pH 7.4), 150 mM NaCl, 0.5% NP-40 (v/v)), cells were incubated for 1 h at room temperature with primary antibody diluted in wash buffer. Cells were washed several times in wash buffer and incubated for 1 h at room temperature in darkness with secondary antibody diluted in wash buffer. Nuclei were stained with DAPI (Invitrogen) and cells were washed several times in wash buffer. Coverslips were mounted on slides with VectaShield mounting medium (Vector Labs, Burlingame, CA, USA). Immunostained cells were visualized with an Axioplan2 imaging microscope (Carl Zeiss, Oberkochen, Germany) and imaged with an Axiocam HRM digital camera (Carl Zeiss).

2.2.12 Immunofluorescence microscopy of endogenous DDR proteins

Cells grown on glass coverslips were initially treated for 5 min with Triton-X buffer (0.5% Triton-X, 20 mM HEPES-KOH, pH 7.9, 50 mM NaCl, 3 mM MgCl2 and 300 mM sucrose). Fixation was undertaken for 10 min with a PBS solution containing 3% paraformaldehyde, 2%

sucrose, followed by permabilization for 10 min with Triton-X buffer. Blocking was undertaken for 30 min at 37 °C in a PBS solution containing 0.5% BSA and 0.2% gelatin followed by incubation with anti-γ-H2AX (Millipore). Cells were then incubated with secondary TRITC-conjugated antibody (Jackson ImmunoResearch) in a PBS solution containing 0.5% BSA, 0.2% gelatin and 0.005% normal donkey serum. Nuclei were stained with DAPI (Invitrogen) and cells were mounted in Slowfade (Invitrogen). Images were captured using a 63 × 1.4 numerical aperture objective mounted onto a Zeiss Axioplan 2 microscope equipped with a Hamamatsu Orca ER camera (Hamamatsu Photonics, Hamamatsu, Japan). 12 bit gray scale images were captured using Openlab software version 5.5.1 (Perkin Elmer, Waltham, MA, USA) before being merged into 8 bit color images using Adobe Photoshop. The sum cellular intensities of γ-H2AX per μm2 (nuclear area determined by DAPI staining) were calculated using Velocity software version 5.5 (Perkin Elmer). Fifty cells per sample were quantified and experiments were performed in triplicate.

2.2.13 Neutral comet assay

Cells were collected at indicated time points after 15 Gy γ-IR and processed on ice. Cells were mixed with 0.1% low-melting point agarose, pipetted onto pre-coated microscope slides, and allowed to solidify at 4 °C. Slides were placed in cold lysis solution (Trevigen, Gaithersburg, MD, USA) for 1 h at 4 °C and electrophoresed in cold 0.5 × tris-borate-EDTA (TBE) buffer (pH 8.5) at 32 V for 25 min. Slides were fixed in cold methanol, dried overnight and stained with SYBR green I. 12 bit gray scale images were captured using Openlab software version 5.5.1 (Perkin Elmer) and a Zeiss Axioplan 2 microscope fitted with a × 20 objective and a Hamamatsu Orca ER camera. Comets were analyzed with Komet software version 6.0 (Andor Technology, South Windsor, CT, USA) to determine olive tail moments of individual nuclei. A total of 100 nuclei per sample were analyzed. Experiments were performed in triplicate.

2.2.14 HR Assay

A U2OS subclone stably reconstituted with the DR-GFP homologous recombination reporter has been previously described[242]. For quantification of homologous recombination, U2OS DR-GFP cells were transfected with the indicated siRNA. 24h later, the cells were transfected with an I-SceI expressing plasmid (pCBASce) to induce DSBs and incubated for an additional 48h before analysis. The cells were harvested by trypsinization, washed once with PBS, resuspended in

PBS and filtered through a cell strainer. The percentage of GFP-positive cells was determined by flow cytometry on a BD FACScalibur flow cytometer and analyzed using FlowJo (Tree Star, Ashland, OR, USA).

2.2.15 NHEJ Assay

NHEJ efficiency was assessed by examining the re-circularization of a luciferase construct. The luciferase plasmid pGL3 was linearized with BamHI or PaeI and PCR purified using a QIAquick PCR purification kit according to the manufacturer's instructions (Qiagen). U2OS cells were transfected with siVHL, siLIG4, or non-targeting siScr as described in section 2.2.6. Twenty-four hours later, cells were transfected with the linearized pGL3 DNA as described in section 2.2.5. Cells were harvested 48hrs after transfection and assayed for luciferase activity using a Promega luciferase assay kit according to the manufacturer's instructions (Promega). 20µL of cleared lysate was added to an opaque 96-well plate and analyzed with a Mithras LB 940 plate reader (Berthold Technologies, Bad Wildbad, Germany). BamHI cleaves the pGL3 construct upstream of the promoter and even unrepaired DNA should express luciferase. This represents the maximal luciferase activity. PaeI cleaves the DNA within the luciferase gene and only cells which precisely repair the break by NHEJ will express luciferase (See Appendix, **Fig. A.5**). % NHEJ repair was then calculated as follows:

% NHEJ repair = (luciferase activity of PaeI-digested pGL3) / (luciferase activity of BamHI-digested pGL3) × 100.

2.3 Results

2.3.1 SOCS1 binds VHL in the nucleus

Expression of FLAG-SOCS1 in the osteosarcoma cell line U2OS showed diffuse nuclear staining and HA-VHL alone was primarily cytoplasmic (**Fig. 2.1A**), which is consistent with the reported cellular localization of these proteins[169, 243]. However, co-expression of FLAG-SOCS1 and HA-VHL showed redistribution to distinct nuclear foci (**Fig. 2.1A**). It is important to note that the HA-VHL construct used in this study was the full-length 30kDa VHL isoform. Consistent with the immunofluorescence microscopy data, cellular fractionation in HEK293A cells confirmed that co-expression of FLAG-SOCS1 redistributes HA-VHL from the cytoplasm to the nucleus, suggesting that they may cooperate for a nuclear function (**Fig. 2.1B**). In addition, FLAG-SOCS1 co-precipitated with HA-VHL in the nuclear fraction (**Fig. 2.1C**). Notably, VHL showed a striking slower-migrating pattern on a reducing SDS-PAGE when co-expressed with SOCS1, suggesting a novel covalent modification of VHL in nuclear-association with SOCS1 (**Fig. 2.1C**).

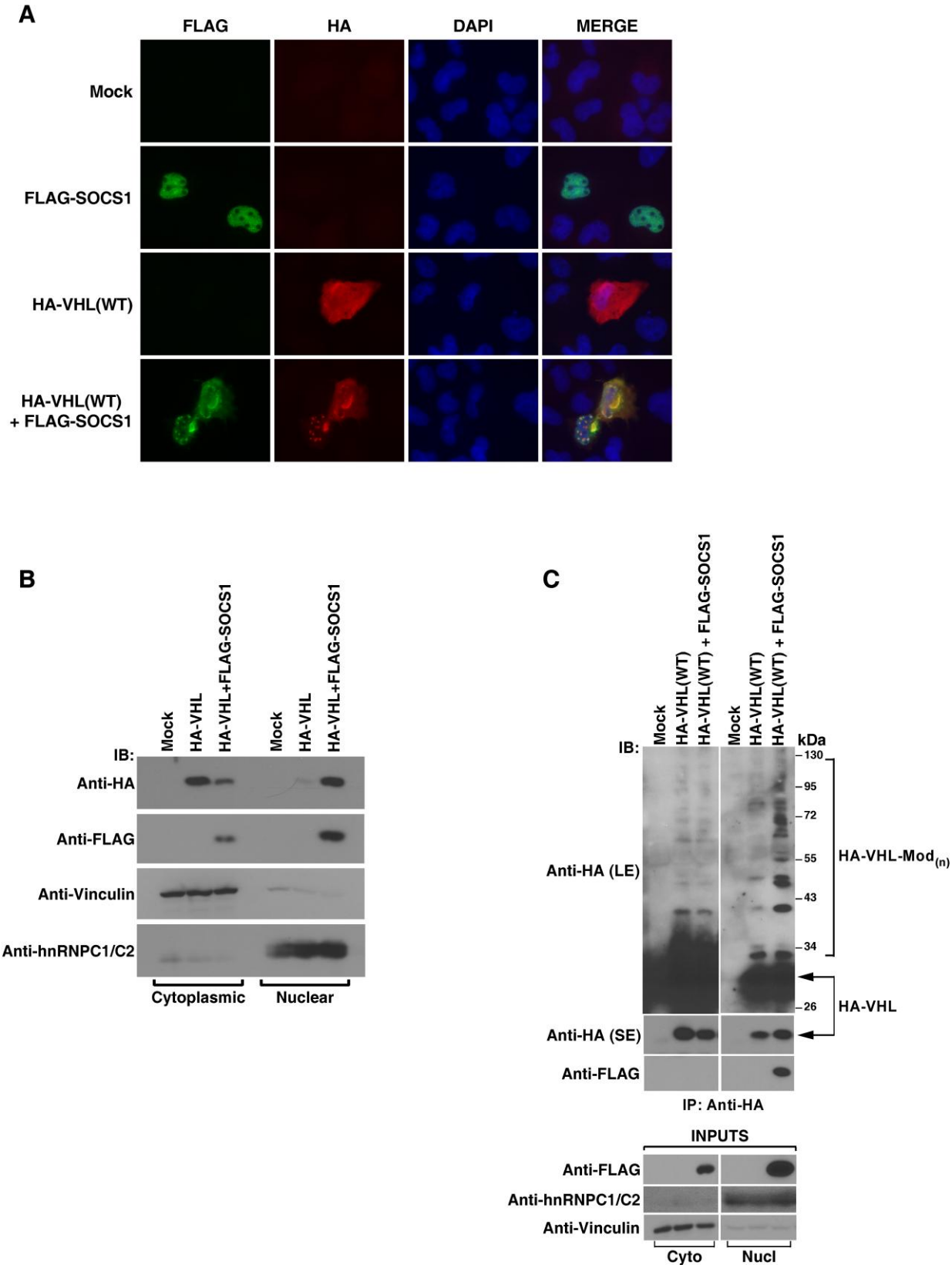
A
FLAG
HA
DAPI
MERGE
Mock
FLAG-SOCS1
HA-VHL(WT)
HA-VHL(WT)
+ FLAG-SOCS1
B
Mock
HA-VHL
HA-VHL+FLAG-SOCS1
Mock
HA-VHL
HA-VHL+FLAG-SOCS1
IB:
Anti-HA
Anti-FLAG
Anti-Vinculin
Anti-hnRNPC1/C2
Cytoplasmic
Nuclear
C
Mock
HA-VHL(WT)
HA-VHL(WT) + FLAG-SOCS1
Mock
HA-VHL(WT)
HA-VHL(WT) + FLAG-SOCS1
IB:
kDa
130
95
72
55
43
34
26
Anti-HA (LE)
HA-VHL-Mod(n)
HA-VHL
Anti-HA (SE)
Anti-FLAG
IP: Anti-HA
INPUTS
Anti-FLAG
Anti-hnRNPC1/C2
Anti-Vinculin
Cyto
Nucl

Figure 2.1. SOCS1 binds VHL in the nucleus. (**A**) U2OS cells were transfected with the indicated plasmids and immunostained with polyclonal anti-HA (red) and monoclonal anti-FLAG (green) antibodies. Blue, DAPI (4,6-diamidino-2-phenylindole) staining. (**B**) HEK293A cells transfected with the indicated plasmids were fractionated into cytoplasmic (cyto) and nuclear (nucl) pools and immunoblotted with the indicated antibodies or (**C**) fractionated, immunoprecipitated (IP) with monoclonal mouse anti-HA, and immunoblotted (IB) with monoclonal rabbit anti-HA and polyclonal rabbit anti-FLAG (top). Unmodified, IP HA-VHL is shown in the lower anti-HA panel with a short exposure (SE) and higher-molecular-weight-modified VHL (HA-VHL-$Mod_{(n)}$) is shown in the upper anti-HA panel with a long exposure (LE). Equal amounts of cytoplasmic or nuclear fractions (Inputs) were also IB with the indicated antibodies (bottom).

2.3.2 SOCS1 promotes modification of VHL on lysine residues

VHL(L118R) and VHL(F119S) mutants, which have reduced binding to SOCS1 relative to wild-type VHL (**Fig. 2.2A** and [228]), exhibited reduced modification in the presence of SOCS1 (**Fig. 2.2A**). These results suggest that SOCS1 directly promotes the undefined modification of VHL. The modification profile of VHL was, however, reminiscent of a polyubiquitin or poly-ubiquitin-like (UBL) pattern. Ubiquitylation and other UBL conjugations such as SUMOylation, NEDDylation, and ISGylation occur on lysine residues. VHL contains three lysine residues (K159, K171, and K196) and substitution of all three lysines to arginines abolished the modification (**Fig. 2.2B**). Further amino acid substitution analysis revealed that while all lysine residues are capable acceptor sites, K196 is the major acceptor site of this modification (**Fig. 2.2C**). Importantly, all lysine to arginine mutants, including VHL(RRR), retained the ability to bind SOCS1 (**Fig. 2.2C**). These results suggest that the defect in modification was due to the absence of the lysine acceptor sites and not a failure in binding SOCS1.

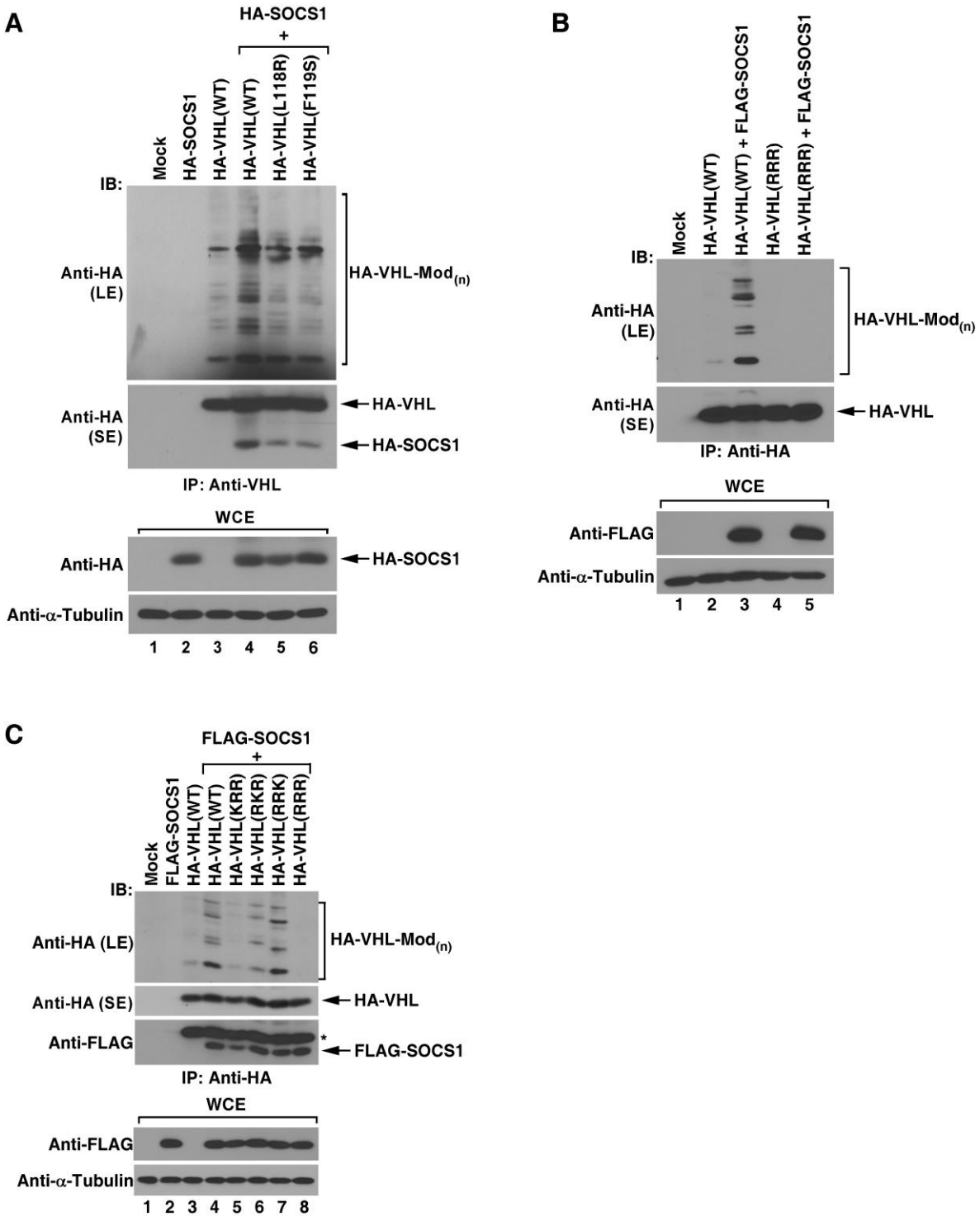

Figure 2.2. SOCS1 promotes covalent modification of VHL on lysine residues. (**A-C**) Lysates from HEK293A cells transfected with the indicated plasmids were immunoprecipitated (IP) with the mouse antibodies indicated and immunoblotted (IB) with the indicated rabbit antibodies (top). Equal amounts of cell lysates were immunoblotted with anti-HA or anti-FLAG and anti-α-tubulin (bottom). *Nonspecific protein band. LE, long exposure; SE, short exposure; WCE, whole-cell extract.

2.3.3 SOCS1 promotes K63-ubiquitylation of VHL

VHL has been shown to be modified by ubiquitin, as well as NEDD8 and SUMO[240, 244]. SOCS1 is a substrate-conferring component of an E3 ubiquitin ligase[245]. Thus, we asked whether the observed SOCS1-mediated modification of VHL was ubiquitylation. HA-VHL immunoprecipitated from HEK293A cells expressing both HA-VHL and FLAG-SOCS1 showed robust ubiquitylation in comparison to cells only expressing HA-VHL (**Fig. 2.3A**). Interestingly, the whole cell extracts revealed no discernable changes in total VHL protein level irrespective of SOCS1 co-expression in the absence of proteasomal inhibitors (**Fig. 2.3A**). These results suggest that SOCS1, while promoting VHL ubiquitylation, did not appreciably promote VHL degradation.

The ubiquitin moiety contains seven lysine residues that can act as acceptor sites for polyubiquitylation[246]. The lysine residue used for the attachment of ubiquitin chains determines the functional outcome. For example, ubiquitin K48-linked chains typically target proteins for degradation, while K63-linked chains often act as regulatory signals for cellular pathways such as endocytosis, vesicular trafficking, NFκB-mediated transcription, and DNA repair[93]. Since modification of VHL was not associated with alteration in total VHL protein level, we asked whether the polyubiquitylation of VHL occurred via K63-linkages. We utilized ubiquitin mutants in which all lysine residues have been substituted to arginine, except for either K48 or K63. T7-VHL was robustly ubiquitylated in the presence of either Ub(WT) or Ub(K63), but only weakly by Ub(K48) when co-transfected with FLAG-SOCS1 (**Fig. 2.3B**). The experiment was performed in the presence of proteasomal inhibitor MG132 in the event that polyubiquitylation, especially via K48 linkage, induced VHL degradation. In addition, K63-ubiquitylation of VHL was enhanced in the presence of FLAG-SOCS1 (**Fig. 2.3C**). These results demonstrate that SOCS1 mediates K63-ubiquitylation of VHL.

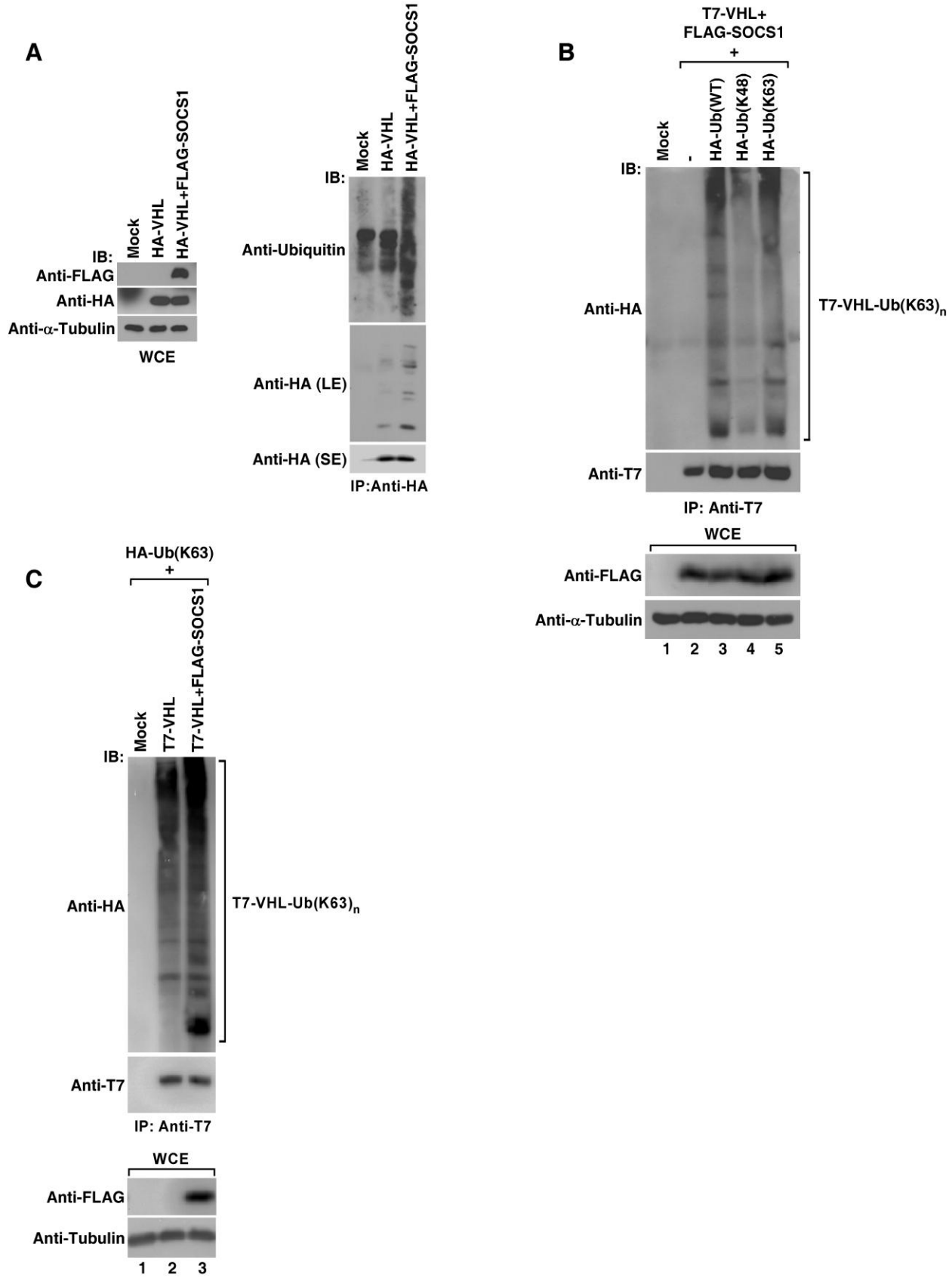
A
Mock
HA-VHL
HA-VHL+FLAG-SOCS1
IB:
Anti-FLAG
Anti-HA
Anti-α-Tubulin
WCE
Anti-Ubiquitin
Anti-HA (LE)
Anti-HA (SE)
IP:Anti-HA
B
T7-VHL+
FLAG-SOCS1
+
Mock
-
HA-Ub(WT)
HA-Ub(K48)
HA-Ub(K63)
IB:
Anti-HA
T7-VHL-Ub(K63)n
Anti-T7
IP: Anti-T7
WCE
Anti-FLAG
Anti-α-Tubulin
1 2 3 4 5
C
HA-Ub(K63)
+
Mock
T7-VHL
T7-VHL+FLAG-SOCS1
IB:
Anti-HA
T7-VHL-Ub(K63)n
Anti-T7
IP: Anti-T7
WCE
Anti-FLAG
Anti-Tubulin
1 2 3

Figure 2.3. SOCS1 induces K63-ubiquitylation of VHL. (**A**) HEK293A cells transfected with the indicated plasmids were lysed in the absence of MG132 and immunoblotted (IB) with the indicated antibodies (left) or immunoprecipitated (IP) with mouse monoclonal anti-HA and IB with rabbit monoclonal anti-HA (top panel) or anti-ubiquitin (bottom panel). *Nonspecific protein band. (**B**) HEK293A cells transfected with the indicated plasmids were treated with 5 μg/ml MG132 for 4 h before lysis. Cell lysates were IP with anti-T7 and IB with the indicated antibodies (top). Equal amounts of cell lysates were also IB with the indicated antibodies (bottom). (**C**) Lysates from HEK293A cells transfected with the indicated plasmids were IP with anti-T7 and IB with the indicated antibodies (top). Equal amounts of cell lysates were also IB with anti-FLAG and anti-α-tubulin (bottom). LE, long exposure; SE, short exposure; WCE, whole-cell extract.

2.3.4 K63-ubiquitylation of VHL is induced by DSBs

Given that SOCS1 has been reported to localize to DNA-damage foci and K63-ubiquitylation of repair proteins is a common mechanism of recruitment to sites of DNA damage, we asked whether K63-ubiquitylation of VHL was induced by DNA damage. Treatment of HEK293A cells with the topoisomerase II inhibitor, doxorubicin, induced the modification of VHL remarkably similar to co-expression with SOCS1 in the absence of doxorubicin (**Fig. 2.4A**). Although VHL can be modified by SOCS1 over-expression alone, the presence of doxorubicin-induced DNA damage led to markedly increased levels of modified VHL, suggesting that SOCS1 mediates modification of VHL in response to DNA damage (**Fig. 2.4A**). As expected, doxorubicin treatment was associated with increased levels of γH2AX, which is consistent with the induction of DSBs. We next asked whether SOCS1 influenced doxorubicin-induced modification of VHL in human CCRCC cell line. Knockdown of endogenous SOCS1 using lentivirus-shSOCS1 in 786-O CCRCC cells stably reconstituted with wild-type HA-VHL (786-VHL(WT)) attenuated DSB-induced VHL modification in comparison to a non-targeting scrambled shRNA (**Fig. 2.4B**). The knockdown efficiency was determined by RT-PCR (**Fig. 2.4B**, bottom) due to the suboptimal quality of commercially available SOCS1 antibodies in detecting endogenous SOCS1 (**Appendix, Fig. A.1**). For this reason, it remains to be determined whether SOCS1 and VHL interact in the absence of overexpression. Furthermore, siRNA-mediated knockdown of the K63 E2 ubiquitin-conjugating enzyme, Ubc13, resulted in decreased modification of ectopic VHL (**Fig. 2.4C**). These results demonstrate that SOCS1 mediates K63-ubiquitylation of VHL in response to DSBs.

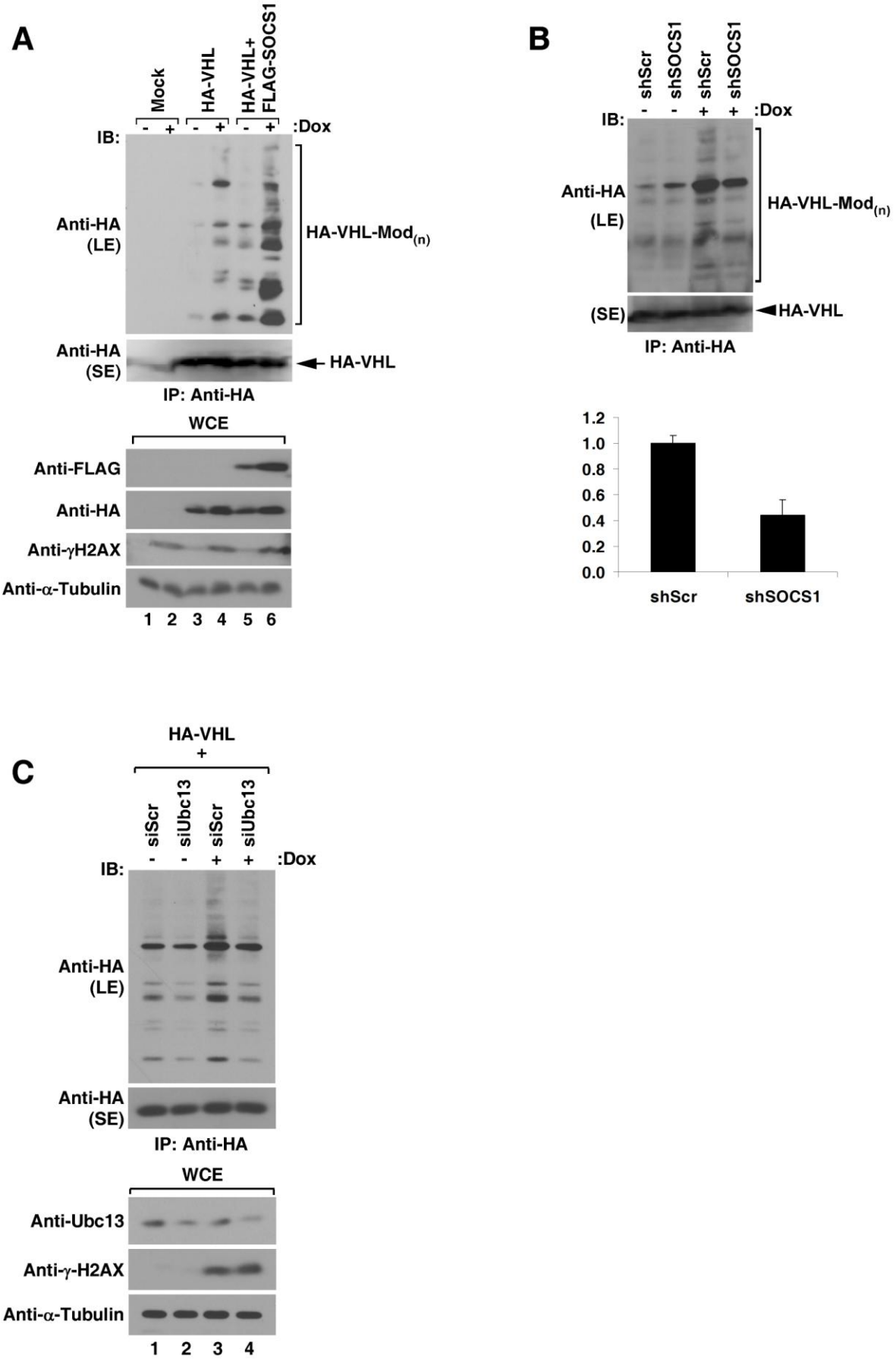
A
Mock
HA-VHL
HA-VHL+ FLAG-SOCS1
- + - + - +
:Dox
IB:
Anti-HA (LE)
HA-VHL-Mod(n)
Anti-HA (SE)
HA-VHL
IP: Anti-HA
WCE
Anti-FLAG
Anti-HA
Anti-γH2AX
Anti-α-Tubulin
1 2 3 4 5 6
B
- shScr
- shSOCS1
+ shScr
+ shSOCS1
:Dox
IB:
Anti-HA (LE)
HA-VHL-Mod(n)
(SE)
HA-VHL
IP: Anti-HA
1.2
1.0
0.8
0.6
0.4
0.2
0.0
shScr
shSOCS1
C
HA-VHL +
- siScr
- siUbc13
+ siScr
+ siUbc13
:Dox
IB:
Anti-HA (LE)
Anti-HA (SE)
IP: Anti-HA
WCE
Anti-Ubc13
Anti-γ-H2AX
Anti-α-Tubulin
1 2 3 4

Figure 2.4. SOCS1 mediates K63-ubiquitylation of VHL in response to DSBs. (A) HEK293A cells were transfected with the indicated plasmids. 24 hrs post-transfection, cells were treated with (+) or without (-) 300ng/mL doxorubicin for 16 hrs. Lysates were immunoprecipitated (IP) with mouse monoclonal anti-HA, and immunoblotted (IB) with rabbit monoclonal anti-HA (top). Equal amounts of whole cell extracts (WCEs) were also IB with the indicated antibodies (bottom). **(B)** 786-VHL(WT)-shScr and –shSOCS1 cells were treated with (+) or without (-) 300ng/mL doxorubicin for 16 hrs. Lysates were IP with mouse monoclonal anti-HA and IB with rabbit monoclonal anti-HA. Equal amounts of whole cell extracts were IB with anti-tubulin (top). RNA was also extracted and mRNA levels of SOCS1 were determined by quantitative real-time PCR and normalized to *β-Actin*. The relative level of SOCS1 transcript levels in 786-VHL-shScr cells was set to 1.0 (bottom). **(C)** HEK293A cells were transfected with siScr or siUbc13. 24 hrs later cells were transfected with HA-VHL. 48hrs later cells were treated with (+) or without (-) 300ng/mL doxorubicin for 16hrs. Lysates were IP with mouse monoclonal anti-HA and IB with rabbit monoclonal anti-HA (top). Equal amounts of whole cell extracts were IB with anti-Ubc13, anti-γH2AX, and anti-α-tubulin (bottom).

2.3.5 VHL is required for activation of the DDR

K63-ubiquitylation of proteins is a key signalling mechanism that promotes the accumulation and spreading of repair factors along the damaged chromatin[93]. Thus, K63-ubiquitylation of VHL in response to DSBs suggests that VHL may have a role in the DDR. Additional support for this idea is provided by the observation that overexpression of VHL results in increased basal levels of γH2AX in untreated cells in comparison to mock-transfected cells **(Fig. 2.4A).** To further investigate the role of VHL in the cellular response to DNA damage, we investigated the activation of DNA damage signalling proteins in VHL-null CCRCC cell lines, 786-O and RCC10, reconstituted with empty plasmid (Mock) or wild-type HA-VHL. The phosphorylation of H2AX and Chk1 was noticeably attenuated in VHL-null cells in comparison to VHL-reconstituted cells upon treatment with doxorubicin (**Fig. 2.5A**). In addition, siRNA-mediated knockdown of endogenous VHL in the kidney cell lines, HEK293A and ACHN, as well as primary renal proximal tubule epithelial cells (RPTECs), which are thought to be the cells of origin for CCRCC[148-150], under physiological oxygen tension (3% O_2) attenuated pChk1 and γH2AX in response to doxorubicin-induced DNA damage (**Fig. 2.5B**). Similar results were obtained in HEK293A and ACHN cells under 21% oxygen suggesting that the observed effects are oxygen-independent (**Appendix, Fig. A.2**). Notably, all other experiments were likewise performed at 21% O_2. These results demonstrate that VHL is required for the optimal activation of key DDR proteins.

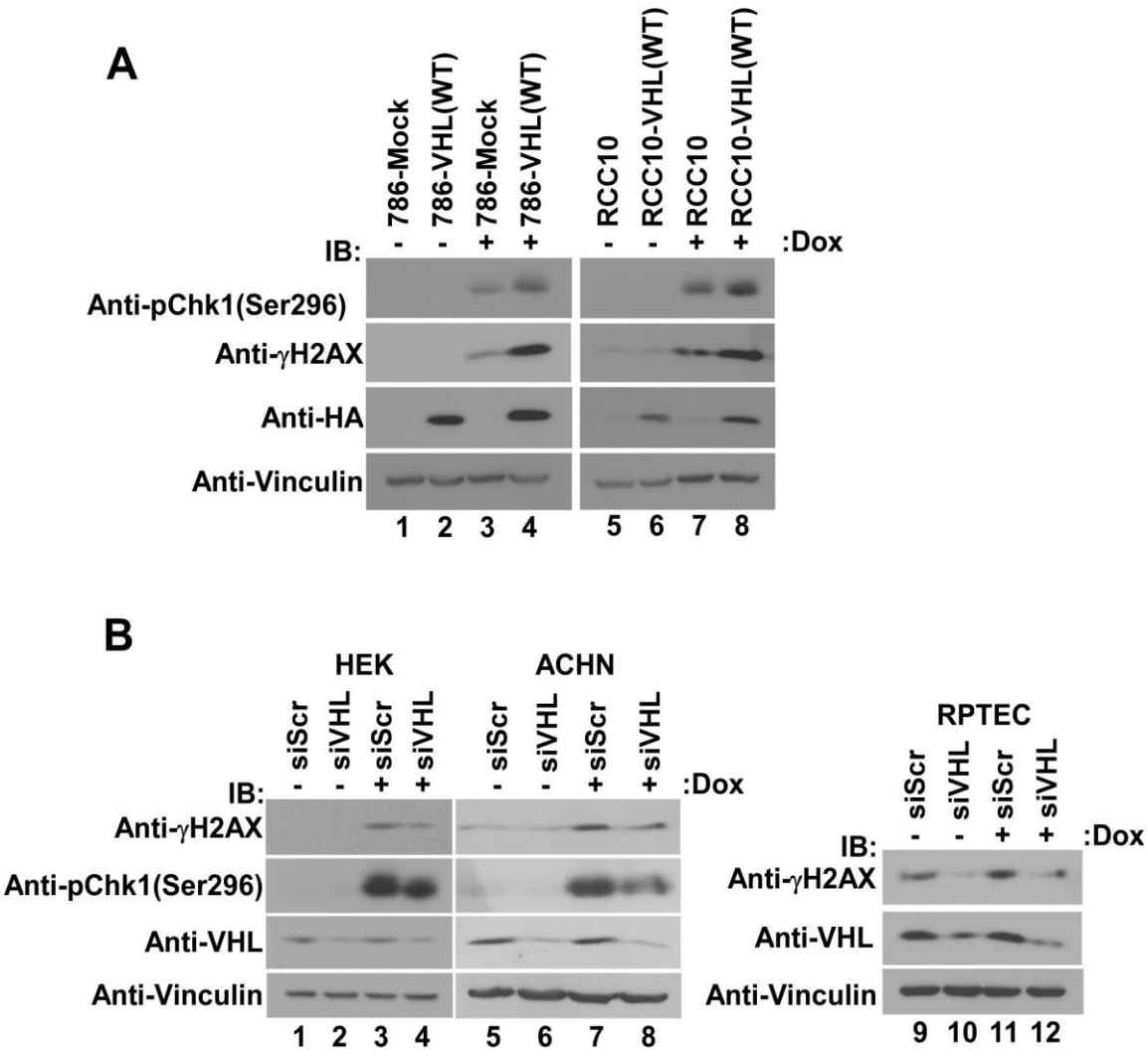

Figure 2.5. Loss of VHL attenuates the DDR. (A) Indicated cell lines were treated with (+) or without (-) 300ng/mL doxorubicin for 16 hrs. Equal amounts of whole cell extracts were immunoblotted with the indicated antibodies. **(B)** HEK293A, ACHN, or renal proximal tubule epithelial cells (RPTEC) were transfected with siScr or siVHL and incubated at 3% O_2. 48 hrs post-transfection, cells were treated with (+) or without (-) 300ng/mL doxorubicin for 16 hrs. Equal amounts of whole cell lysates were immunoblotted with the indicated antibodies.

2.3.6 SOCS1-mediated K63-ubiquitylation of VHL is required for activation of the DDR

We next asked whether SOCS1-mediated ubiquitylation of VHL is necessary for the DDR. siRNA-mediated knockdown of endogenous SOCS1 in HEK293 cells attenuated the activation of Chk1 and H2AX (**Fig. 2.6A**). Consistent with a role of SOCS1-mediated VHL ubiquitylation in the DDR, 786-O cells stably expressing empty plasmid (Mock) or VHL(RRR) mutant, which is unable to be ubiquitylated (see **Fig. 2.2B**), or VHL(L118R and F119S), which have reduced SOCS1 binding and K63-ubiquitylation (see **Fig. 2.2A**), showed attenuated phosphorylation of Chk1 and H2AX in comparison to cells reconstituted with wild-type VHL (**Fig. 2.6B**). In addition, radiation-induced phosphorylation of H2AX was determined 4 hours after irradiation by indirect immunofluorescence and quantified per unit area of the nucleus. 786-VHL(WT) cells displayed robust γH2AX staining, while comparatively 786-Mock, 786-VHL(RRR) and 786-VHL(F119S) cells showed 45%, 30%, and 35% reduction in γH2AX staining, respectively ($p<0.0001$) (**Fig. 2.6C**). Notably, VHL(RRR), VHL(L118R) and VHL(F119S) retain the ability to properly regulate HIFα **(Appendix Fig. A3A** and [228, 240]), and knockdown of HIF2α in 786-Mock, 786-VHL(WT) and 786-VHL(RRR) had no discernible effect on γH2AX expression levels (**Appendix Fig. A3B)**. These results suggest that the DDR defect in VHL-null and Ub(K63)-deficient VHL mutants is HIF-independent.

To further elucidate the DDR defect, we examined upstream activators of γH2AX, ATM and Mre11. VHL-null and Ub(K63)-deficient VHL mutant-expressing cells contained less phosphorylated ATM after doxorubicin-induced DNA damage in comparison to wild-type VHL-reconstituted cells (**Fig. 2.6D**). Additionally, when examined four hours after irradiation, Ionizing Radiation Induced Foci (IRIF) of Mre11 were significantly impaired in VHL-null and Ub(K63)-deficient VHL mutants compared to wild-type VHL cells, suggesting that there is a defect in the activation of the MRN-dependent DDR and recruitment or retention of repair proteins to the DNA lesion (**Fig. 2.6E**).

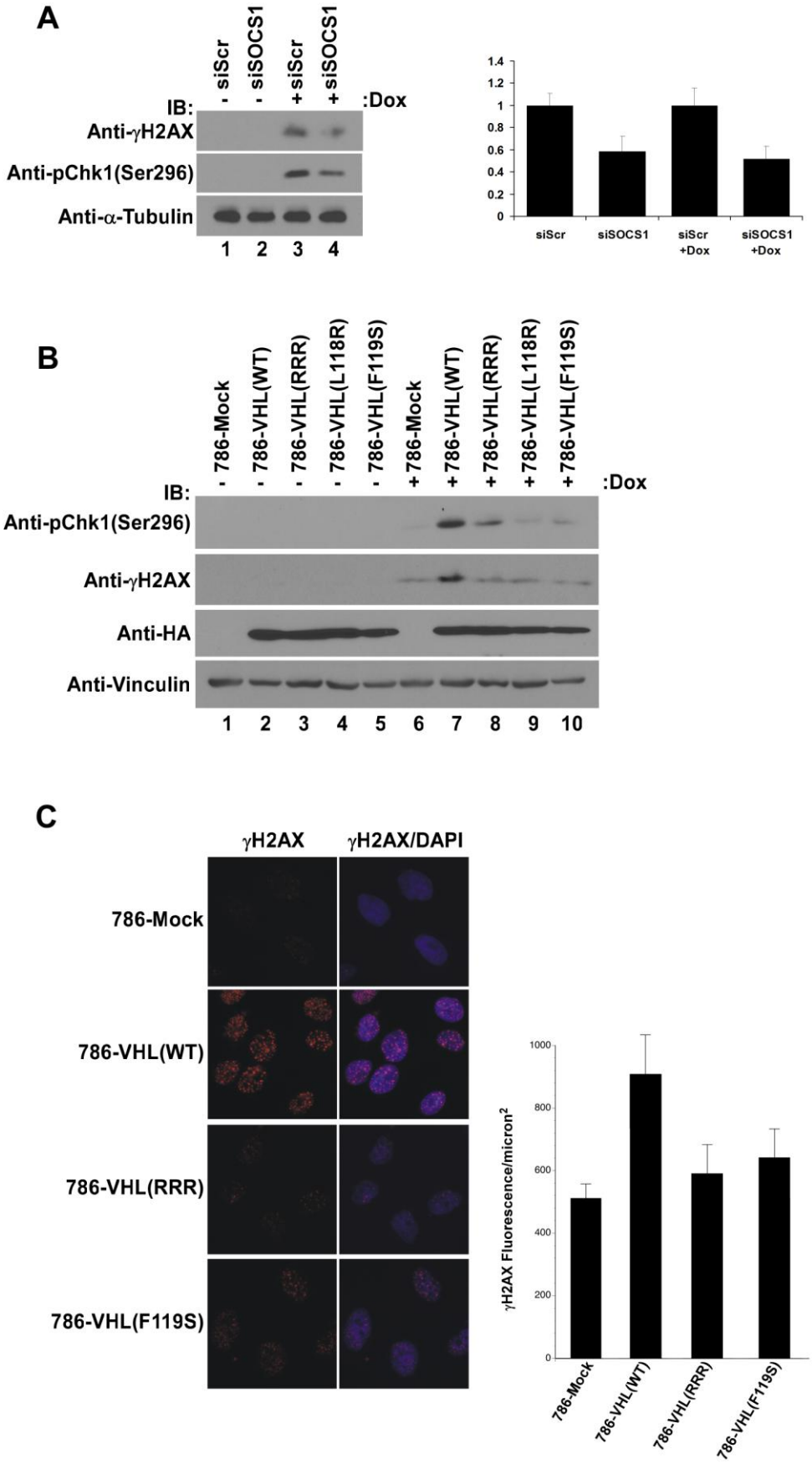
A
- siScr
- siSOCS1
+ siScr
+ siSOCS1
IB:
:Dox
Anti-γH2AX
Anti-pChk1(Ser296)
Anti-α-Tubulin
1 2 3 4
1.4
1.2
1
0.8
0.6
0.4
0.2
0
siScr
siSOCS1
siScr +Dox
siSOCS1 +Dox
B
- 786-Mock
- 786-VHL(WT)
- 786-VHL(RRR)
- 786-VHL(L118R)
- 786-VHL(F119S)
+ 786-Mock
+ 786-VHL(WT)
+ 786-VHL(RRR)
+ 786-VHL(L118R)
+ 786-VHL(F119S)
IB:
:Dox
Anti-pChk1(Ser296)
Anti-γH2AX
Anti-HA
Anti-Vinculin
1 2 3 4 5 6 7 8 9 10
C
γH2AX
γH2AX/DAPI
786-Mock
786-VHL(WT)
786-VHL(RRR)
786-VHL(F119S)
γH2AX Fluorescence/micron²
1000
800
600
400
200
0
786-Mock
786-VHL(WT)
786-VHL(RRR)
786-VHL(F119S)

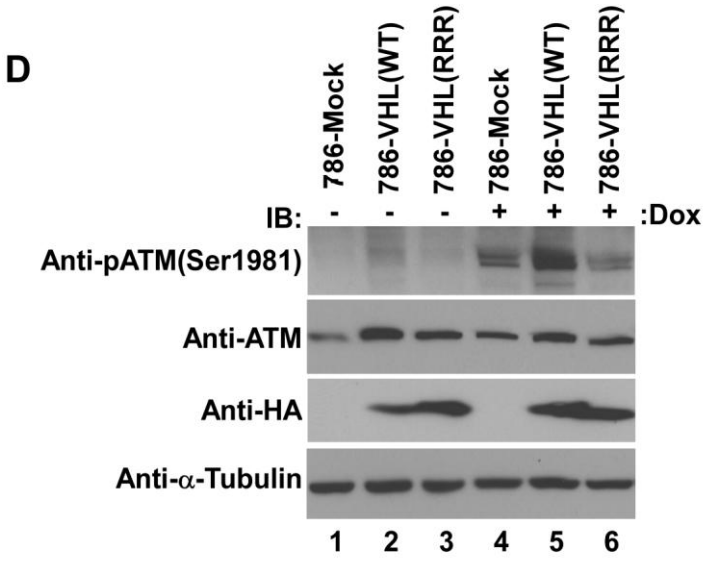
D
786-Mock
786-VHL(WT)
786-VHL(RRR)
786-Mock
786-VHL(WT)
786-VHL(RRR)
IB:
- - - + + + :Dox
Anti-pATM(Ser1981)
Anti-ATM
Anti-HA
Anti-α-Tubulin
1 2 3 4 5 6

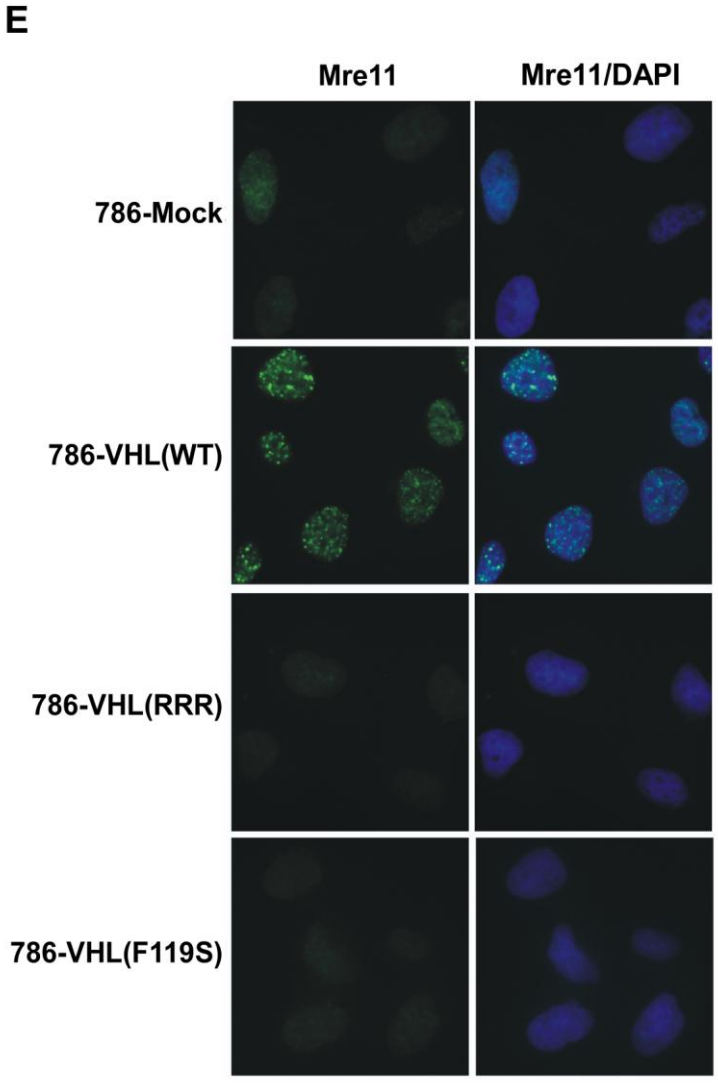
E
Mre11
Mre11/DAPI
786-Mock
786-VHL(WT)
786-VHL(RRR)
786-VHL(F119S)

Figure 2.6. Loss of SOCS1 or K63-ubiquitylation of VHL attenuates the DDR. (A) siScr or siSOCS1 was transfected into HEK293A cells and 48 hrs post-transfection cells were treated with (+) or without (-) 300ng/mL doxorubicin for 16 hrs. Cell lysates were immunoblotted with the indicated antibodies. RNA was also extracted and mRNA levels of SOCS1 were determined by quantitative real-time PCR and normalized to *β-Actin*. **(B)** Indicated cell lines were treated as in (a) and immunoblotted with the indicated antibodies. **(C)** Indicated cell lines were irradiated with 10Gy of γ-radiation and incubated at 37°C for 4 hr prior to detection of γ-H2AX by indirect immunofluorescence (red) (left). 50 cells per sample were quantified for the level of γ-H2AX per unit area of the nucleus (as determined by DAPI staining) (N=3 ± SD) (right). **(D)** Indicated cell lines were treated with (+) or without (-) 300ng/mL doxorubicin for 16hrs and lysed. Equal amounts of whole cells extracts were immunoblotted with anti-pATM(Ser1981) and anti-ATM. **(E)** Indicated cell lines were irradiated with 10Gy γ-radiation and incubated at 37°C for 4 hr. Cells were immunostained with anti-Mre11 (green). Nuclei were stained with DAPI (blue).

2.3.7 Loss of VHL inhibits repair of DSBs by HR

We next asked whether the loss of VHL or K63-ubiquitylation of VHL compromised the repair of damaged DNA. A neutral comet assay in which single cells are electrophoresed to separate damaged from intact DNA was performed to measure the extent of DSBs persisting after 15Gy γ-radiation. 786-VHL(WT) cells had fewer unrepaired DSBs 6 hours post-irradiation than 786-Mock, -VHL(RRR), -VHL(F119S), and VHL(L118R) cells, as indicated by the shorter comet tails in 786-VHL(WT) cells (**Fig. 2.7A** and **Appendix, Fig. A.4**). The relative extent of unrepaired DSBs was quantified by calculating the average tail moment, which is a measure of the amount of DNA present in the comet tail. At 0.5 and 1 hour post-irradiation the tail moments were similar for all five cell lines, indicating that initial DSB rejoining is largely independent of VHL. However, at 3 and 6 hours post-irradiation, the extent of DSB rejoining in the 786-VHL(WT) cells was significantly greater than that of the 786-Mock, -VHL(RRR), -VHL(F119S), and VHL(L118R) cells (**Fig. 2.7A** and **Appendix, Fig. A.4**). These results suggest that VHL specifically contributes to a late phase of DSB repair and that SOCS1-mediated K63-ubiquitylation of VHL is necessary to orchestrate this process.

K63-ubiquitylation has been reported to play a key role in orchestrating DNA repair by HR[22, 247]. Furthermore, the late 3 and 6 hour DNA repair defect revealed by the neutral comet assay is consistent with a defect in HR, based on the previously reported kinetics of HR factors[248]. To determine whether VHL is involved in the repair of DSBs by HR, we utilized a direct repeat-green fluorescent protein (DR-GFP) reporter assay[242]. This reporter consists of a two non-

functional GFP genes oriented as tandem repeats: one full-length GFP gene mutated to contain a rare-cutting I-SceI restriction site and a truncated wild-type GFP gene that acts as a donor for HR. Thus, repair of the I-SceI-generated DSB by HR restores the expression of the GFP gene. U2OS DR-GFP cells were treated with siRNA directed against *VHL*, *RAD51*, or non-targeting siRNA (**Fig. 2.7B**). Cells were transfected 24 hours later with an I-SceI expression plasmid (pcBASce) to induce DSBs, and HR was quantitated by measuring the percentage of GFP-positive cells by flow cytometry. Knockdown of endogenous *RAD51*, which is an essential HR protein, attenuated the repair of DSBs by 3 to 4-fold (**Fig. 2.7B**). Notably, knockdown of endogenous *VHL* resulted in a 2-fold reduction in HR (**Fig. 2.7B**). In contrast, knockdown of VHL had no observable effect on NHEJ (**Appendix, Fig. A5**). These results demonstrate that VHL plays a critical role in the repair of DSBs by HR.

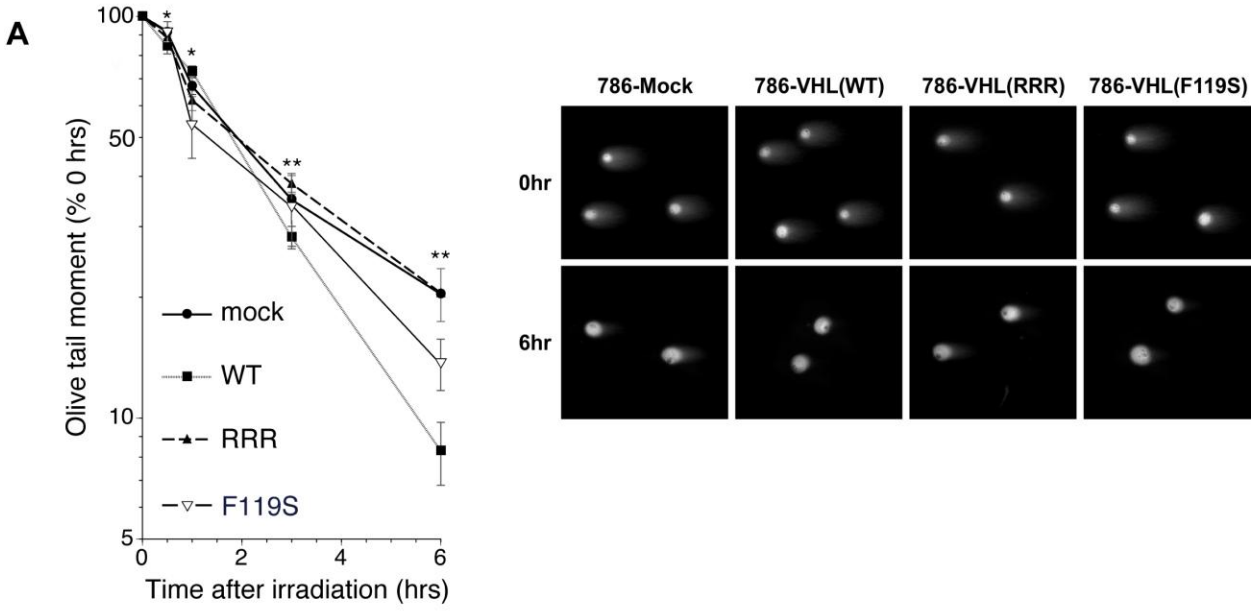
A
Olive tail moment (% 0 hrs)
Time after irradiation (hrs)
mock
WT
RRR
F119S
786-Mock
786-VHL(WT)
786-VHL(RRR)
786-VHL(F119S)
0hr
6hr

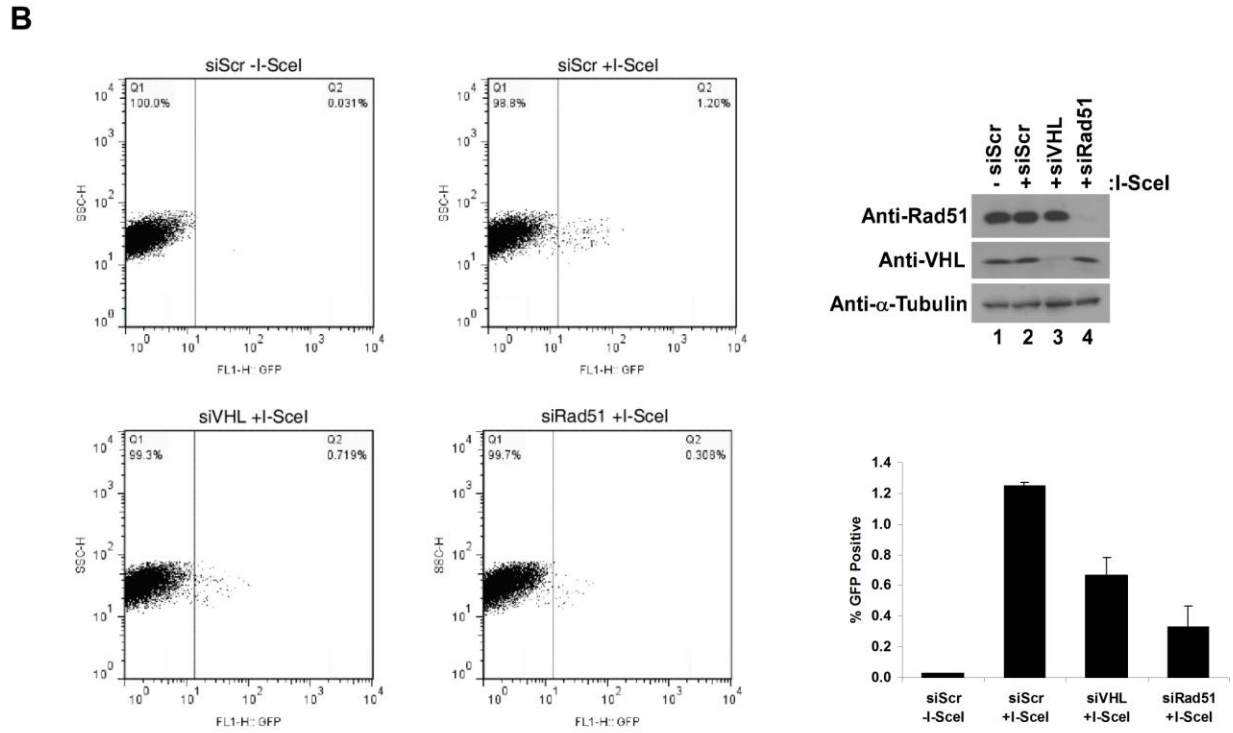
B
siScr -I-SceI
siScr +I-SceI
siVHL +I-SceI
siRad51 +I-SceI
SSC-H
FL1-H:: GFP
- siScr
+siScr
+siVHL
+siRad51
:I-SceI
Anti-Rad51
Anti-VHL
Anti-α-Tubulin
1 2 3 4
% GFP Positive
siScr -I-SceI
siScr +I-SceI
siVHL +I-SceI
siRad51 +I-SceI

Figure 2.7. Loss of VHL inhibits repair of DSBs by HR. (A) The indicated cell lines were exposed to 15 Gy γ-irradiation and a neutral comet assay was performed. 100 cells per sample were analyzed and average tail moment was calculated using Komet software v6.0 (Andor Technology). The relative extent of unrepaired DSBs was quantified by calculating the average olive tail moment as a percentage of the initial olive tail moment at time 0 hr (N=3 ±SE). Tail moments for WT cells were compared to tail moments for Mock, RRR, and F119S cells using unpaired t-tests, with $p>0.06$ indicated by *, and $p<0.03$ indicated by **. Representative images for 0 hr and 6 hrs are shown (right). **(B)** U2OS DR-GFP cells were transfected with siScr, siVHL, or siRad51. 24 hrs later cells were transfected without (-) or with (+) I-SceI to induce DSBs. 48 hrs later cells were analyzed by flow cytometry to determine the percentage of GFP-positive cells. Experiment was performed in triplicate. A representative experiment is shown in scatter plots, displaying GFP-positive cells to the right of vertical line (left) and Western blotting was performed to confirm knockdown (right, top). The bar graph shows the mean % of GFP-positive cells (N=3 ± SD) (right, bottom).

2.4 Discussion

VHL shuttles between the nucleus and cytoplasm in response to cell density or transcriptional arrest[169, 170]. Notably, the nuclear localization of VHL and its dynamic nuclear-cytoplasmic shuttling capabilities have been shown to be essential for its tumour suppressor activity[170, 173]. The present work reveals a novel nuclear function for VHL in the repair of DSBs by HR, identifying VHL as a caretaker for genome stability and extending our current understanding of its diverse tumour suppressor activities.

We show here that SOCS1 promotes nuclear redistribution and K63-ubiquitylation of VHL in response to DNA damage. Thus, SOCS1 is involved in K63-linked as well as K48-linked ubiquitylation. This is, however, not unique to SOCS1 as several E3 ligases that can catalyze both K63-linked and K48-linked ubiquitylation have been identified, including RNF8, Itch, and BRCA1[249, 250]. These E3 ligases bind to multiple E2 ubiquitin-conjugating enzymes to direct the formation of different types of ubiquitin chains. Currently, the only E2 capable of mediating K63-ubiquitylation is the Ubc13-Uev1 complex[251]. Endogenous knockdown of Ubc13 attenuated VHL K63-ubiquitylation in response to DNA damage similar to SOCS1 knockdown, but whether SOCS1 acts as the E3 ligase for this modification through direct interaction with the Ubc13-Uev1 complex remains unresolved.

K63-ubiquitylation has been shown to act as a regulatory signal for the recruitment of DNA repair proteins to the DNA lesions[93]. Here, we found that the loss of VHL or an inability to ubiquitylate VHL via SOCS1 attenuates the activation or recruitment of several key DNA damage signalling proteins, including Chk1, H2AX, ATM, and Mre11. Notably, the defect in DDR was independent of HIF activity since, for example, the DDR-deficient VHL(RRR) mutant retains the ability to negatively regulate HIFα. Interestingly, SOCS1 has previously been reported to associate with ATM during STAT5-mediated oncogene-induced senescence[229]. These observations suggest that VHL, SOCS1 and ATM may collaborate at the DNA lesion to activate downstream DNA damage signalling for the recruitment of additional repair factors.

We show here that VHL facilitates HR repair of DSBs; most notably illustrated by a marked reduction in HR following knockdown of endogenous VHL in U2OS DR-GFP cells. Rapid repair of DSBs in mammalian cells primarily occurs via NHEJ, while HR factors accumulate at sites of DNA damage with delayed kinetics (>1hr post-damage)[248]. Consistent with a role of VHL in HR, the neutral comet assay indicated a late defect in DSB repair in cells devoid of VHL or expressing VHL mutants defective in K63-ubiquitylation. Furthermore, the defect in late DSB repair correlated with attenuated activation of ATM and impaired recruitment or retention of Mre11 at unrepaired DSBs at 4hrs post-irradiation, which is in agreement with the reported role of ATM and Mre11 in slow-repairing DSBs[125]. The defect in HR and persistence of DNA breaks that result from a loss of VHL or mutations that compromise K63-ubiquitylation of VHL would be predicted to generate genomic instability and an increased propensity to accumulate additional mutations that characterize and promote CCRCC.

Unlike normal cells, which initiate apoptosis under condition of excessive or irreparable DNA damage, cancer cells have defects in this intrinsic protective mechanism that allows them to accumulate DNA damage without triggering cell death. CCRCC cells devoid of functional VHL have been shown to have elevated levels of NFκB-target pro-survival proteins such as c-FLIP, survivin and c-IAP-1/2, which block the activities of caspases 8 and 3, and suppress p53-mediated pro-apoptotic activity[222, 252]. These anti-apoptotic activities were shown to be associated with a failure in the oxygen-dependent ubiquitin-mediated negative regulation of HIFα upon the loss of VHL function[222, 252]. Intriguingly, VHL was also shown to function as an adaptor protein that promotes casein kinase 2-mediated inhibitory phosphorylation of the NFκB

agonist Card9[225], which suggests that the loss of VHL, independent of HIF, can also enhance the cellular survival capacity. These observations support the notion that defects in the apoptotic pathway and DDR network act synergistically in VHL-defective cells to permit the accumulation of DNA damage and genomic instability that ultimately drive CCRCC, as well as potentially other VHL-associated malignancies.

Chapter 3

3 Differentiating the role of VHL19 versus VHL30 in the DNA damage response

3.1 Introduction

Von Hippel-Lindau (VHL) is the substrate recognition component of an E3 ubiquitin ligase complex, composed of ElonginB/C, Cul2, and Rbx1 (ECV) [161, 174-176]. The most well-characterized function of VHL is the negative regulation of the heterodimeric transcription factor, hypoxia-inducible factor (HIF) [200, 233]. Under normal oxygen tension, HIFα is hydroxylated on conserved proline residues by prolyl hydroxylase enzymes and targeted for ubiquitylated destruction through the proteasome pathway[196, 198, 200, 201]. In an adaptive response to low oxygen tension (hypoxia), HIFα escapes degradation, dimerizes with HIFβ and translocates to the nucleus where it activates the transcription of several hypoxia-inducible genes involved in cellular processes such as angiogenesis, glucose transport, erythropoiesis, and cell proliferation[196, 197, 203]. However, inactivating mutations in VHL, found in the majority of clear-cell renal cell carcinoma (CCRCC), allows HIF to escape degradation and aberrantly upregulates HIF-target genes under conditions of normal oxygen tension[155].

The *VHL* mRNA encodes two protein isoforms: a 213 amino acid protein with a molecular weight of 30-kilodaltons (VHL30) and a shorter 19-kilodalton protein (VHL19) produced from an internal translational start site at methionine 54[161]. Both VHL30 and VHL19 can regulate HIF normally and have been shown independently to suppress tumour formation in nude mouse xenograft assays[162-164]. However, several disease-associated mutations are found within the first 53aa of VHL that would presumably allow the transcription of functional VHL19, suggesting that the N-terminal domain of VHL30 may have HIF-independent tumour suppressor functions [165-167]. In support of this notion, Lolkema *et al.* have demonstrated that VHL is phosphorylated by casein kinase 2 (CK2) in the N-terminal domain, which is necessary for proper fibronectin matrix deposition and suppression of tumour formation[168]. In addition, Lai *et al*. have reported that VHL30, but not VHL19 binds ARF and recruits the arginine methyltransferase, PRMT3 to

methylate p53[253]. Although, the physiological consequences were not explored, these results provide further evidence for functional differences between VHL30 and VHL19. Since most studies do not differentiate between VHL30 and VHL19 isoforms, there is likely additional unidentified tumour suppressor functions mediated through the unique N-terminal domain of VHL30.

In addition to the hypoxic profile, CCRCC is associated with high genomic instability with frequent chromosomal translocations and deletions[153]. However, the link between loss of VHL and genomic instability has remained elusive until now. We have recently shown that SOCS1 K63-ubiquitylates VHL in response to DSBs, which is essential for the activation and/or recruitment of key proteins in the DDR such as ATM, Mre11, Chk1, and γH2AX (Chapter 2 and [254]). Furthermore, VHL was shown to contribute to the repair of DSBs by HR, identifying VHL as a critical regulator of genome stability[254].

While mapping the SOCS1 binding interface on VHL, we found that SOCS1 binds the N-terminal domain of VHL (aa1-53). Consequently, SOCS1 interacts with VHL30, but not VHL19. We demonstrated in Chapter 2 that K63-ubiquitylation of VHL30, mediated through interactions with SOCS1, promotes the repair of DSBs by HR[255]. Therefore, we hypothesized that since VHL19 is unable to interact with SOCS1, that it would be defective for activating the DDR.

3.2 Materials and Methods

3.2.1 Cells

786-O, HEK293A, and U2OS cells were obtained from the American Type Culture Collection (Rockville, MD). 786-O subclones ectopically expressing HA-VHL(30), HA-VHL(19), or empty plasmid (Mock) were previously described[228, 239, 240]. Polyclonal populations of U2OS shVHL cells were generated by the stable integration of the pGIPZ shVHL construct as described in Chapter 2, section 2.2.9). Cell lines were maintained in DMEM supplemented with 10% fetal bovine serum (Wisent, St.-Bruno, QC, Canada) at 37°C in a humidified 5% CO2 atmosphere. 786-O subclones were maintained with 0.25mg/mL G418 and U2OS shVHL with 2µg/mL puromycin in culture medium.

3.2.2 Plasmids

Triple-FLAG-tagged SOCS1 (FLAG-SOCS1) was gene synthesized (Mr. Gene, Regensburg, Germany) and subcloned into pcDNA3. HA-VHL30 (1-213), HA-VHL19 (54-213), HA-VHL (Δ114-154), HA-VHL(1-155), T7-VHL30, and T7-VHL19 were previously described[162, 168, 170, 174, 202, 256]. HA-Ub(K63) was a generous gift from Dr. Zhijian Chen (UTSW Medical Centre, Dallas, TX).

3.2.3 Chemicals

Doxorubicin was obtained from Santa Cruz Biotechnology, MG132 was obtained from Peptides International, and chloroquine (CQ) was purchased from Bioshop (Burlington, ON, Canada).

3.2.4 Antibodies

The following antibodies were used: mouse monoclonal anti-FLAG(M2) (Sigma-Aldrich, Oakville, ON, Canada), rabbit monoclonal anti-HA (Cell Signaling, Danvers, MA, USA), mouse monoclonal anti-HA(12CA5) (Roche Applied Science, Laval, QC, Canada), mouse monoclonal anti-T7 (Novagen), goat polyclonal anti-T7 (AbCam), mouse monoclonal anti-vinculin (Sigma-Aldrich), rabbit polyclonal anti-FLAG (Novus Biologicals, Oakville, ON, Canada), mouse monoclonal anti-α-tubulin (Sigma-Aldrich), rabbit polyclonal anti-γH2AX (Cell Signaling), rabbit polyclonal anti-pChk1 (Cell Signaling), mouse monoclonal anti-MDC1 (Sigma), rabbit

polyclonal anti-LC3B (Cell Signaling), and rabbit polyclonal anti-H3 (AbCam). Horseradish peroxidase goat anti-rabbit, goat anti-mouse, and rabbit anti-goat secondary antibodies were obtained from ThermoScientific. AlexaFluor 488-conjugated goat anti-mouse secondaries were obtained from Invitrogen.

3.2.5 Transfection

Performed as described in Chapter 2, Section 2.2.5.

3.2.6 Immunoprecipitation and Immunoblotting

Immunoprecipitation and immunoblotting were performed as described in Chapter 2, section 2.2.7.

3.2.7 Immunofluorescence microscopy

Immunofluorescence was performed as described in Chapter 2, section 2.2.11, with the following modification. After fixation, cells were permeabilized with 0.5% Triton-X-100 in PBS for 10min at room temperature.

3.2.8 Alkaline comet assay

Comet assay was performed using OxiSelect Comet Assay kit according to the manufacturer's instructions (Cell Biolabs, Inc, San Diego, CA). Alkalynation was followed by electrophoresis under neutral buffer conditions. DNA was stained with SYBR green and cells were visualized using an inverted Nikon Eclipse TE200 microscope. 50 cells per sample were analyzed and average tail moment was calculated using TriTek CometScore freeware. Experiments were performed in triplicate.

3.2.9 Cellular fractionation

Performed as described in Chapter 2, section 2.2.8, with the following modification. For insoluble nuclear fraction, EBC buffer with protease inhibitors was added to the insoluble nuclear pellet and sonicated 3 times for 5sec. Lysates were clarified by centrifugation at 14,000 rpm for 10min at 4°C.

3.3 Results

3.3.1 SOCS1 binds VHL30, but not VHL19

To determine the region on VHL necessary for interaction with SOCS1, we generated several HA-tagged VHL truncations and internal deletion constructs. HEK293 cells were co-transfected with FLAG-SOCS1 and full-length or truncation/deletion mutants of HA-VHL. Immunoprecipitation for HA-VHL revealed that SOCS1 binds full-length VHL(1-213) and the C-terminal deletion mutant VHL(1-155) with high affinity, with weak binding to the internal deletion mutant VHL (Δ114-154) (**Fig. 3.1A**). Strikingly, N-terminal deletion of VHL (54-213) completely abolished the interaction with SOCS1 (**Fig. 3.1A**, lane 4**)**. These results indicate that the N-terminal domain of VHL (aa1-53) is the primary binding site for SOCS1, while residues 114-154 may provide additional contacts to enhance the stability of the interaction.

Our recent data has revealed that VHL and SOCS1 interact in the nucleus for a novel role in the DDR (Chapter 2 and [255]). Therefore, we next examined the ability of SOCS1 to bind VHL30 and VHL19 in response to DSBs. In the presence of the topoisomerase II inhibitor, doxorubicin, SOCS1 binding to VHL30 (aa1-213) was significantly enhanced, but VHL19 (aa54-213) remained unable to interact (**Fig. 3.1B**). These results suggest that VHL30 cooperates with SOCS1 for a unique function in the DDR, not shared with the VHL19 isoform.

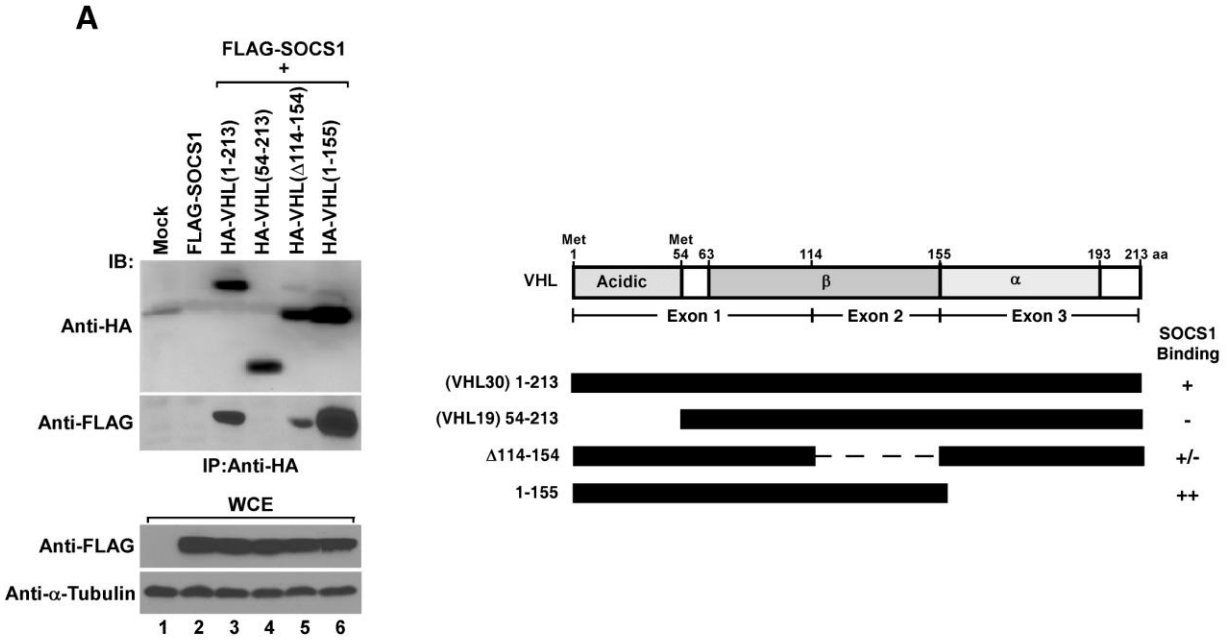
A
FLAG-SOCS1
+
Mock
FLAG-SOCS1
HA-VHL(1-213)
HA-VHL(54-213)
HA-VHL(Δ114-154)
HA-VHL(1-155)
IB:
Anti-HA
Anti-FLAG
IP:Anti-HA
WCE
Anti-FLAG
Anti-α-Tubulin
1 2 3 4 5 6
Met 1
Met 54
63
114
155
193
213 aa
VHL
Acidic
β
α
Exon 1
Exon 2
Exon 3
SOCS1 Binding
(VHL30) 1-213
+
(VHL19) 54-213
-
Δ114-154
+/-
1-155
++

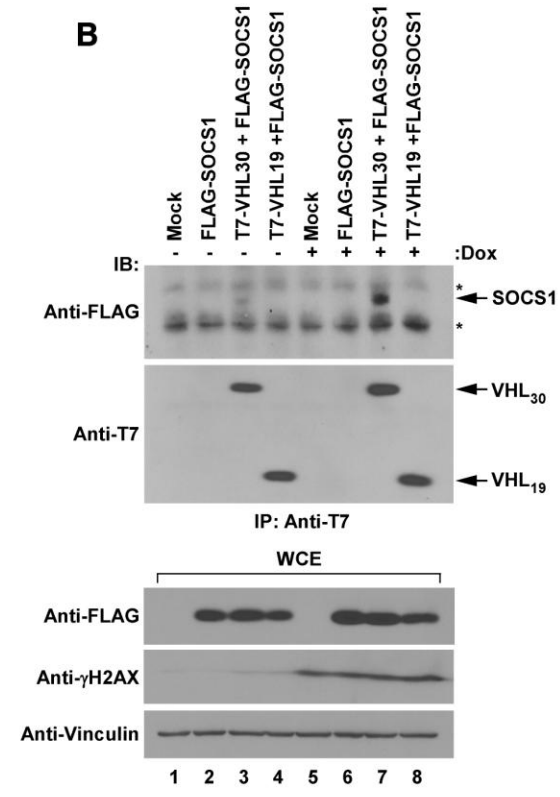
B
- Mock
- FLAG-SOCS1
- T7-VHL30 + FLAG-SOCS1
- T7-VHL19 +FLAG-SOCS1
+ Mock
+ FLAG-SOCS1
+ T7-VHL30 + FLAG-SOCS1
+ T7-VHL19 +FLAG-SOCS1
:Dox
IB:
Anti-FLAG
SOCS1
Anti-T7
VHL30
VHL19
IP: Anti-T7
WCE
Anti-FLAG
Anti-γH2AX
Anti-Vinculin
1 2 3 4 5 6 7 8

Figure 3.1. SOCS1 binds VHL30 N-terminus upon induction of DSBs. (A) HEK293A cells were transfected with the indicated plasmids. Forty-eight hours post-transfection, cells were lysed, immunoprecipitated (IP) with mouse monoclonal anti-HA, and immunoblotted (IB) with rabbit monoclonal anti-HA and rabbit polyclonal anti-FLAG antibodies. Equal amounts of whole-cell extracts (WCE) were also immunoblotted with mouse monoclonal anti-FLAG or anti-α-Tubulin. A schematic illustrating the VHL deletion constructs used and there binding to SOCS1 is shown on right. **(B)** HEK293A cells were transfected with the indicated constructs. Twenty-four hours post-transfection, cells were treated with (+) or without (-) 300ng/mL doxorubicin (Dox) for 16hrs. Cell lysates were IP with mouse monoclonal anti-T7 and IB with goat polyclonal anti-T7 and rabbit polyclonal anti-FLAG. Equal amounts of WCE were also immunoblotted with the indicated antibodies. *, indicates non-specific band.

3.3.2 K63-ubiquitylation of VHL19 is attenuated with DNA damage

We showed previously that SOCS1 mediates DNA damage-induced K63-ubiquitylation of VHL30 and binding to SOCS1 is necessary for this modification (Chapter 2, Section 2.3.2-2.3.3 and [255]). Therefore, the inability of VHL19 to interact with SOCS1 in the presence of DNA damage would be predicted to result in a defect in K63-ubiquitylation. To test this hypothesis, HEK293 cells were co-transfected with plasmids encoding T7-VHL30 or T7-VHL19 and the ubiquitin mutant, HA-Ub(K63), where all lysine have been mutated to arginine except lysine 63. Cells were treated with the DNA-damaging agent, doxorubicin and immunoprecipitated for VHL with anti-T7. As expected, K63-ubiquitylation of VHL30 was induced in the presence of doxorubicin, while VHL19 showed negligible levels of K63-ubiquitylation in the presence or absence of DNA damage (**Fig. 3.2**).

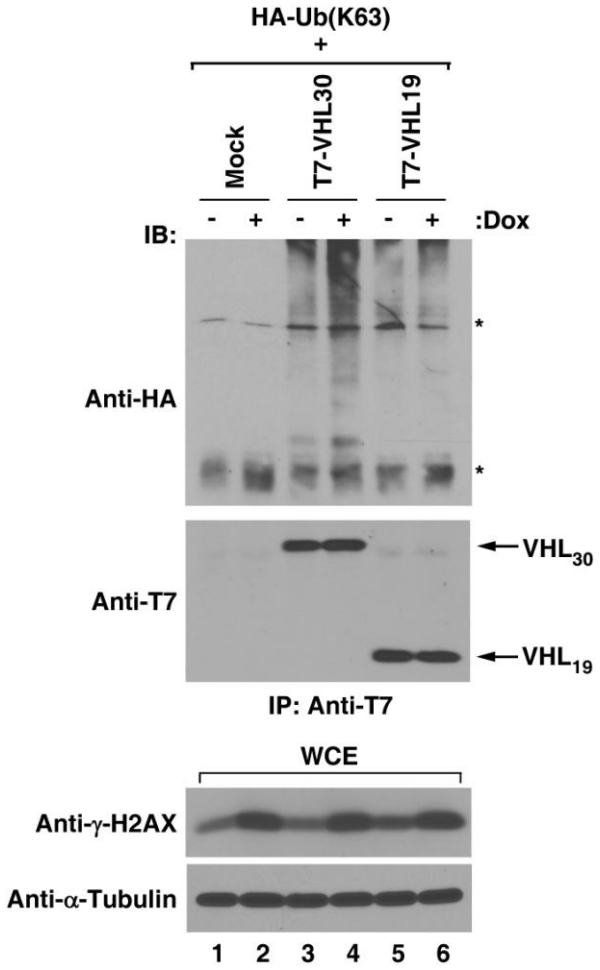

Figure 3.2. K63-Ubiquitylation of VHL19 is inhibited with DNA damage. HEK293A cells were transfected with the indicated plasmids. Twenty-four hours later, cells were treated with (+) or without (-) 300ng/mL doxorubicin for 16hrs. Lysates were immunoprecipitated (IP) with mouse monoclonal anti-T7 and immunoblotted (IB) with rabbit polyclonal anti-HA and goat polyclonal anti-T7. Equal amounts of whole cell extracts (WCE) were immunoblotted with the indicated antibodies. *, denotes non-specific band

3.3.3 VHL19 is defective in the activation of the DDR

K63-ubiquitylation of VHL is necessary to activate the DDR (Chapter 2, Section 2.3.5 and [255]). Thus, we predicted that since VHL19 is deficient for DNA damage-induced K63-ubiquitylation, that this isoform would be defective for activating the DDR. To investigate the role of VHL19 versus VHL30 in the DDR we utilized the VHL-null CCRCC cell line, 786-O, reconstituted with either vector alone (Mock), HA-VHL30, or HA-VHL19. In response to doxorubicin-induced DNA damage, the activation of H2AX and Chk1 were significantly attenuated in VHL-null and VHL19 cells in comparison to VHL30-expressing cells (**Fig. 3.3A**). Intriguingly, the expression of VHL19 was also significantly reduced in the presence of DNA damage (**Fig. 3.3A**). In addition, the intensity of IRIF of MDC1 were impaired in both VHL-null and VHL19 cells in comparison to VHL30 and showed a more diffuse nuclear staining pattern, suggesting that there is a defect in the recruitment of DNA repair proteins to the DNA lesion (**Fig. 3.3B**). Collectively, these results indicate that VHL30 has a non-overlapping function with VHL19 for the activation of the DDR.

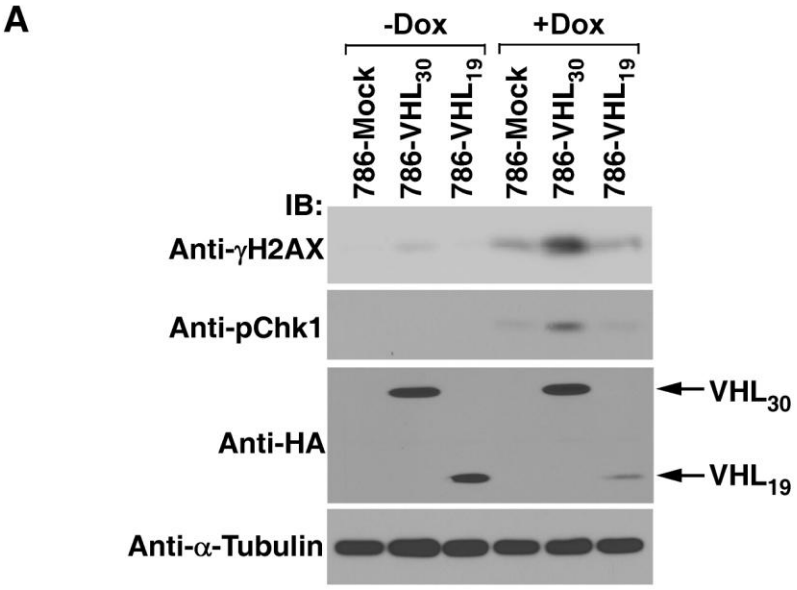
A
-Dox
+Dox
786-Mock
786-VHL30
786-VHL19
786-Mock
786-VHL30
786-VHL19
IB:
Anti-γH2AX
Anti-pChk1
Anti-HA
VHL30
VHL19
Anti-α-Tubulin

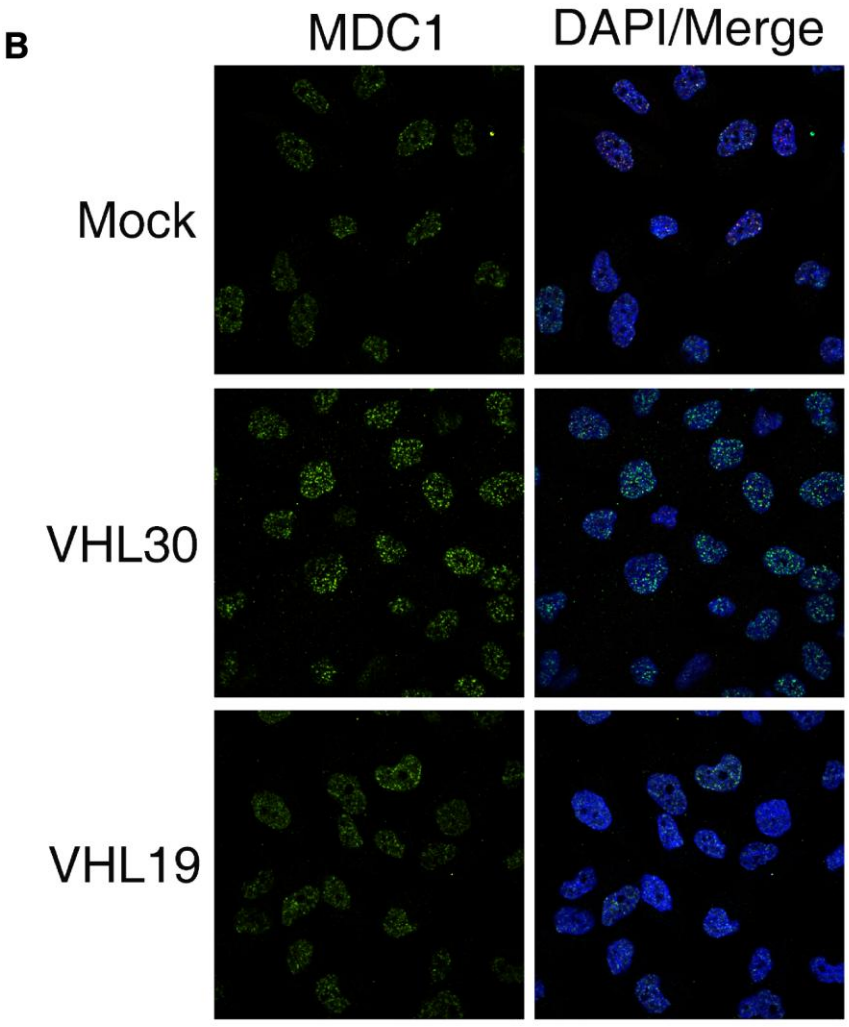
B
MDC1
DAPI/Merge
Mock
VHL30
VHL19

Figure 3.3. VHL19 is defective in activation of the DDR. (A) Indicated cell lines were treated with or without 300ng/mL doxorubicin (Dox) for 16hrs. Equal amounts of whole-cell extracts were immunoblotted with the indicated antibodies. **(B)** Indicated cell lines were irradiated with 5Gy γ-radiation and incubated for 4hrs prior to detection of MDC1 by indirect immunofluorescence. Nuclei were stained with 4,6-diamidino-2-phenylindole (DAPI) staining and merged images are shown.

3.3.4 VHL19 is defective for DNA repair

A defect in the DDR would be expected to inhibit DNA repair and promote an accumulation of DNA damage in the cell. Therefore, the ability of VHL30 versus VHL19 to mediate DNA repair was assessed using an alkaline comet assay which detects both single- and double-stranded DNA breaks in the cell. After induction of DNA damage, single cells are electrophoresed to separate damaged DNA from intact DNA. Undamaged DNA is less mobile and remains within the comet head, while damaged, fragmented DNA, migrates into the comet tail. After treatment with doxorubicin, VHL-null (Mock) and VHL19 cells had many cells with long comet tails, indicative of unrepaired DNA breaks, while VHL30 cells had no visible comet tails and the DNA remained immobilized within the head (**Fig. 3.4**). The relative extent of DNA damage persisting in the cells was measured by calculating the average tail moment, which is a measure of the amount of DNA present in the comet tail. After treatment with doxorubicin, 786-Mock and VHL19 cells had approximately 10 and 20-fold more DNA damage, respectively, than VHL30 cells (**Fig. 3.4**). These results suggest that VHL30 contributes to the repair of doxorubicin-induced DNA breaks, while VHL19 is defective in this function.

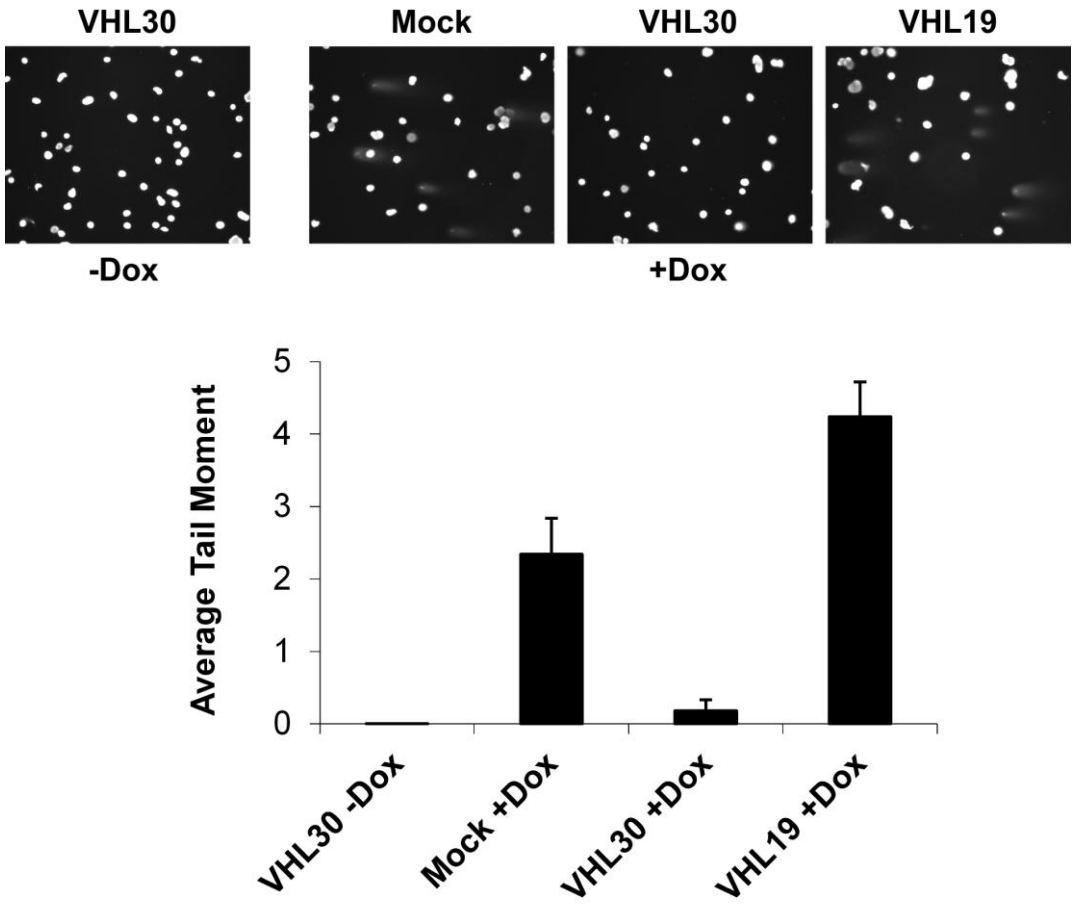

Figure 3.4. VHL19 is defective for DNA repair. 786-Mock, -VHL30, and -VHL19 were treated with 300ng/mL doxorubicin (+Dox) or untreated (-Dox) for 16hrs and an alkaline comet assay was performed. Fifty cells per sample were analyzed and average tail moment was calculated (N=3 ± SD). A representative image for each sample is shown.

3.3.5 VHL19 has a dominant-negative effect on the DDR

The presence of approximately 2-fold more DNA damage in VHL19-expressing cells in comparison to VHL-null cells suggests that VHL19 may not be merely defective for activating the DDR, but actually inhibitory (**Fig. 3.4**). To investigate whether VHL19 has an inhibitory effect on the DDR, U2OS shVHL cells were transfected with vector alone (Mock), VHL19, VHL30, or co-transfected with VHL30 and VHL19. DNA damage was induced with doxorubicin and the activation of H2AX was examined by immunoblot. γH2AX was modestly attenuated with ectopic expression of VHL19 relative to Mock transfected (**Fig. 3.5**). In addition, co-expression of VHL19 with VHL30 resulted in reduced activation of γH2AX in comparison to VHL30 alone (**Fig. 3.5)**. These results suggest that overexpression of VHL19 has a dominant-negative effect on the activation of the DDR by VHL30.

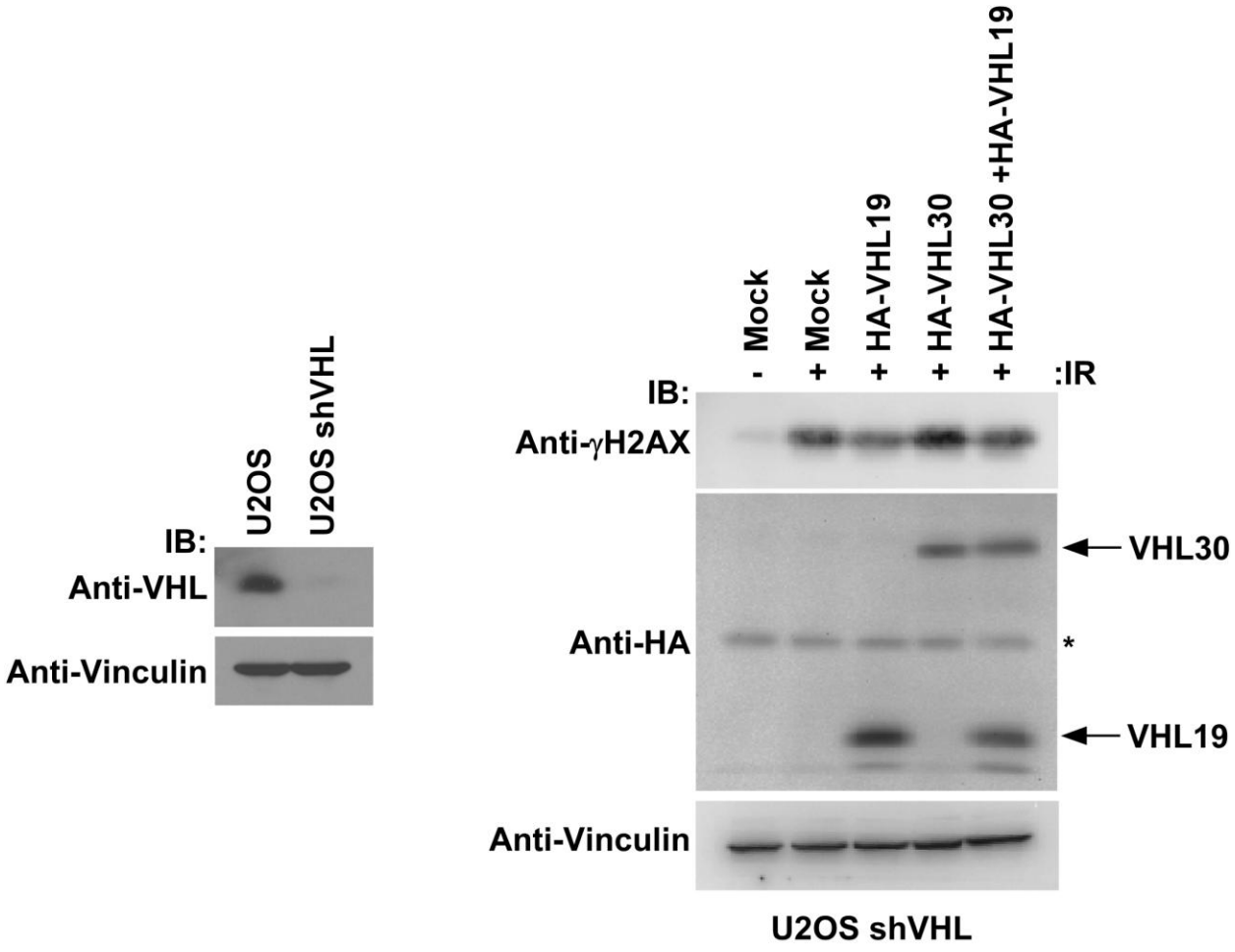

Figure 3.5. VHL19 has a dominant negative effect on the DDR. U2OS shVHL cells were transfected with the indicated plasmids and irradiated with (+) or without (-) 10Gy IR. Cells were lysed 1hr post-IR and equal amounts of whole cell extracts were immunoblotted with the indicated antibodies. *, denotes non-specific band

3.3.6 VHL19 is removed from chromatin upon induction of DSBs

We next sought to determine how VHL19 exhibited its inhibitory effect on the DDR. We hypothesized that VHL19 may bind chromatin similar to VHL30, but its defect in K63-ubiquitylation and recruitment of DDR proteins would inhibit DNA repair. Thus, the dominant-negative effect of exogenous VHL19 on the DDR may be exerted by binding chromatin and blocking the recruitment of VHL30 to inhibit its ability to activate the DDR. To investigate whether both isoforms were capable of binding chromatin, we performed cellular fractionation experiments in 786-VHL30 and 786-VHL19 cells in the presence or absence of doxorubicin-induced DNA damage. Under basal conditions, VHL19 was associated with the insoluble nuclear fraction, while VHL30 was excluded from this fraction (**Fig. 3.6**, lanes 4 & 8). Strikingly, after induction of DNA damage, VHL30 was redistributed to the insoluble fraction and VHL19 was no longer present in this fraction (**Fig. 3.6**, lanes 12 & 16). These results suggest that under normal conditions VHL19 is bound to chromatin, but in the presence of DNA damage it is removed from the damaged chromatin and VHL30 is actively recruited.

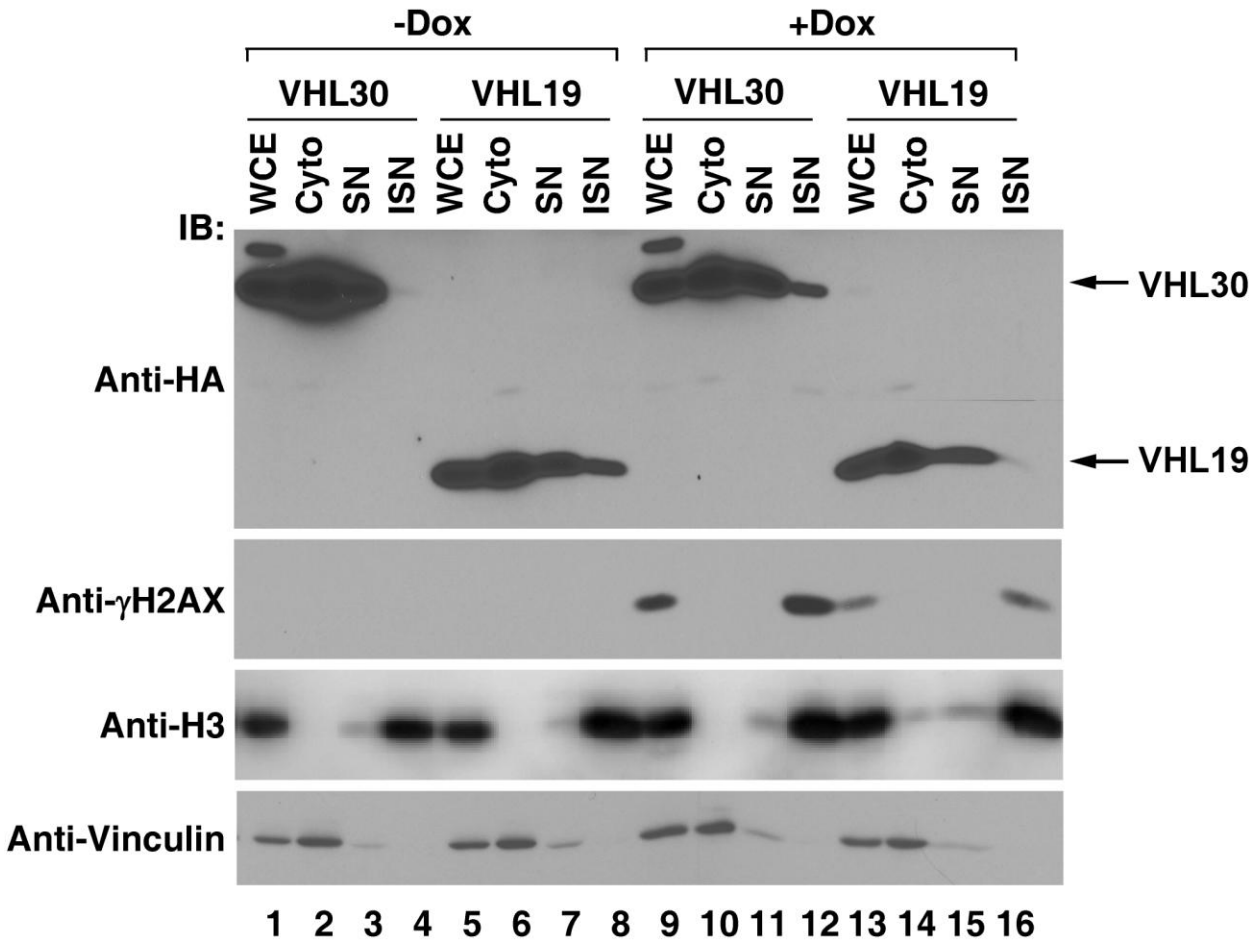

Figure 3.6. VHL19 is removed from chromatin upon induction of DSBs. 786-O cells stably expressing HA-VHL30 or HA-VHL19 were treated with (+Dox) or without (-Dox) 300ng/mL doxorubicin for 16hrs. Cells were trypsinized and resuspended in growth medium. One-tenth of the cells were lysed for whole cell extract (WCE) and remainder were washed in PBS and fractionated into cytoplasmic (Cyto), soluble nuclear (SN), and insoluble nuclear (ISN) fractions. Equal amounts of each fraction were immunoblotted with the indicated antibodies.

3.3.7 VHL19 is degraded through the proteasome with DNA damage

Interestingly, we previously observed that the expression of exogenous VHL19 is significantly reduced in the presence of the DNA-damaging agent, doxorubicin (**Fig. 3.3A**). Therefore, we hypothesized that VHL19 may be removed from the chromatin through degradation. In support of this notion, doxorubicin-induced attenuation of VHL19 was rescued in the presence of the proteasomal inhibitor MG132, while the lysosomal inhibitor chloroquine (CQ) had a minimal effect (**Fig. 3.7**). Importantly, LC3B, which is degraded through the lysosomal pathway, was induced with CQ treatment, confirming the efficiency of the lysosomal inhibitor (**Fig. 3.7)**. These results suggest that VHL19 is primarily degraded through the proteasomal pathway in response to DNA damage. Based on these findings, we propose that VHL19 is targeted for degradation upon induction of DSBs to remove its inhibitory effect on the DDR and promote repair by VHL30.

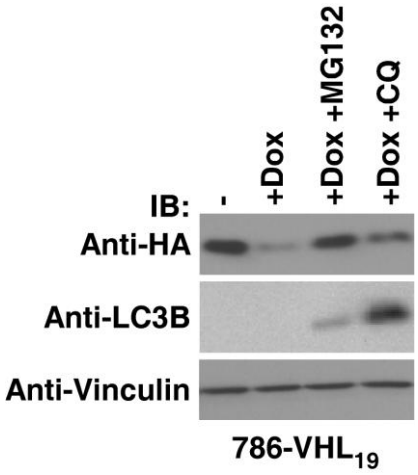

Figure 3.7. VHL19 is degraded through the proteasome with DNA damage. 786-VHL19 cells were treated with 300ng/mL doxorubicin alone or in combination with 5µg/mL MG132 or 50µM choloroquine (CQ) for 16hrs. Equal amounts of cell lysates were immunoblotted with the indicated antibodies.

3.4 Discussion

We have previously shown that VHL30 is required for activation of the DDR. However, we now demonstrate that VHL30 and VHL19 isoforms have non-overlapping roles in the DDR. In contrast to VHL30, VHL19 fails to bind SOCS1 in the presence of DNA damage, resulting in a defect in K63-ubiquitylation and activation/recruitment of DDR proteins to the DNA lesion. Interestingly, we show that VHL30 and VHL19 have opposing roles in the DDR; VHL30 activates the DDR, while VHL19 inhibits this cellular response. The molecular mechanisms underlying this inhibition have not been fully elucidated, but our current data supports the following model: VHL19 is bound to chromatin under steady-state conditions, but upon induction of a nearby DSB, is unable to recruit DNA repair factors due to its diminished K63-ubiquitylation. To alleviate this inhibition, VHL19 is removed from the chromatin through proteasomal degradation, allowing for the recruitment of VHL30. K63-ubiquitylation of VHL30 then mediates recruitment of DNA repair proteins to the lesion.

The present data suggests that VHL30 and VHL19 have important functional differences in the DDR, but a number of important questions remain. Why would cells have a form of VHL that is inhibitory for the DDR and what is the functional significance of the exchange between VHL19 and VHL30 isoforms at damaged chromatin? We have shown in Chapter 2 that VHL is necessary for the late repair of DSBs. Notably, DSBs within heterochromatin have been shown to be repaired with slow-kinetics, suggesting that VHL may play a role in the repair of these breaks[122]. According to recent work by Chiolo *et al*., DSBs within heterochromatin are relocalized to the periphery of the heterochromatin domain prior to the recruitment of the HR protein Rad51, which is necessary for the homology search on the sister chromatid[121]. The tightly packed, highly repetitive structure of heterochromatin makes this a particularly dangerous environment for HR to occur, which relies on homologous sequences for template-mediated repair. The authors speculate that the relocalization of heterochromatic DBSs may prevent erroneous strand invasion in non-homologous regions[121]. Based on this study, we hypothesize that VHL19 may be bound to heterochromatin and repress the DDR until the break can be relocalized for repair by VHL30. Alternatively, we can speculate that VHL19 may be involved in suppressing the DDR at naturally-occurring DNA ends or telomeres.

The human *VHL* gene is conserved in mice, worms, and flies. However, the N-terminal region is highly divergent, with only 19 of the 53 N-terminal amino acids conserved in mice[257]. Our current data suggests that mouse VHL, which is most similar to VHL19, may lack the DNA repair function of human VHL30. Although we have not formally tested the ability of mouse VHL to bind SOCS1 or regulate the DDR, it is interesting to note that homozygous deletion of VHL in mice has been unable to recapitulate CCRCC. These mice develop renal cysts, the precursors of CCRCC, but do not form tumours[258]. In addition, the lack of conservation in other organisms suggests that VHL30 may have evolved for a unique function in human cells. Therefore, we hypothesize that the increased genome size and chromatin complexity of human cells may necessitate additional DDR proteins such as VHL30 for repair.

Chapter 4

4 VHL mediates repair of DSBs by regulating the chromatin association of HP1α

4.1 Introduction

Upon induction of a DSB, ATM is rapidly autophosphorylated and recruited to the DNA lesion by the MRN complex[14, 15]. Activated ATM then phosphorylates H2AX and the downstream effector kinases Chk1/2 to initiate a complex signalling cascade that serves to arrest the cell cycle, initiate DNA repair, or activate apoptosis if the damage is too extensive or cannot be repaired[17, 23, 28, 29]. In mammalian cells, DSBs are repaired by two major pathways: non-homologous end joining (NHEJ) and homologous recombination (HR). NHEJ directly ligates the DNA ends and is intrinsically error-prone. In contrast, HR uses a homologous chromosome or sister chromatid as a template for very accurate repair during S/G_2 phases of the cell cycle.

Recent evidence suggests that the chromatin environment in which the DSB arises has a significant impact on DNA repair. Eukaryotic DNA is organized into open, transcriptionally active euchromatin and highly compact, transcriptionally inert heterochromatin. The highly compact nature of heterochromatin poses a significant barrier to DDR signalling and DNA repair. Studies have shown that γH2AX expansion within heterochromatin is inhibited and DSBs arising in heterochromatin relocalize to the periphery of heterochromatic regions, suggesting that heterochromatin restricts the access of DNA repair proteins to the DSB [119-121, 123].

Local chromatin expansion and decondensation has been observed following DSBs and this dynamic reorganization plays a critical role in repair[126, 135]. Recently, KRAB-associated protein (KAP-1), heterochromatin protein 1 (HP1), and the histone deacetylase Tip60, have been shown to be critical mediators of heterochromatin relaxation following DSBs. KAP-1 promotes chromatin condensation by recruiting HP1, which binds H3K9me3 to stabilize nucleosome compaction[117]. While the dynamic reorganization of heterochromatin proteins following DSBs has not been fully elucidated, recent studies support the following model: In response to DSBs, HP1β is phosphorylated by casein kinase 2 and released from H3K9me3[133]. The exposed

H3K9me3 is then bound by the acetyltransferase Tip60, which acetylates ATM, resulting in autophosphorylation and activation of ATM[129, 137]. The heterochromatin protein KAP-1 is phosphorylated by activated ATM which results in chromatin relaxation and increased spacing between nucleosomes to allow for the recruitment of repair factors[122, 138].

ATM is dispensable for the repair of the majority of DSBs (~85%), but is specifically required for the repair of DSBs within heterochromatin[122]. Notably, the majority of DSBs within heterochromatin are repaired by HR[259]. Thus, the newly identified role of VHL in HR and its requirement for ATM signalling, suggests that VHL may be involved in the repair of DSBs within heterochromatin, perhaps through chromatin remodelling. We have previously shown that loss of VHL attenuates the activation of ATM and recruitment of Mre11, suggesting that VHL acts upstream of these proteins in the DDR (Chapter 2 and [254]). Based on the current proposed model for the repair of DSBs within heterochromatin, dissociation of HP1 from H3K9me3 precedes the recruitment of the MRN complex and ATM. Interestingly, VHL contains an HP1 binding motif (PxVxL) between aa81-85 and has recently been reported to bind HP1γ[260]. Therefore, we hypothesized that VHL may regulate the chromatin association of HP1 to promote decondensation and facilitate DNA repair.

4.2 Materials and Methods

4.2.1 Cells

786-O and HEK293A were obtained from the American Type Culture Collection (Rockville, MD). 786-O subclones ectopically expressing HA-VHL(WT) or empty plasmid (Mock) were previously described[239]. 786-O cells stably expressing HA-VHL(P81S) were generated as previously described[239]. Cell lines were maintained in Dulbecco's modified Eagle's medium (DMEM) supplemented with 10% fetal bovine serum (Wisent, St.-Bruno, QC, Canada) at 37°C in a humidified 5% CO2 atmosphere. 786-O subclones were maintained with 0.25mg/mL G418 (Sigma) in culture medium.

4.2.2 Plasmids

Full-length HA-VHL(WT) (aa1-213) has been previously described[162]. HA-VHL(P81S) was generated using QuikChange site-directed mutagenesis kit (Stratagene, La Jolla, CA, USA) and mutations verified by direct DNA sequencing. FLAG-VHL(WT) and FLAG-VHL(P81S) were generated as follows. First, a triple-FLAG tag was incorporated into the pcDNA3 vector between the HindIII and BamHI restriction sites. 50µM of the following oligos were annealed together in 1× Oligo annealing buffer (10mM Tris-HCl, pH 8.0, 1mM EDTA, pH 8.0, 0.1M NaCl) by heating at 94°C for 4min and cooling slowly to 50°C : forward 5'-AGCTTAGACTACAAAGACCATGACGGTGATTATAAAGATCATGACATCGATTACAAGGATGACGATGACAAGTG-3' and reverse 5'-GATCCACTTGTCATCGTCATCCTTGTAATCGATGTCATGATCTTTATAATCACCGTCATGGTCTTTGTAGTCTA-3'. pcDNA3 was digested with HindIII and BamHI (Thermo Scientific) and purified using a QIAquick PCR purification kit (Qiagen). The annealed oligo was diluted 100-fold in 1× Oligo annealing buffer and ligated with 0.35ng of linearized pcDNA3 using T4 DNA ligase (Invitrogen). The ligation reaction was transformed into DH5α *E.coli* (Invitrogen) and plasmid DNA was isolated by maxi prep using a NucleoBond Xtra Maxi kit (Macherey-Nagel, Düren, Germany). VHL(WT) and VHL(P81S) were amplified from HA-VHL(WT) and HA-VHL(P81S) constructs, respectively using the following primers: forward 5'-GACGACGGATCCCCCCGGAGGGCGGAGAAC-3' and reverse 5'-GACGACCTCGAGTCAATCTCCCATCCGTTGATG-3' . 50µL PCR reactions containing 1×PCR buffer (Invitrogen), 3mM $MgCl_2$ (Invitrogen), 0.2mM dNTPs (Invitrogen), 0.5µM each

forward and reverse primers, and 2.5U of Pfu Turbo DNA polymerase (Agilent Technologies, Mississauga, ON, Canada) were cycled using the following conditions: 94°C for 30 s, 54°C for 30 s, and 72°C for 90 s for 30 cycles. Reactions were PCR purified, digested with BamHI and XhoI (Fermentas), and re-purified. FLAG-pcDNA3 was also digested with BamHI and XhoI and PCR purified. Digested VHL(WT) or VHL(P81S) was ligated into the linearized FLAG-pcDNA3 vector using T4 DNA ligase, transformed into DH5α and maxi prepped as described above. HA-HP1α (#24078), HA-HP1β (#24079), and HA-HP1γ (#24080) were obtained from AddGene.

4.2.3 Transfection

Performed as described in Chapter 2, Section 2.2.5.

4.2.4 Immunoprecipitation and Immunoblotting

Performed as described in Chapter 2, Section 2.2.7.

4.2.5 Antibodies

The following monoclonal antibodies were used: anti-FLAG(M2), anti-vinculin, and anti-α-tubulin were obtained from Sigma, mouse anti-HA(12CA5) was obtained from Roche, rabbit anti-HA was purchased from Cell Signaling, and anti-hnRNPC1/C2 from AbCam. The following polyclonal antibodies were used: anti-γH2AX, anti-pChk1(Ser296), anti-pKAP-1(Ser824), anti-HP1α were obtained from Cell Signaling, anti-FLAG was obtained from Novus Biologicals, anti-HIF2α was purchased from Novus Biologicals and anti-acetyl-H3 was purchased from Millipore.

4.2.6 Chemicals

Doxorubicin was obtained from Santa Cruz Biotechnology and valproic acid (VPA) was obtained from Sigma Aldrich.

4.2.7 Cellular Fractionation

Performed as described in Chapter 3, section 3.2.8.

4.3 Results

4.3.1 VHL binds HP1α upon induction of DSBs

Three HP1 isoforms have been identified in humans: α, β, and γ. Each of these isoforms contains a highly conserved chromodomain (CD), which interacts with chromatin, and a chromoshadow domain (CSD), which mediates dimerization of HP1 proteins and interactions with other binding partners (**Fig. 4.1A**)[261-264]. The CD and CSD are separated by a more divergent hinge domain, which may affect the chromatin binding affinities or protein-protein interactions of the different HP1 isoforms[265, 266] . Interestingly, the N-terminus of HP1α contains a unique CK2 phosphorylation motif (aa11-17), suggesting that HP1α may be differentially regulated (**Fig. 4.1A**). Both HP1α and HP1β have been shown to be associated with heterochromatin, however, HP1α appears to be most specific for pericentric heterochromatin, with HP1β showing more diffuse nuclear staining[267-269]. HP1γ on the other hand, is primarily associated with euchromatin[267-269].

Based on the predicted role of VHL in the repair of heterochromatic DSBs, we investigated the ability of full-length (30kDa) VHL to bind human HP1 α, β, and γ, upon induction of DSBs. Strikingly, upon induction of DSBs with doxorubicin, VHL was found to specifically interact with HP1α (**Fig. 4.1B**). These results suggest that VHL may interact with HP1α for a role in the DDR.

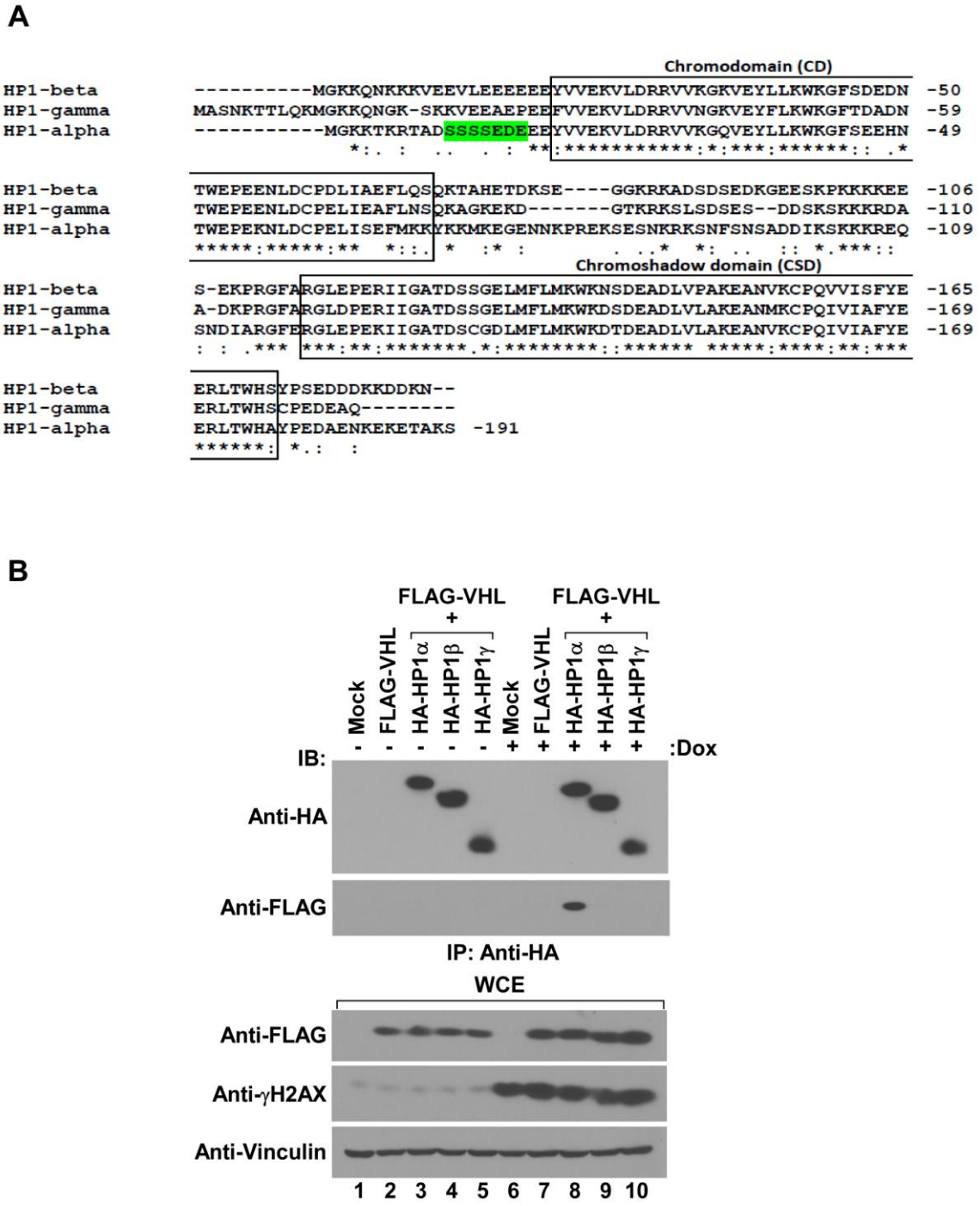

Figure 4.1. VHL binds HP1α upon induction of DSBs. (**A**) ClustalW sequence alignment of human HP1α, β, and γ [270]. An N-terminal CK2 phosphorylation motif unique to HP1α is highlighted in green. (**B**) HEK293A cells were transfected with the indicated constructs. Twenty-four hours later cells were treated with (+) or without (-) 300ng/mL doxorubicin for 16hrs. Cell lysates were immunoprecipitated (IP) with monoclonal mouse anti-HA and immunoblotted (IB) with rabbit monoclonal anti-HA and polycloncal rabbit anti-FLAG antibodies. Equal amounts of whole cell extracts (WCE) were also immunoblotted with the indicated antibodies (bottom).

4.3.2 VHL(P81S) is defective for HP1α binding, but retains HIF function

In an attempt to elucidate the function of the VHL-HP1α interaction, we utilized a naturally-occurring VHL mutant, VHL(P81S), that was previously reported to be defective for HP1γ binding[260]. We first extended the previously reported findings of Lai *et al*. by demonstrating that VHL(P81S) is unable to bind HP1α, but retains HIF function (**Fig. 4.2A,B** and [260]).

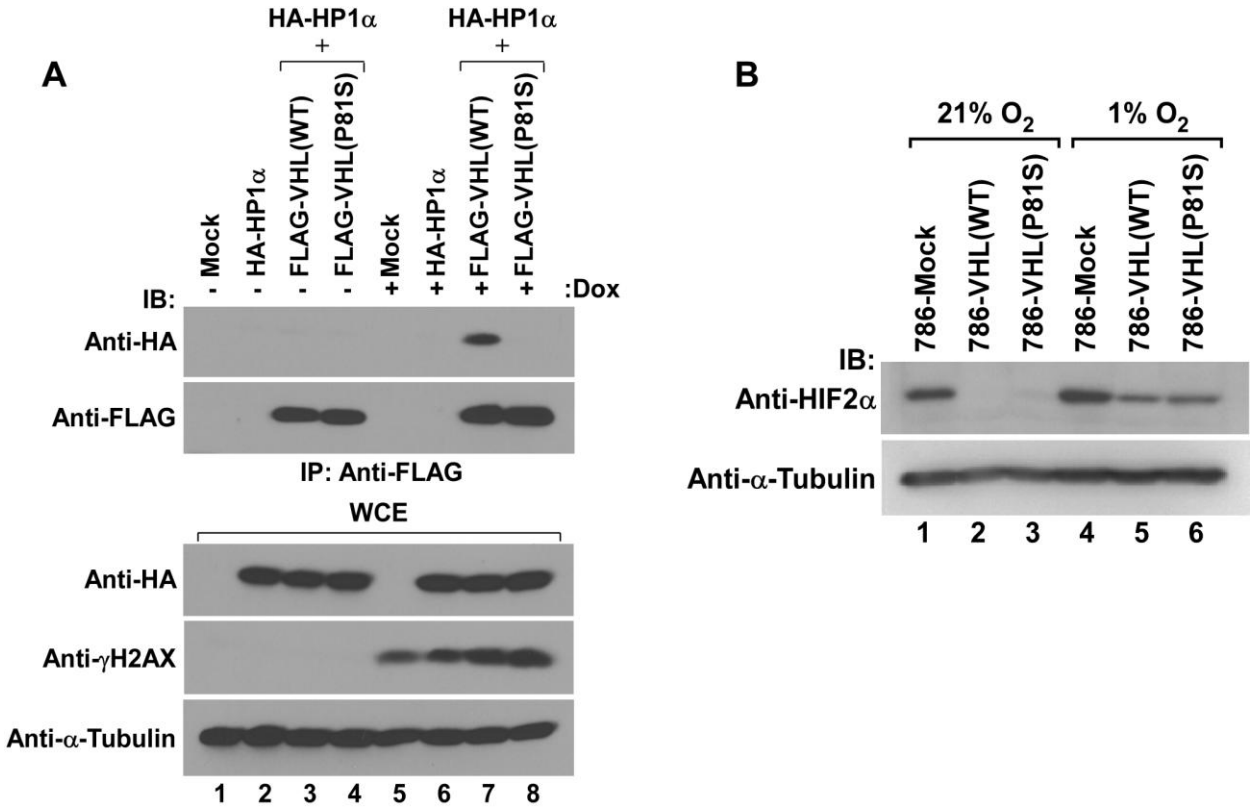

Figure 4.2. VHL(P81S) is defective for HP1α binding, but retains HIF function. (A) HEK293A cells were transfected with the indicated plasmids and treated with (+) or without (-) 300ng/mL doxorubicin for 16hrs. Cell lysates were immunoprecipitated (IP) with anti-FLAG and immunoblotted (IB) with the indicated antibodies. Equal amounts of whole cell extracts (WCE) were also IB with the indicated antibodies. **(B)** 786-Mock, -VHL(WT), and –VHL(P81S) were incubated at 21% or 1% O_2 for 16hrs. WCE were immunoblotted with anti-HIF2α and anti-α-tubulin.

4.3.3 VHL binding to HP1α is necessary for activation of the DDR

We then asked whether the VHL-HP1α interaction is necessary for activation of the DDR. We investigated the activation of key DDR proteins in the VHL-null CCRCC cell line, 786-O, stably reconstituted with empty plasmid (Mock), HA-VHL(WT) or HA-VHL(P81S). In response to doxorubicin-induced DNA damage, the phosphorylation of H2AX, Chk1, and KAP-1 were all significantly attenuated in VHL-null and VHL(P81S) cells comparison to VHL(WT) (**Fig. 4.3)**. However, VHL(P81S) binds SOCS1 and is K63-ubiquitylated to levels comparable with VHL(WT) in the presence of doxorubicin, suggesting that the DDR defect in VHL(P81S) cells is due to a defect in binding HP1α and not SOCS1-mediated K63-ubiquitylation (**Appendix, Fig. A.6 & A.7**). Therefore, these results imply that the VHL-HP1α interaction is necessary for the activation of the DDR.

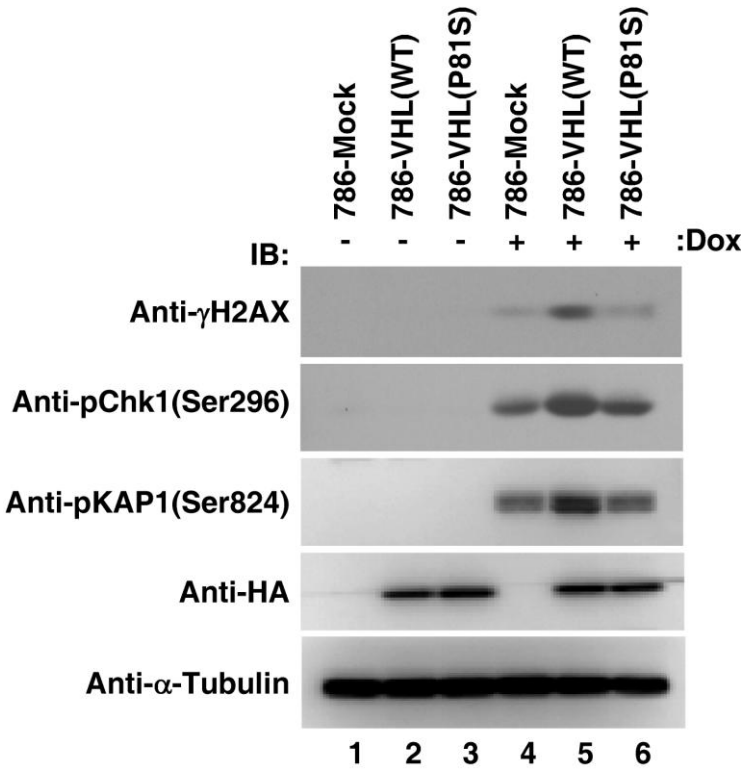

Figure 4.3. VHL(P81S) is defective for activation of the DDR. 786-Mock, -VHL(WT), and VHL(P81S) cells were treated with (+) or without (-) 300ng/mL doxorubicin for 16hrs. Equal amounts of whole cell extracts were immunoblotted with the indicated antibodies.

4.3.4 VHL binding to HP1α promotes its dissociation from chromatin

The next question we wanted to address was how VHL binding to HP1α promoted activation of the DDR. Dissociation of HP1β has previously been shown to induce heterochromatin relaxation to promote repair[271]. Based on the current model for DSB heterochromatin remodelling, HP1 dissociation precedes Tip60/ATM and Mre11 recruitment. Given our previous findings that ATM activation and Mre11 IRIF are defective in VHL-null cells, we hypothesized that VHL may alter HP1α association with chromatin upon induction of DSBs.

786-Mock, -VHL(WT), and VHL(P81S) cell lines were irradiated with 5Gy γ-irradiation and fractionated into cytoplasmic, soluble nuclear, and insoluble nuclear fractions at 1hr and 4hrs post-IR. Examination of the chromatin-bound HP1α in the insoluble nuclear fraction (ISN) revealed a transient dissociation of HP1α at 1hr post-IR in VHL(WT) cells, with re-association at 4hrs (**Fig. 4.4**, lanes 11 & 12). In contrast, the chromatin association of HP1α increased with DNA damage and remained stable at 4hrs post-IR in VHL(P81S) cells (**Fig. 4.4**, lanes 23 & 24). These data suggest that upon induction of DSBs, the interaction of VHL with HP1α may promote the transient dissociation of HP1α from chromatin.

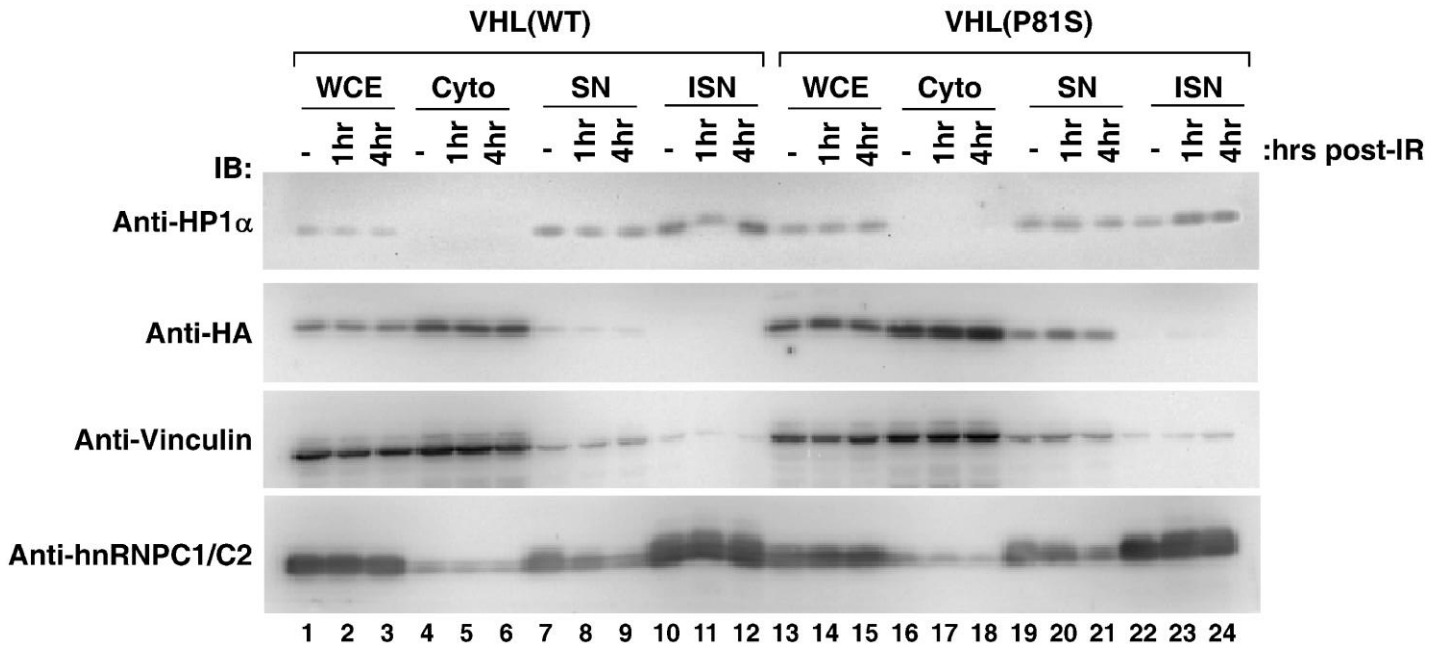

Figure 4.4. VHL binding to HP1α induces DSB-induced dissociation of HP1α. 786-VHL(WT) and 786-VHL(P81S) cells were irradiated with 5Gy γ-radiation and fractionated 1hr and 4hrs later. Equal amounts of whole cell extracts (WCE), cytoplasmic (Cyto), soluble nuclear (SN), and insoluble nuclear (ISN) fractions were immunoblotted with the indicated antibodies.

4.3.5 Chromatin relaxation rescues the DDR defect in VHL-null and VHL(P81S) cells

If the function of the VHL-HP1α interaction is to dissociate HP1α to induce chromatin relaxation, then we hypothesized that we should be able to rescue the DDR defect in VHL-null and VHL(P81S) cells by chemically inducing chromatin relaxation. 786-Mock, -VHL(WT), and -VHL(P81S) cells were treated with the HDACI, valproic acid (VPA), for 24hrs prior to induction of DSBs by IR. In the absence of HDACI, IR increased the levels of acetyl-H3 in VHL(WT) in comparison to Mock and VHL(P81S) cells, supporting the notion that VHL induces chromatin relaxation upon induction of DSBs (**Fig. 4.5,** compare lanes 4-6). After treatment with HDACI, all cells had significantly increased levels of acetyl-H3, indicative of chromatin relaxation (**Fig. 4.5,** lanes 7-9**)**. Remarkably, pre-treatment with the HDACI increased IR-induced γH2AX expression in Mock and VHL(P81S) cells to levels comparable to VHL(WT), rescuing the DDR defect in these cells (**Fig. 4.5,** lanes 7-9). These results suggest that VHL induces chromatin relaxation after DSB induction through its interaction with HP1α and DDR defects in VHL mutant cells can be efficiently restored with HDACIs.

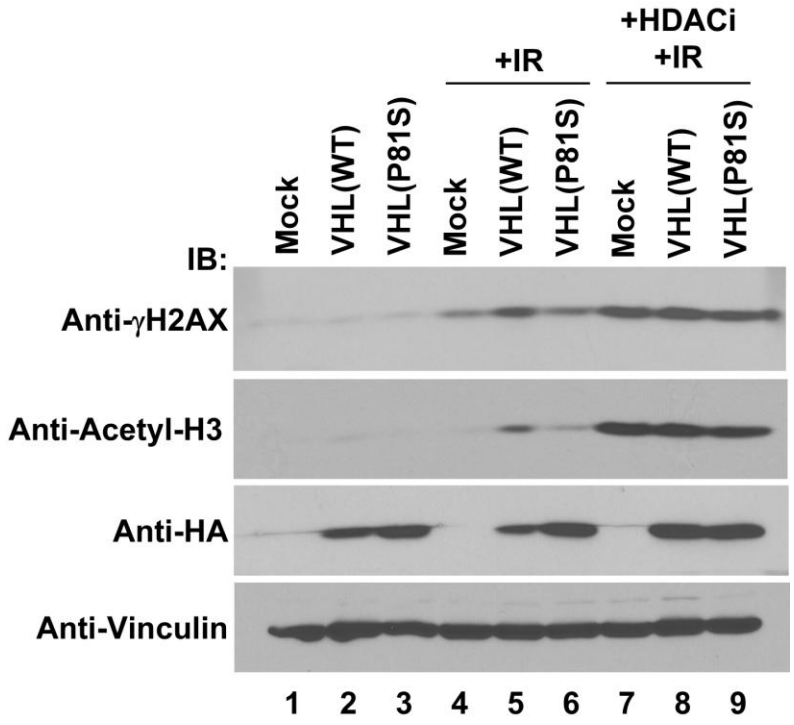

Figure 4.5. HDCAI rescues DDR in VHL-null and VHL(P81S) cells. 786-Mock, -VHL(WT), and VHL(P81S) were treated with the histone deactylase inhibitor (HDACI) valproic acid (10mM) for 24hrs or untreated and then irradiated (IR) with 5Gy γ-radiation. Cells were lysed 1hr post-IR and equal amounts of whole cell extracts were immunoblotted with the indicated antibodies.

4.4 Discussion

Here we show that VHL interacts with HP1α upon induction of DSBs, which is necessary for full activation of the DDR. The interaction between VHL and HP1α promotes transient dissociation of HP1α from chromatin, which is predicted to result in chromatin decondensation.

HP1 dynamics in response of DNA damage have been poorly characterized to date, with several conflicting reports. HP1 has been shown to be recruited to chromatin to promote repair, while others have reported that HP1 is inhibitory for repair and dissociates upon induction of DSBs[271, 272]. As a result of these studies, a bimodal model for HP1 dynamics has emerged whereby HP1 first dissociates from chromatin to relieve chromatin compaction and later re-associates to enhance DDR signalling[133]. Consistent with the bimodal model of DSB-induced HP1 dynamics, we have shown that HP1α dissociates from chromatin at 1hr post-IR and re-associates at 4hr in VHL(WT) cells, but remains constitutively associated with chromatin in VHL(P81S) cells. The tight chromatin association of HP1α in VHL(P81S) cells is predicted to inhibit chromatin decondensation and the DDR. Consistent with this notion, increased levels of acetyl-H3 were observed in VHL(WT) cells, but not VHL(P81S) cells upon induction of DSBs. Furthermore, the DDR defect in VHL-null and VHL(P81S) cells was fully rescued by chemically inducing chromatin relaxation with an HDACI. These results imply that the DNA damage-induced VHL-HP1α interaction promotes chromatin decondensation to activate the DDR.

DNA damage-induced decondensation is thought to facilitate the recruitment of DNA repair proteins to the lesion. This response is particularly important in highly condensed heterochromatic regions. We have shown that VHL interacts exclusively with HP1α, which is most specific for pericentric heterochromatin[267-269]. Consistent with these current findings, we have previously shown that VHL is necessary for activation of ATM and late-repairing of DSBs, both of which have previously been linked to heterochromatic DSBs[122]. Collectively, these results suggest that the interaction between VHL and HP1α may specifically facilitate heterochromatin decondensation to promote repair. However, a small fraction of HP1α is also found within euchromatin and presently we cannot exclude the possibility that VHL may also promote euchromatin decondensation after DSB induction. Further studies are necessary to differentiate the role of VHL in the repair of heterochromatic versus euchromatic DSBs.

The molecular mechanism underlying the transient dissociation of HP1α from damaged chromatin remains unresolved. Phosphorylation of HP1β by casein kinase 2 (CK2) has been shown to disrupt the interaction with H3K9me3[133, 271]. Intriguingly, VHL has previously been shown to act as an adaptor for CK2 to promote its kinase activity[225]. In addition, HP1α is unique among the three mammalian isoforms in that it contains a CK2 phosphorylation motif in its N-terminus. Therefore, we predict that VHL promotes CK2 activity to phosphorylate HP1α and transiently disrupt its association with H3K9me3. Unmasking of the H3K9me3 promotes recruitment/activation of the MRN complex and Tip60/ATM. ATM-dependent phosphorylation of KAP-1 and H2AX, in addition to acetylation of H3 and H4 by Tip60, then promotes heterochromatin relaxation surrounding the DSB. However, further studies are necessary to validate this proposed model.

Chapter 5

5 Summary, Future Directions, and Implications for CCRCC

5.1 Predicted model of VHL-mediated HR repair

We have shown that VHL is K63-ubiquitylated by SOCS1 in response to DSBs, which mediates the activation/recruitment of DNA repair proteins to the lesion. Loss of VHL or K63-ubiquitylation inhibits the repair of DSBs by HR and results in the persistence of breaks in the cell. We further show that this novel role of VHL in HR repair is unique to VHL30, as VHL19 fails to bind SOCS1 and is defective in K63-ubiquitylation. Intriguingly, VHL19 has an opposing role in the DDR and is degraded upon induction of DSBs, presumably to relieve its inhibitory effect on the DDR. Finally, we show that in the presence of DNA damage, VHL binds HP1α to dissociate it from chromatin, which is thought to promote chromatin relaxation and allow for the recruitment of DNA repair proteins to the lesion.

The relationship between K63-ubiquitylation of VHL and binding to HP1α remains unclear, but we hypothesize that these mechanisms are part of a larger coordinated DDR response. Based on our current data we propose the following model for VHL-mediated DSB repair. Under normal conditions, VHL19 is associated with chromatin. Upon induction of a DSB, VHL19 may initially repress DNA repair at heterochromatic breaks until the lesion is relocalized to the periphery of the heterochromatin domain. Once the DSB is relocalized, VHL19 may be exported to the cytoplasm and degraded through the proteasome, while VHL30 is recruited to the DNA lesion. Binding of VHL to HP1α promotes its dissociation from chromatin to induce decondensation and K63-ubiquitylation of VHL by SOCS1 promotes the recruitment of DNA repair factors to the now accessible damaged DNA (**Fig. 5.1**). Conceivably, this coordinated response could protect heterochromatic breaks from being repaired prematurely in the tightly packed chromatin prior to relocalization to less condensed regions. Therefore, DNA repair proteins are only recruited once the DNA is in a decondensed state that is conducive for repair.

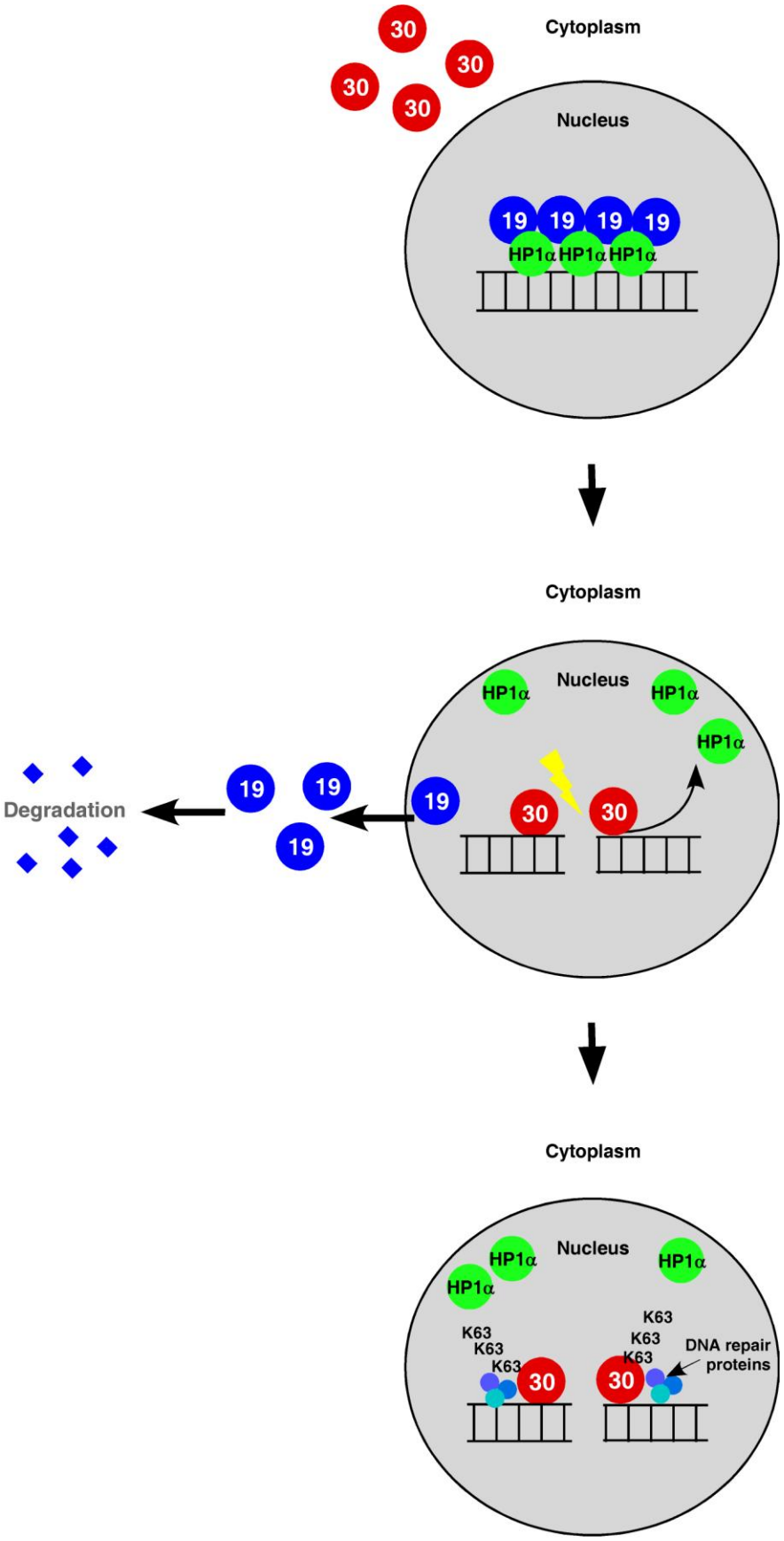
Cytoplasm
30
30
30
30
Nucleus
19
19
19
19
HP1α
HP1α
HP1α
Cytoplasm
Nucleus
HP1α
HP1α
HP1α
Degradation
19
19
19
19
30
30
Cytoplasm
Nucleus
HP1α
HP1α
HP1α
K63
K63
K63
K63
K63
K63
DNA repair
proteins
30
30

Figure 5.1. Proposed model of VHL-mediated DSB repair. Under basal conditions, VHL19 is bound to chromatin and VHL30 is predominantly cytoplasmic. Upon induction of a DSB, VHL19 is exported to the cytoplasm and degraded, while VHL30 relocalized to the nucleus and binds the damaged chromatin. Binding of VHL30 to HP1α promotes its dissociation and chromatin decondensation. SOCS1-mediated K63-ubiquitylation of VHL30 then promotes the recruitment of DNA repair proteins to the accessible DNA lesion.

5.2 Link between loss of VHL and genomic instability in CCRCC

CCRCC is associated with high genomic instability, with frequent chromosomal translocations and deletions. However, the cause of this instability has not been fully elucidated. Recently, mutations in the *PBRM1* chromatin remodelling gene have been identified in ~41% of cases, however the majority of CCRCC patients harbour no mutations in any known chromatin remodelling or DNA repair genes. The most common mutation in CCRCC is in the tumour suppressor *VHL*, which is inactivated in >80% of cases. Here we show for the first time, that VHL is essential for the repair of DSBs by HR. Loss of VHL leads to the persistence of DSBs, which is predicted to generate genomic instability that characterize and promote tumourigenesis.

VHL inactivation is thought to be an early event in the development of CCRCC, as loss of VHL has been observed in pre-neoplastic renal cysts[214]. Based on this evidence, it is thought that loss of VHL is insufficient to initiate CCRCC and additional mutations must be acquired to promote tumourigenesis. In support of this notion, Kaelin and colleagues have shown that loss of VHL in murine fibroblasts leads to Rb-dependent cellular senescence, suggesting that additional mutations would be required to overcome this barrier and promote tumour growth[236]. In agreement with this previous report, the persistence of DSBs resulting from loss of VHL would normally trigger apoptosis or cellular senescence. Therefore, among the many mutations that cancer cells acquire, we predict that mutations that inactivate the apoptotic and/or cellular senescence pathways are critical to promote CCRCC. Consistent with the mutator phenotype hypothesis (described in Chapter 1, section 1.4.1), we now show that loss of VHL inhibits DNA repair, which would presumably accelerate the accumulation of these additional mutations necessary to drive tumourigenesis.

The majority of DSBs within heterochromatin are repaired by HR[259]. We have now shown that VHL plays an essential role in the repair of DSBs by HR and its interaction with HP1α further suggests that VHL may be particularly important for the repair of DSBs within heterochromatin. The close proximity of highly repetitive sequences in heterochromatin is extremely dangerous for HR, which uses a homologous sequence for repair. Recent studies in *Drosophila*, have shown that HR proteins are rapidly recruited to DSBs within heterochromatin, but later relocalize to the periphery of the heterochromatin domain to complete repair[121]. Time-lasped microscopy revealed that the heterochromatin domain is expanded and HP1a is removed from the periphery of the domain prior to the recruitment of Rad51[121]. This delicate spatiotemporal regulation of DSBs within heterochromatin is predicted to protect against erroneous strand invasion at nonhomologous sequences, which could generate chromosomal rearrangements and genomic instability. Likewise, we predict that in human cells VHL may coordinate the organization of heterochromatin to facilitate accurate repair by HR. Loss of VHL and the retention of HP1α at heterochromatic breaks would prevent local chromatin decondensation that could result in recombination at nonhomologous sequences, which may give rise to the frequent chromosomal translocations observed in CCRCC.

5.3 Future Directions

5.3.1 Apoptosis and genomic instability in CCRCC

Unrepaired DSBs typically result in apoptosis or cellular senescence. Therefore, it is generally assumed that cancer cells must acquire additional mutations to disarm this cellular defence mechanism. An *et al.* have shown that VHL-null cells have an upregulation of NFκB pro-survival genes and we predict that this defect in the apoptotic pathway results in the persistence of DSBs in CCRCC cells[222]. To test this hypothesis, clonogenic survival assays could be performed to measure cell survival after DNA damage. Furthermore, we predict that the persistence of unrepaired DSBs in VHL-null and DDR-deficient cells generates genomic instability; however, this was not formally examined in this study. Chromosomal instability could be investigated in future studies using metaphase spreads to detect gross chromosomal aberrations in VHL-null and DDR-deficient cell lines. These studies will validate whether the

observed DNA repair defect underlies the genomic instability in CCRCC and significantly advance our understanding of the pathogenesis of this aggressive disease.

5.3.2 Regulation of VHL nuclear redistribution

Nuclear redistribution of VHL is undoubtedly important for its newly described role in DSB repair and elucidating the molecular mechanisms that regulate this dynamic response will be important for future studies. Previously, VHL was shown to localize to the nucleus upon transcriptional arrest or low pH[170, 171]. Intriguingly, in the study by Lee *et al.*, transcription was arrested using actinomycin D, which intercalates DNA resulting in DSBs[170, 273]. In addition, low pH has been shown to induce topoisomerase II-mediated DNA damage, suggesting that the nuclear relocalization of VHL in these earlier studies may actually be a cellular response to DNA damage[274]. Consistent with this notion, we have observed an increase in nuclear VHL after DNA damage (discussed in Chapter 3, see **Fig. 3.7**). However, the molecular mechanism underlying this dynamic cellular relocalization remains unknown. VHL contains both a NLS between aa1-60 and a NES between aa114-154, which may be critical for DNA damage-induced shuttling of VHL. We have shown that binding to SOCS1 promotes nuclear redistribution of VHL. Since SOCS1 binding to VHL is essential for it K63-ubiquitylation, we originally hypothesized that this modification of VHL may regulate its nuclear redistribution. Surprisingly, VHL(RRR) which is defective for K63-ubiquitylation, but retains binding to SOCS1, is also redistributed to the nucleus when co-expressed with SOCS1 (data not shown). This result suggests that binding to SOCS1, not K63-ubiquitylation, may regulate the nuclear relocalization of VHL. Unexpectedly, we found that VHL19, which is defective for binding SOCS1, is bound to chromatin under normal conditions. This suggests that VHL binding to SOCS1 is not necessary for its nuclear localization under normal conditions. Therefore, we predict that SOCS1 binding blocks DNA-damage induced nuclear export of VHL to promote the nuclear retention of VHL in the presence of DSBs. Since VHL19 cannot bind SOCS1, it is exported to the cytoplasm in the presence of DSBs. Mutation or deletion of the NLS and NES will help to define the role of these regulatory elements in the DNA-damage induced nuclear redistribution of VHL. We propose that binding to SOCS1 may induce a conformational change in VHL which may physically block the NES. X-ray crystallography of the VHL-SOCS1 complex and comparison to the resolved ECV complex would yield important structural information to determine if such a conformational change occurs. Undoubtedly, the results of these studies will

contribute to a greater understanding of how VHL's diverse tumour suppressor functions are regulated.

5.3.3 Mechanism of DSB-induced VHL19 degradation

Elucidating the molecular mechanisms underlying the DNA damage-induced degradation of VHL19 is critical for understanding how VHL regulates the DDR. The data presented in Chapter 3 indicates that VHL19 is degraded through the proteasome, suggesting that it may be targeted for K48-ubiquitylation in the presence of DNA damage. *In-vivo* ubiquitylation assays using Ub(K48), where all lysine have been mutated to arginine except K48, could be used to formally test this prediction. If VHL19 is K48-ubiquitylated after DNA damage, then identifying its E3 ligase will be crucial. Jung *et al.* have previously shown that the E2-EPF ubiquitin carrier protein (UCP) targets VHL for E3-independent proteasome-mediated degradation [275]. To date, E2-EPF UCP is the only known protein that targets VHL for degradation, making it a likely candidate for DNA-damage induced degradation of VHL19. If siRNA-knockdown of *E2-EPF* (*UBE2S*) in 786-VHL19 cells stabilizes VHL19 after DNA damage, then this strongly suggests that E2-EPF regulates VHL19 degradation. These findings could then be further validated with *in-vitro* or *in-vivo* ubiquitylation assays.

5.3.4 Inhibition of the DDR by VHL19

Once the mechanism underlying VHL19 degradation has been clearly defined, we can begin to investigate how VHL19 inhibits activation of the DDR. For example, if E2-EPF is found to degrade VHL19 in the presence of DSBs, then we can examine the recruitment of VHL19 and VHL30 to DSBs after E2-EPF inhibition using chromatin immunoprecipitation (ChIP)-based assays. If VHL19 blocks the recruitment of VHL30, then inhibition of E2-EPF would be predicted to result in retention of VHL19 and exclusion of VHL30 from DSBs.

A major limitation to the work presented in Chapter 3 is the reliance on CCRCC cell lines with overexpressed levels of VHL30 and VHL19. Although the functional differences between VHL19 and VHL30 can be clearly distinguished in these cell lines, the expression, localization, and dynamic regulation of endogenous VHL19 and VHL30 after DNA damage should be investigated in future studies.

5.3.5 VHL-dependent chromatin remodelling

The data presented in Chapter 4 provides evidence that VHL may mediate DSB-induced chromatin remodelling via regulation of HP1α. However, unravelling the molecular mechanisms that underlie this response will be critical for understanding the role of VHL in DSB repair.

Given that phosphorylation of HP1 has been shown to regulate its binding to chromatin, the effect of VHL on HP1α phosphorylation following DSB induction should be the focus of future studies. A number of approaches could feasibly be used to determine if VHL affects the phosphorylation status of HP1α. First, HP1α could be immunoprecipitated from HEK293A cells expressing ectopic VHL(WT) or VHL(P81S) in the presence or absence of DSBs. Since site-specific HP1α phospho-serine antibodies are not commercially available, the phosphorylation status of HP1α could be investigated by immunoblotting with a pan phospho-serine specific antibody. These experiments could be complemented with endogenous studies which examine the phosphorylation status of endogenous HP1α in cells with stable knockdown of VHL.

If VHL is found to have an effect on HP1α phosphorylation following DNA damage, then the specific phosphorylation site could be mapped. A previous study has revealed that mouse HP1α is phosphorylated *in-vivo* on two major sites: Ser14 and S93[276]. In addition, HP1α was shown to be phosphorylated *in-vitro* by CK2[276], but it remains to be determined whether HP1α is a CK2 target *in-vivo* and if this plays a role in the DDR. Based on these studies, it is likely that VHL mediates phosphorylation of HP1α on Ser14 and/or Ser93 upon induction of DSBs. However, sequence alignment of human HP1α, β, and γ reveal that Ser93 is conserved among the three isoforms, while Ser14 is present only in HP1α (**Fig. 4.1A)**. The binding specificity of VHL for HP1α therefore suggests that Ser14 is the most probable phosphorylation site. HP1α-S14A and -S92A (human homolog of S93 in mouse) mutants could then be used to determine the specific phosphorylation site and the functional effects on chromatin binding. Finally, CK2 inhibitors would be particularly useful in determining if VHL promotes CK2-mediated phosphorylation of HP1α and its effect on the DDR.

The data presented in Chapter 4 implies that VHL promotes chromatin decondensation; however, an *in-vivo* micrococcal nuclease (MNase) digestion assay could be used to directly assess the effect of VHL on DSB-induced chromatin accessibility and further validate the proposed model. MNase preferentially cleaves DNA between nucleosomes. Thus, the tight compaction of nucleosomes protects DNA from MNase digestion. DNA gel electrophoresis is then used to examine the extent of DNA digestion following MNase treatment, as a measure of nucleosome compaction. MNase digestion of nuclear fractions obtained from 786-Mock, -VHL(WT), and –VHL(P81S) in the absence or presence of DSBs could determine if VHL plays a role in chromatin relaxation following DSB induction and if HP1α interaction is necessary for this response.

5.3.6 Role of VHL in the repair of heterochromatic DSBs

Finally, determining whether VHL is necessary for the repair of DSB within heterochromatin and/or euchromatin will be an important question to address in future studies. Generally, γH2AX foci within DAPI-dense regions are classified as heterochromatic DSBs. However, the γH2AX defect in VHL-null and VHL(P81S) cells limits our ability to detect and monitor the repair of these breaks cytogenetically. Furthermore, the prominent heterochromatin-rich domains (chromocentres) found in murine cells are not observed in human cells. Since the VHL in murine cells is most similar to VHL19, which has an inhibitory effect on the DDR (discussed in Chapter 3), our studies are unfortunately restricted to human cells. An alternative method to examine heterochromatic DSB would be through the use of a modified DR-GFP construct. The DR-GFP construct used in this study was randomly integrated into the genome. Flanking the DR-GFP sequence with targeting arms homologous for a heterochromatic or euchromatic locus could conceivably allow for introduction of a DSB specifically within either heterochromatin or euchromatin. However, the compact nature heterochromatin would likely significantly reduce the integration efficiency. To overcome this barrier, cells could be treated transiently with an HDACI to increase the integration efficiency without permanently affecting the genomic integrity of the cells.

5.4 Therapeutic Implications for CCRCC

Several poly(ADP-ribose) polymerase (PARP) inhibitors are currently in clinical trials and have shown great promise for the treatment of a wide spectrum of cancers[277]. The family of PARP enzymes plays a key role in the repair of SSBs. Inhibition of PARP leads to the persistence of SSBs, which are converted into DSBs during S phase and repaired through HR[277]. However, if cells have a defect in HR repair mechanisms, inhibition of PARP would result in the accumulation of unrepaired DSBs and apoptosis. This synergistic effect is known as "synthetic lethality"[278]. In 2005, two independent research groups first demonstrated that BRCA1- and BRCA2-deficient cells were remarkably sensitive to PARP inhibitors, resulting in increased cell death[279, 280]. The great therapeutic advantage of PARP inhibitors is that cancer cells with HR defects are selectively killed and healthy cells, which retain the ability to repair DSBs through HR, remain relatively unaffected.

PARP inhibitors are currently being investigated as a novel therapy for BRCA1/2-deficient tumours such as breast and ovarian, and as well as other cancers with HR-defects including pancreatic and colorectal[281]. Clinical trials are investigating the therapeutic potential of PARP inhibitors as both single agents and combined treatment with DNA-damaging chemotherapy agents or radiotherapy[281]. Phase II trials with the PARP inhibitor, olaparib has shown encouraging response rates of 33% and 41% for BRCA1/2-deficient ovarian and breast cancers, respectively[282, 283] Although numerous pre-clinical studies have shown increased sensitivity to combined treatment with PARP inhibitors and cytotoxic agents such as alkylating agents, topoisomerase inhibitors, platinums, temozolomide, and radiotherapy, determining the effective dose combination has proven to be extremely challenging[284]. Myelosuppression is a common dose-limiting toxicity observed in these combination studies that has limited their success in the clinic[284]. Determining the optimal dosing schedule to maximize cytotoxicity in cancer cells and limit the toxicity to healthy cells is critical for the future success of combination therapy.

The data presented in Chapter 3 reveals a novel role for VHL in HR. Based on the selectivity of PARP inhibitors for HR-defective tumours, we hypothesize that loss of VHL in CCRCC would confer synthetic lethality to PARP inhibitors. In addition, the lack of treatment options for advanced stage CCRCC necessitates the investigation of PARP inhibitors as a novel treatment option for this highly aggressive cancer. While chemotherapy alone has shown poor response

rates in CCRCC, combined treatment with PARP inhibitors may augment the effects due to inactivation of both SSB and DSB repair pathways. Preliminary sensitivity assays using CCRCC cells treated with PARP inhibitors alone or in combination with chemotherapy agents such as doxorubicin should be of utmost importance for future studies to determine whether this is a potentially viable treatment option for CCRCC. Since many PARP inhibitors are in late-stage clinical trials already, their application to other HR-deficient tumours will hopefully hasten the time from bench to bedside.

Despite the encouraging response rates to PARP inhibitors in clinical trials, there remains a serious concern about long-term genotoxicity and secondary malignancies that may result from prolonged inhibition of DNA repair pathways. An alternative therapeutic approach would be to correct the DDR defect. In Chapter 4, **Fig. 4.5**, we demonstrated that the DDR defect in VHL-null cells could be successfully rescued by pre-treatment with an HDACI, rationalizing their use for the treatment of CCRCC. HDACs remove acetyl groups from histones to promote nucleosome compaction and gene silencing. Increased levels of HDACs have been reported in several cancers including, kidney, bladder, prostate, and testis, suggesting that these chromatin remodelling proteins may be an important therapeutic target[285-288]. In addition, many cancers show increased heterochromatization and may benefit from the chromatin decondensation effects of HDACIs[289]. Similar to PARP inhibitors, HDACIs are promising cancer therapeutics because they are preferentially toxic to cancer cells[289]. Several HDACIs are currently in early phase clinical trials and have been shown to be well tolerated and have good anti-tumour activities in a variety of hematopoietic malignancies and solid tumours[290]. Notably, Jones *et al.* have demonstrated the therapeutic potential of the HDACI VPA in CCRCC cell lines, where treatment with VPA led to significant growth arrest, blocked the attachment of tumour cells to ECM, and inhibited tumour growth in *in-vitro* and *in-vivo* models[291, 292]. Synergistic anti-tumour effects in kidney cancer have also been shown for combination therapies of HDACIs with mTOR inhibitors, epithelial growth factor (EGF)/VEGF receptor inhibitors, and topoisomerase I inhibitors[293-295]. These studies provide pre-clinical evidence for the therapeutic potential of HDACIs in CCRCC and rationalize their use for clinical trials. Based on our current data, we hypothesize that combined treatment with HDACIs and DNA-damaging agents such as doxorubicin may augment the DDR in CCRCC cells, sensitizing them to apoptosis.

In summary, the identification of VHL as a novel HR protein provides insight into the genomic instability associated with CCRCC and opens a realm of new therapeutic opportunities that may improve the outcome and quality of life for these patients.

Appendix

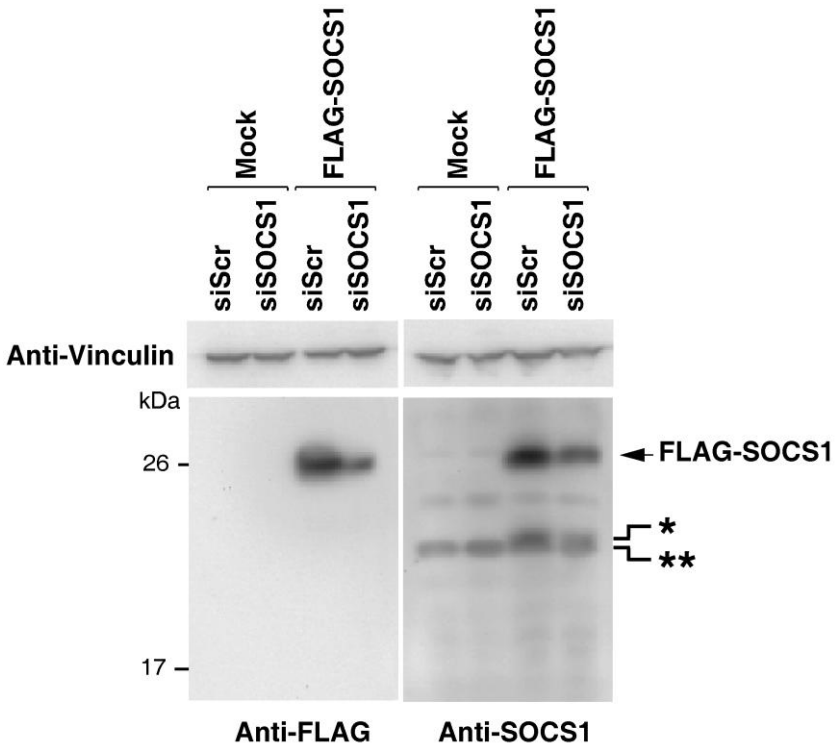

Figure A.1. Commercially available SOCS1 antibodies are unable to detect endogenous SOCS1. HEK293A cells were transfected with siScr or siSOCS1. 24 hrs post-transfection, cells were transfected with empty plasmid alone (Mock) or FLAG-SOCS1. 48 hrs later, cells were lysed and equal amounts of whole cell extracts were immunoblotted with monoclonal anti-FLAG (left), anti-SOCS1 (right), and anti-α-tubulin antibodies. *, N-terminal degradation product of FLAG-SOCS1; **, non-specific background band.

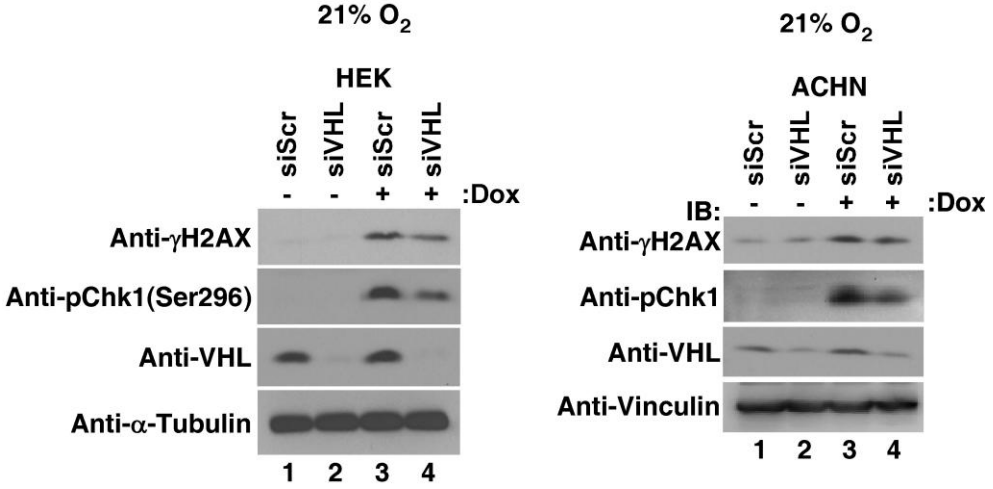

Figure A.2. Loss of VHL attenuates DDR signalling at 21% oxygen conditions. HEK293A or ACHN cells were transfected with siScr or siVHL and incubated at 21% O_2. 48 hrs post-transfection, cells were treated with (+) or without (-) 300ng/mL doxorubicin for 16 hrs. Equal amounts of whole cell lysates were immunoblotted with the indicated antibodies.

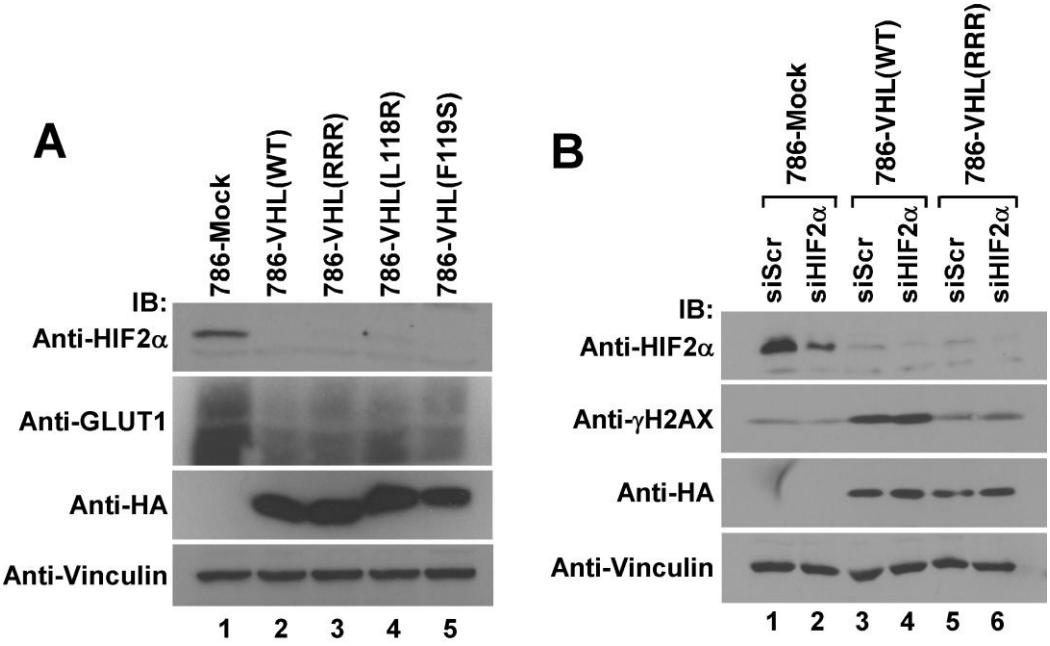

Figure A.3. VHL mutants with normal HIF regulatory function have defects in the DDR. **(a)** 786-Mock or 786-VHL(WT, RRR, L118R, or F119S) were lysed under normal oxygen conditions (21% O_2) and immunoblotted with the indicated antibodies. **(b)** 786-Mock, -VHL(WT), and -VHL(RRR) cells were transfected with siScr or siHIF2α. 48 hrs later cells were treated with 300ng/mL doxorubicin for 16 hrs. Cells were lysed and equal amounts of whole cell extracts were immunoblotted with the indicated antibodies.

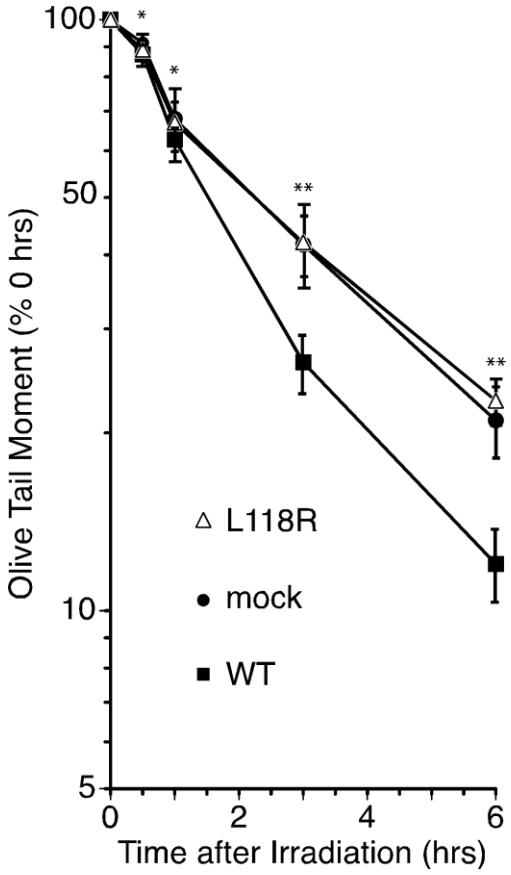

Figure A.4. VHL(L118R) is defective for repair of DSBs. 786-Mock, -VHL(WT), and –VHL(L118R) were exposed to 15 Gy γ-irradiation and a neutral comet assay was performed. 100 cells per sample were analyzed and average tail moment was calculated using Komet software v6.0 (Andor Technology). The relative extent of unrepaired DSBs was quantified by calculating the average olive tail moment as a percentage of the initial olive tail moment at time 0 hr (N=3 ±SE).

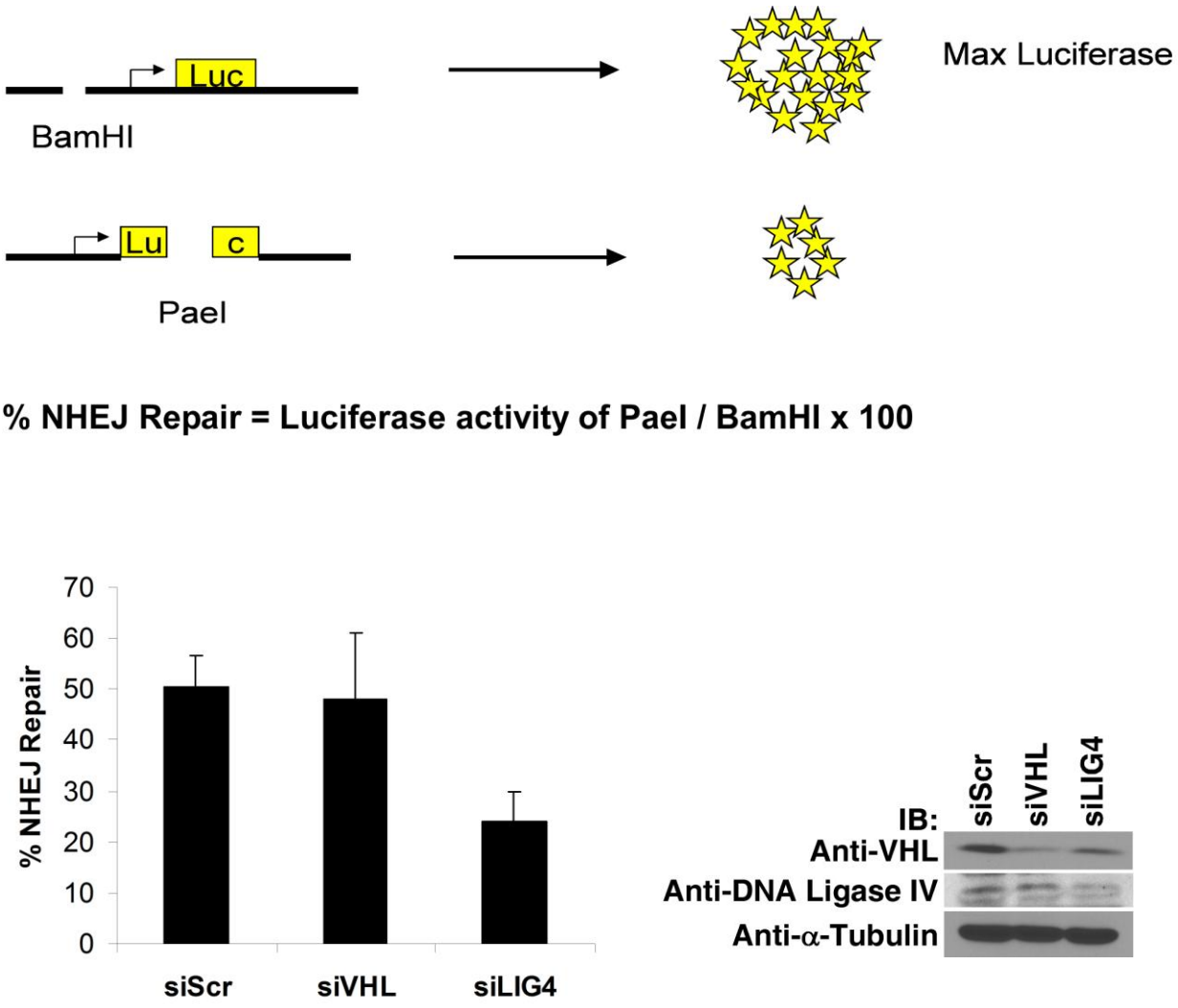

Figure A.5. Repair by NHEJ is unaffected by VHL knockdown. U2OS cells were transfected with siVHL, siLIG4, or a non-targeting control (siScr). Twenty-four hours later, cells were transfected with BamHI- or PaeI-digested pGL3. Forty-eight hours later, cells were harvested and luciferase activity was measured. Equal amounts of whole cell extracts were also immunoblotted with the indicated antibodies to assess knockdown efficiency.

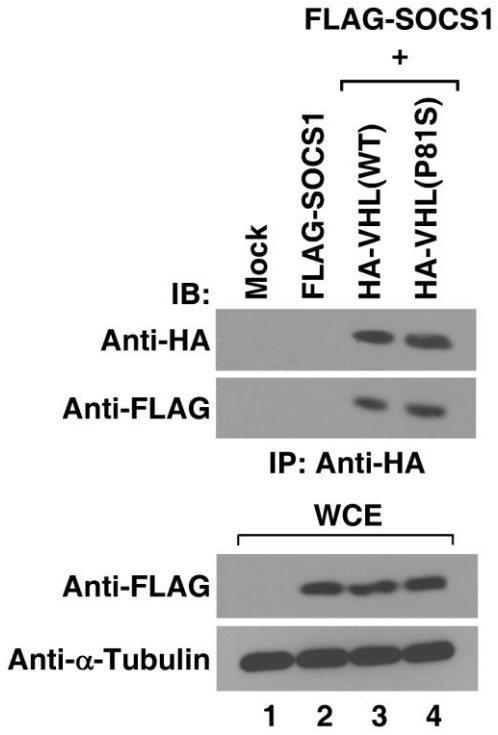

Figure A.6. SOCS1 binds VHL(WT) and VHL(P81S). HEK293A cells were transfected with the indicated plasmids. Forty-eight hours post-transfection cells were lysed and immunoprecipitated with mouse monoclonal anti-HA and immunoblotted with rabbit monoclonal anti-HA or rabbit polyclonal anti-FLAG. Equal amounts of whole cell extracts (WCE) were are immunoblotted with mouse monoclonal anti-FLAG or mouse monoclonal anti-α-tubulin.

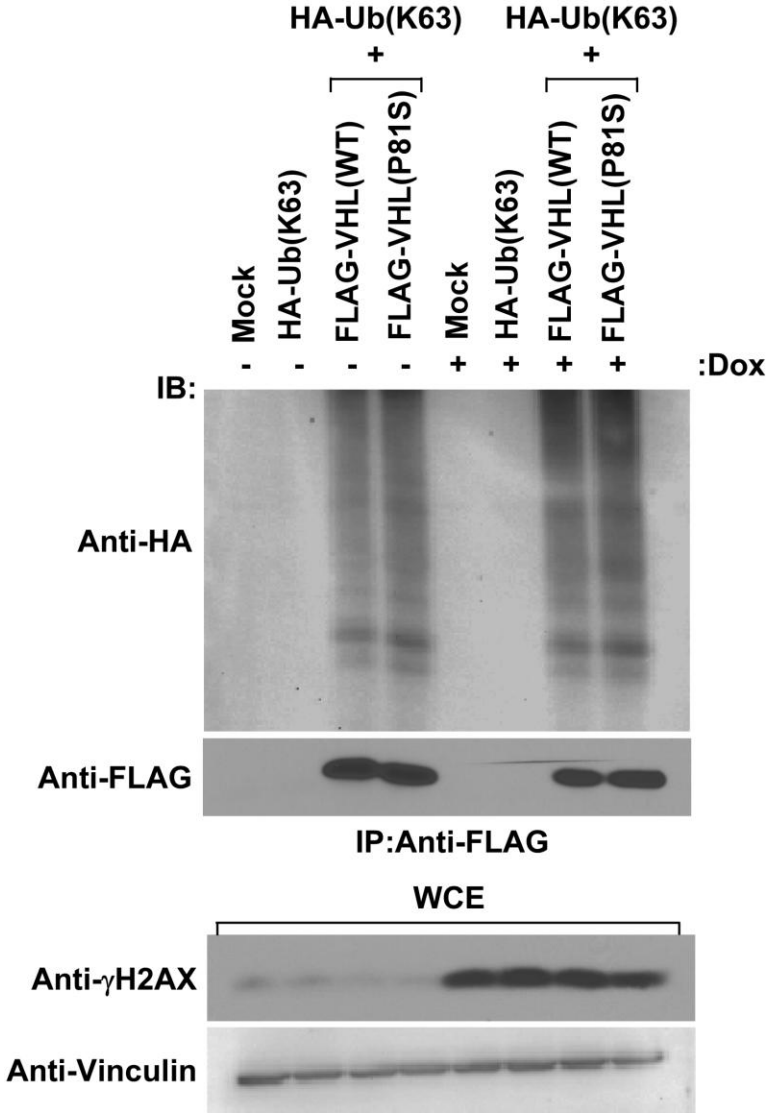

Figure A.7. VHL(P81S) retains the ability to be K63-ubiquitylated. HEK293A cells were transfected with the indicated constructs and 24hrs later were treated with (+) or without (-) 300ng/mL doxorubicin for 16hrs. Cell lysates were immunoprecipitated (IP) with anti-FLAG and immunoblotted (IB) with the indicated antibodies. Equal amounts of whole cell extracts (WCE) were also immunoblotted with anti-γH2AX and anti-α-tubulin.

References

1. Lindahl, T. & Barnes, D.E. Repair of endogenous DNA damage. *Cold Spring Harb Symp Quant Biol* 2000; **65**: 127-133.

2. Olive, P.L. & Johnston, P.J. DNA damage from oxidants: influence of lesion complexity and chromatin organization. *Oncol Res* 1997; **9**: 287-294.

3. Cadenas, E. Biochemistry of oxygen toxicity. *Annu Rev Biochem* 1989; **58**: 79-110.

4. Kawanishi, S., Hiraku, Y., Pinlaor, S. & Ma, N. Oxidative and nitrative DNA damage in animals and patients with inflammatory diseases in relation to inflammation-related carcinogenesis. *Biol Chem* 2006; **387**: 365-372.

5. Bassing, C.H. & Alt, F.W. The cellular response to general and programmed DNA double strand breaks. *DNA Repair (Amst)* 2004; **3**: 781-796.

6. d'Adda di Fagagna, F. *et al.* A DNA damage checkpoint response in telomere-initiated senescence. *Nature* 2003; **426**: 194-198.

7. Lempiainen, H. & Halazonetis, T.D. Emerging common themes in regulation of PIKKs and PI3Ks. *EMBO J* 2009; **28**: 3067-3073.

8. Lavin, M.F. ATM and the Mre11 complex combine to recognize and signal DNA double-strand breaks. *Oncogene* 2007; **26**: 7749-7758.

9. Smith, G.C. & Jackson, S.P. The DNA-dependent protein kinase. *Genes Dev* 1999; **13**: 916-934.

10. Cimprich, K.A. & Cortez, D. ATR: an essential regulator of genome integrity. *Nat Rev Mol Cell Biol* 2008; **9**: 616-627.

11. Bannister, A.J., Gottlieb, T.M., Kouzarides, T. & Jackson, S.P. c-Jun is phosphorylated by the DNA-dependent protein kinase in vitro; definition of the minimal kinase recognition motif. *Nucleic Acids Res* 1993; **21**: 1289-1295.

12. Kim, S.T., Lim, D.S., Canman, C.E. & Kastan, M.B. Substrate specificities and identification of putative substrates of ATM kinase family members. *J Biol Chem* 1999; **274**: 37538-37543.

13. Lovejoy, C.A. & Cortez, D. Common mechanisms of PIKK regulation. *DNA Repair (Amst)* 2009; **8**: 1004-1008.

14. Lee, J.H. & Paull, T.T. ATM activation by DNA double-strand breaks through the Mre11-Rad50-Nbs1 complex. *Science* 2005; **308**: 551-554.

15. Bakkenist, C.J. & Kastan, M.B. DNA damage activates ATM through intermolecular autophosphorylation and dimer dissociation. *Nature* 2003; **421**: 499-506.

16. Weterings, E. & Chen, D.J. The endless tale of non-homologous end-joining. *Cell Res* 2008; **18**: 114-124.

17. Rogakou, E.P., Pilch, D.R., Orr, A.H., Ivanova, V.S. & Bonner, W.M. DNA double-stranded breaks induce histone H2AX phosphorylation on serine 139. *J Biol Chem* 1998; **273**: 5858-5868.

18. Stucki, M. *et al.* MDC1 directly binds phosphorylated histone H2AX to regulate cellular responses to DNA double-strand breaks. *Cell* 2005; **123**: 1213-1226.

19. Lou, Z. *et al.* MDC1 maintains genomic stability by participating in the amplification of ATM-dependent DNA damage signals. *Mol Cell* 2006; **21**: 187-200.

20. Doil, C. *et al.* RNF168 binds and amplifies ubiquitin conjugates on damaged chromosomes to allow accumulation of repair proteins. *Cell* 2009; **136**: 435-446.

21. Kolas, N.K. *et al.* Orchestration of the DNA-damage response by the RNF8 ubiquitin ligase. *Science* 2007; **318**: 1637-1640.

22. Stewart, G.S. *et al.* The RIDDLE syndrome protein mediates a ubiquitin-dependent signaling cascade at sites of DNA damage. *Cell* 2009; **136**: 420-434.

23. Matsuoka, S. *et al.* ATM and ATR substrate analysis reveals extensive protein networks responsive to DNA damage. *Science* 2007; **316**: 1160-1166.

24. Zhang, J. *et al.* Chk2 phosphorylation of BRCA1 regulates DNA double-strand break repair. *Mol Cell Biol* 2004; **24**: 708-718.

25. Shiloh, Y. ATM and related protein kinases: safeguarding genome integrity. *Nat Rev Cancer* 2003; **3**: 155-168.

26. Goodarzi, A.A., Block, W.D. & Lees-Miller, S.P. The role of ATM and ATR in DNA damage-induced cell cycle control. *Prog Cell Cycle Res* 2003; **5**: 393-411.

27. Gatei, M. *et al.* Ataxia-telangiectasia-mutated (ATM) and NBS1-dependent phosphorylation of Chk1 on Ser-317 in response to ionizing radiation. *J Biol Chem* 2003; **278**: 14806-14811.

28. Lavin, M.F. & Kozlov, S. ATM activation and DNA damage response. *Cell Cycle* 2007; **6**: 931-942.

29. Bartek, J. & Lukas, J. Chk1 and Chk2 kinases in checkpoint control and cancer. *Cancer Cell* 2003; **3**: 421-429.

30. Delacote, F., Han, M., Stamato, T.D., Jasin, M. & Lopez, B.S. An xrcc4 defect or Wortmannin stimulates homologous recombination specifically induced by double-strand breaks in mammalian cells. *Nucleic Acids Res* 2002; **30**: 3454-3463.

31. Allen, C., Halbrook, J. & Nickoloff, J.A. Interactive competition between homologous recombination and non-homologous end joining. *Mol Cancer Res* 2003; **1**: 913-920.

32. Couedel, C. *et al.* Collaboration of homologous recombination and nonhomologous end-joining factors for the survival and integrity of mice and cells. *Genes Dev* 2004; **18**: 1293-1304.

33. Pierce, A.J., Hu, P., Han, M., Ellis, N. & Jasin, M. Ku DNA end-binding protein modulates homologous repair of double-strand breaks in mammalian cells. *Genes Dev* 2001; **15**: 3237-3242.

34. Takata, M. *et al.* Homologous recombination and non-homologous end-joining pathways of DNA double-strand break repair have overlapping roles in the maintenance of chromosomal integrity in vertebrate cells. *EMBO J* 1998; **17**: 5497-5508.

35. Fukushima, T. *et al.* Genetic analysis of the DNA-dependent protein kinase reveals an inhibitory role of Ku in late S-G2 phase DNA double-strand break repair. *J Biol Chem* 2001; **276**: 44413-44418.

36. Gottlieb, T.M. & Jackson, S.P. The DNA-dependent protein kinase: requirement for DNA ends and association with Ku antigen. *Cell* 1993; **72**: 131-142.

37. Paull, T.T. & Gellert, M. The 3' to 5' exonuclease activity of Mre 11 facilitates repair of DNA double-strand breaks. *Mol Cell* 1998; **1**: 969-979.

38. Nimonkar, A.V., Ozsoy, A.Z., Genschel, J., Modrich, P. & Kowalczykowski, S.C. Human exonuclease 1 and BLM helicase interact to resect DNA and initiate DNA repair. *Proc Natl Acad Sci U S A* 2008; **105**: 16906-16911.

39. Sartori, A.A. *et al.* Human CtIP promotes DNA end resection. *Nature* 2007; **450**: 509-514.

40. Jazayeri, A. *et al.* ATM- and cell cycle-dependent regulation of ATR in response to DNA double-strand breaks. *Nat Cell Biol* 2006; **8**: 37-45.

41. Myers, J.S. & Cortez, D. Rapid activation of ATR by ionizing radiation requires ATM and Mre11. *J Biol Chem* 2006; **281**: 9346-9350.

42. Somyajit, K., Basavaraju, S., Scully, R. & Nagaraju, G. ATM- and ATR-Mediated Phosphorylation of XRCC3 Regulates DNA Double-Strand Break-Induced Checkpoint Activation and Repair. *Mol Cell Biol* **33**: 1830-1844.

43. Tibbetts, R.S. *et al.* Functional interactions between BRCA1 and the checkpoint kinase ATR during genotoxic stress. *Genes Dev* 2000; **14**: 2989-3002.

44. Davies, S.L., North, P.S., Dart, A., Lakin, N.D. & Hickson, I.D. Phosphorylation of the Bloom's syndrome helicase and its role in recovery from S-phase arrest. *Mol Cell Biol* 2004; **24**: 1279-1291.

45. Mazon, G., Mimitou, E.P. & Symington, L.S. SnapShot: Homologous recombination in DNA double-strand break repair. *Cell* **142**: 646, 646 e641.

46. Chapman, J.R., Taylor, M.R. & Boulton, S.J. Playing the end game: DNA double-strand break repair pathway choice. *Mol Cell* **47**: 497-510.

47. Escribano-Diaz, C. *et al.* A cell cycle-dependent regulatory circuit composed of 53BP1-RIF1 and BRCA1-CtIP controls DNA repair pathway choice. *Mol Cell* **49**: 872-883.

48. Huertas, P. & Jackson, S.P. Human CtIP mediates cell cycle control of DNA end resection and double strand break repair. *J Biol Chem* 2009; **284**: 9558-9565.

49. Yu, X. & Chen, J. DNA damage-induced cell cycle checkpoint control requires CtIP, a phosphorylation-dependent binding partner of BRCA1 C-terminal domains. *Mol Cell Biol* 2004; **24**: 9478-9486.

50. Banin, S. *et al.* Enhanced phosphorylation of p53 by ATM in response to DNA damage. *Science* 1998; **281**: 1674-1677.

51. Nakagawa, K., Taya, Y., Tamai, K. & Yamaizumi, M. Requirement of ATM in phosphorylation of the human p53 protein at serine 15 following DNA double-strand breaks. *Mol Cell Biol* 1999; **19**: 2828-2834.

52. Siliciano, J.D. *et al.* DNA damage induces phosphorylation of the amino terminus of p53. *Genes Dev* 1997; **11**: 3471-3481.

53. Shieh, S.Y., Ahn, J., Tamai, K., Taya, Y. & Prives, C. The human homologs of checkpoint kinases Chk1 and Cds1 (Chk2) phosphorylate p53 at multiple DNA damage-inducible sites. *Genes Dev* 2000; **14**: 289-300.

54. Chehab, N.H., Malikzay, A., Stavridi, E.S. & Halazonetis, T.D. Phosphorylation of Ser-20 mediates stabilization of human p53 in response to DNA damage. *Proc Natl Acad Sci U S A* 1999; **96**: 13777-13782.

55. Dumaz, N. & Meek, D.W. Serine15 phosphorylation stimulates p53 transactivation but does not directly influence interaction with HDM2. *EMBO J* 1999; **18**: 7002-7010.

56. Caspari, T. How to activate p53. *Curr Biol* 2000; **10**: R315-317.

57. Hirao, A. *et al.* DNA damage-induced activation of p53 by the checkpoint kinase Chk2. *Science* 2000; **287**: 1824-1827.

58. Khosravi, R. *et al.* Rapid ATM-dependent phosphorylation of MDM2 precedes p53 accumulation in response to DNA damage. *Proc Natl Acad Sci U S A* 1999; **96**: 14973-14977.

59. Falck, J., Petrini, J.H., Williams, B.R., Lukas, J. & Bartek, J. The DNA damage-dependent intra-S phase checkpoint is regulated by parallel pathways. *Nat Genet* 2002; **30**: 290-294.

60. Wu, L., Luo, K., Lou, Z. & Chen, J. MDC1 regulates intra-S-phase checkpoint by targeting NBS1 to DNA double-strand breaks. *Proc Natl Acad Sci U S A* 2008; **105**: 11200-11205.

61. Varon, R. *et al.* Nibrin, a novel DNA double-strand break repair protein, is mutated in Nijmegen breakage syndrome. *Cell* 1998; **93**: 467-476.

62. Stewart, G.S. *et al.* The DNA double-strand break repair gene hMRE11 is mutated in individuals with an ataxia-telangiectasia-like disorder. *Cell* 1999; **99**: 577-587.

63. Carney, J.P. *et al.* The hMre11/hRad50 protein complex and Nijmegen breakage syndrome: linkage of double-strand break repair to the cellular DNA damage response. *Cell* 1998; **93**: 477-486.

64. Falck, J., Mailand, N., Syljuasen, R.G., Bartek, J. & Lukas, J. The ATM-Chk2-Cdc25A checkpoint pathway guards against radioresistant DNA synthesis. *Nature* 2001; **410**: 842-847.

65. Walter, J. & Newport, J. Initiation of eukaryotic DNA replication: origin unwinding and sequential chromatin association of Cdc45, RPA, and DNA polymerase alpha. *Mol Cell* 2000; **5**: 617-627.

66. Zou, L. & Stillman, B. Assembly of a complex containing Cdc45p, replication protein A, and Mcm2p at replication origins controlled by S-phase cyclin-dependent kinases and Cdc7p-Dbf4p kinase. *Mol Cell Biol* 2000; **20**: 3086-3096.

67. Aparicio, O.M., Stout, A.M. & Bell, S.P. Differential assembly of Cdc45p and DNA polymerases at early and late origins of DNA replication. *Proc Natl Acad Sci U S A* 1999; **96**: 9130-9135.

68. Rotman, G. & Shiloh, Y. ATM: a mediator of multiple responses to genotoxic stress. *Oncogene* 1999; **18**: 6135-6144.

69. O'Connell, M.J., Walworth, N.C. & Carr, A.M. The G2-phase DNA-damage checkpoint. *Trends Cell Biol* 2000; **10**: 296-303.

70. Passalaris, T.M., Benanti, J.A., Gewin, L., Kiyono, T. & Galloway, D.A. The G(2) checkpoint is maintained by redundant pathways. *Mol Cell Biol* 1999; **19**: 5872-5881.

71. Miyashita, T. & Reed, J.C. Tumor suppressor p53 is a direct transcriptional activator of the human bax gene. *Cell* 1995; **80**: 293-299.

72. Nakano, K. & Vousden, K.H. PUMA, a novel proapoptotic gene, is induced by p53. *Mol Cell* 2001; **7**: 683-694.

73. Oda, E. *et al.* Noxa, a BH3-only member of the Bcl-2 family and candidate mediator of p53-induced apoptosis. *Science* 2000; **288**: 1053-1058.

74. Martinou, J.C. & Green, D.R. Breaking the mitochondrial barrier. *Nat Rev Mol Cell Biol* 2001; **2**: 63-67.

75. Ferri, K.F. & Kroemer, G. Organelle-specific initiation of cell death pathways. *Nat Cell Biol* 2001; **3**: E255-263.

76. Toledo, L.I., Murga, M., Gutierrez-Martinez, P., Soria, R. & Fernandez-Capetillo, O. ATR signaling can drive cells into senescence in the absence of DNA breaks. *Genes Dev* 2008; **22**: 297-302.

77. Rebbaa, A., Zheng, X., Chou, P.M. & Mirkin, B.L. Caspase inhibition switches doxorubicin-induced apoptosis to senescence. *Oncogene* 2003; **22**: 2805-2811.

78. Mallette, F.A., Gaumont-Leclerc, M.F. & Ferbeyre, G. The DNA damage signaling pathway is a critical mediator of oncogene-induced senescence. *Genes Dev* 2007; **21**: 43-48.

79. Martens, U.M., Chavez, E.A., Poon, S.S., Schmoor, C. & Lansdorp, P.M. Accumulation of short telomeres in human fibroblasts prior to replicative senescence. *Exp Cell Res* 2000; **256**: 291-299.

80. Di Micco, R. *et al.* Oncogene-induced senescence is a DNA damage response triggered by DNA hyper-replication. *Nature* 2006; **444**: 638-642.

81. Bunz, F. *et al.* Requirement for p53 and p21 to sustain G2 arrest after DNA damage. *Science* 1998; **282**: 1497-1501.

82. Schmitt, C.A. Cellular senescence and cancer treatment. *Biochim Biophys Acta* 2007; **1775**: 5-20.

83. Robles, S.J. & Adami, G.R. Agents that cause DNA double strand breaks lead to p16INK4a enrichment and the premature senescence of normal fibroblasts. *Oncogene* 1998; **16**: 1113-1123.

84. Schmitt, C.A. *et al.* A senescence program controlled by p53 and p16INK4a contributes to the outcome of cancer therapy. *Cell* 2002; **109**: 335-346.

85. Linke, S.P., Clarkin, K.C. & Wahl, G.M. p53 mediates permanent arrest over multiple cell cycles in response to gamma-irradiation. *Cancer Res* 1997; **57**: 1171-1179.

86. Xu, H.J. *et al.* Reexpression of the retinoblastoma protein in tumor cells induces senescence and telomerase inhibition. *Oncogene* 1997; **15**: 2589-2596.

87. Narita, M. *et al.* Rb-mediated heterochromatin formation and silencing of E2F target genes during cellular senescence. *Cell* 2003; **113**: 703-716.

88. Strunnikova, M. *et al.* Chromatin inactivation precedes de novo DNA methylation during the progressive epigenetic silencing of the RASSF1A promoter. *Mol Cell Biol* 2005; **25**: 3923-3933.

89. Tamaru, H. *et al.* Trimethylated lysine 9 of histone H3 is a mark for DNA methylation in Neurospora crassa. *Nat Genet* 2003; **34**: 75-79.

90. Hershko, A. & Ciechanover, A. The ubiquitin system. *Annu Rev Biochem* 1998; **67**: 425-479.

91. Weissman, A.M. Themes and variations on ubiquitylation. *Nat Rev Mol Cell Biol* 2001; **2**: 169-178.

92. Jackson, S.P. & Durocher, D. Regulation of DNA damage responses by ubiquitin and SUMO. *Mol Cell* 2013; **49**: 795-807.

93. Panier, S. & Durocher, D. Regulatory ubiquitylation in response to DNA double-strand breaks. *DNA Repair (Amst)* 2009; **8**: 436-443.

94. Chen, A., Kleiman, F.E., Manley, J.L., Ouchi, T. & Pan, Z.Q. Autoubiquitination of the BRCA1*BARD1 RING ubiquitin ligase. *J Biol Chem* 2002; **277**: 22085-22092.

95. Hashizume, R. *et al.* The RING heterodimer BRCA1-BARD1 is a ubiquitin ligase inactivated by a breast cancer-derived mutation. *J Biol Chem* 2001; **276**: 14537-14540.

96. Wu, L.C. *et al.* Identification of a RING protein that can interact in vivo with the BRCA1 gene product. *Nat Genet* 1996; **14**: 430-440.

97. Yu, X., Fu, S., Lai, M., Baer, R. & Chen, J. BRCA1 ubiquitinates its phosphorylation-dependent binding partner CtIP. *Genes Dev* 2006; **20**: 1721-1726.

98. Shanbhag, N.M., Rafalska-Metcalf, I.U., Balane-Bolivar, C., Janicki, S.M. & Greenberg, R.A. ATM-dependent chromatin changes silence transcription in cis to DNA double-strand breaks. *Cell* **141**: 970-981.

99. Cooper, E.M. *et al.* K63-specific deubiquitination by two JAMM/MPN+ complexes: BRISC-associated Brcc36 and proteasomal Poh1. *EMBO J* 2009; **28**: 621-631.

100. Juang, Y.C. *et al.* OTUB1 co-opts Lys48-linked ubiquitin recognition to suppress E2 enzyme function. *Mol Cell* **45**: 384-397.

101. Wiener, R., Zhang, X., Wang, T. & Wolberger, C. The mechanism of OTUB1-mediated inhibition of ubiquitination. *Nature* **483**: 618-622.

102. Fraile, J.M., Quesada, V., Rodriguez, D., Freije, J.M. & Lopez-Otin, C. Deubiquitinases in cancer: new functions and therapeutic options. *Oncogene* **31**: 2373-2388.

103. Yeh, E.T. SUMOylation and De-SUMOylation: wrestling with life's processes. *J Biol Chem* 2009; **284**: 8223-8227.

104. Galanty, Y. *et al.* Mammalian SUMO E3-ligases PIAS1 and PIAS4 promote responses to DNA double-strand breaks. *Nature* 2009; **462**: 935-939.

105. Morris, J.R. *et al.* The SUMO modification pathway is involved in the BRCA1 response to genotoxic stress. *Nature* 2009; **462**: 886-890.

106. Dou, H., Huang, C., Singh, M., Carpenter, P.B. & Yeh, E.T. Regulation of DNA repair through deSUMOylation and SUMOylation of replication protein A complex. *Mol Cell* **39**: 333-345.

107. Kornberg, R.D. Chromatin structure: a repeating unit of histones and DNA. *Science* 1974; **184**: 868-871.

108. Finch, J.T. & Klug, A. Solenoidal model for superstructure in chromatin. *Proc Natl Acad Sci U S A* 1976; **73**: 1897-1901.

109. Gerchman, S.E. & Ramakrishnan, V. Chromatin higher-order structure studied by neutron scattering and scanning transmission electron microscopy. *Proc Natl Acad Sci U S A* 1987; **84**: 7802-7806.

110. Fan, Y. *et al.* Histone H1 depletion in mammals alters global chromatin structure but causes specific changes in gene regulation. *Cell* 2005; **123**: 1199-1212.

111. Rattner, J.B. & Lin, C.C. Radial loops and helical coils coexist in metaphase chromosomes. *Cell* 1985; **42**: 291-296.

112. Widom, J. & Klug, A. Structure of the 300A chromatin filament: X-ray diffraction from oriented samples. *Cell* 1985; **43**: 207-213.

113. Guenatri, M., Bailly, D., Maison, C. & Almouzni, G. Mouse centric and pericentric satellite repeats form distinct functional heterochromatin. *J Cell Biol* 2004; **166**: 493-505.

114. Yunis, J.J. & Yasmineh, W.G. Heterochromatin, satellite DNA, and cell function. Structural DNA of eucaryotes may support and protect genes and aid in speciation. *Science* 1971; **174**: 1200-1209.

115. Goodarzi, A.A., Jeggo, P. & Lobrich, M. The influence of heterochromatin on DNA double strand break repair: Getting the strong, silent type to relax. *DNA Repair (Amst)* **9**: 1273-1282.

116. Denslow, S.A. & Wade, P.A. The human Mi-2/NuRD complex and gene regulation. *Oncogene* 2007; **26**: 5433-5438.

117. Hediger, F. & Gasser, S.M. Heterochromatin protein 1: don't judge the book by its cover! *Curr Opin Genet Dev* 2006; **16**: 143-150.

118. Cowell, I.G. *et al.* gammaH2AX foci form preferentially in euchromatin after ionising-radiation. *PLoS One* 2007; **2**: e1057.

119. Kim, J.A., Kruhlak, M., Dotiwala, F., Nussenzweig, A. & Haber, J.E. Heterochromatin is refractory to gamma-H2AX modification in yeast and mammals. *J Cell Biol* 2007; **178**: 209-218.

120. Karagiannis, T.C., Harikrishnan, K.N. & El-Osta, A. Disparity of histone deacetylase inhibition on repair of radiation-induced DNA damage on euchromatin and constitutive heterochromatin compartments. *Oncogene* 2007; **26**: 3963-3971.

121. Chiolo, I. *et al.* Double-strand breaks in heterochromatin move outside of a dynamic HP1a domain to complete recombinational repair. *Cell* 2011; **144**: 732-744.

122. Goodarzi, A.A. *et al.* ATM signaling facilitates repair of DNA double-strand breaks associated with heterochromatin. *Mol Cell* 2008; **31**: 167-177.

123. Jakob, B. *et al.* DNA double-strand breaks in heterochromatin elicit fast repair protein recruitment, histone H2AX phosphorylation and relocation to euchromatin. *Nucleic Acids Res* 2011; **39**: 6489-6499.

124. Jakob, B. *et al.* DNA double-strand breaks in heterochromatin elicit fast repair protein recruitment, histone H2AX phosphorylation and relocation to euchromatin. *Nucleic Acids Res* **39**: 6489-6499.

125. Riballo, E. *et al.* A pathway of double-strand break rejoining dependent upon ATM, Artemis, and proteins locating to gamma-H2AX foci. *Mol Cell* 2004; **16**: 715-724.

126. Kruhlak, M.J. *et al.* Changes in chromatin structure and mobility in living cells at sites of DNA double-strand breaks. *J Cell Biol* 2006; **172**: 823-834.

127. Kruhlak, M.J., Celeste, A. & Nussenzweig, A. Spatio-temporal dynamics of chromatin containing DNA breaks. *Cell Cycle* 2006; **5**: 1910-1912.

128. Falk, M., Lukasova, E., Gabrielova, B., Ondrej, V. & Kozubek, S. Chromatin dynamics during DSB repair. *Biochim Biophys Acta* 2007; **1773**: 1534-1545.

129. Sun, Y., Jiang, X., Chen, S., Fernandes, N. & Price, B.D. A role for the Tip60 histone acetyltransferase in the acetylation and activation of ATM. *Proc Natl Acad Sci U S A* 2005; **102**: 13182-13187.

130. Sun, Y. *et al.* Histone H3 methylation links DNA damage detection to activation of the tumour suppressor Tip60. *Nat Cell Biol* 2009; **11**: 1376-1382.

131. Bird, A.W. *et al.* Acetylation of histone H4 by Esa1 is required for DNA double-strand break repair. *Nature* 2002; **419**: 411-415.

132. Ikura, T. *et al.* DNA damage-dependent acetylation and ubiquitination of H2AX enhances chromatin dynamics. *Mol Cell Biol* 2007; **27**: 7028-7040.

133. Ayoub, N., Jeyasekharan, A.D. & Venkitaraman, A.R. Mobilization and recruitment of HP1: a bimodal response to DNA breakage. *Cell Cycle* 2009; **8**: 2945-2950.

134. Luijsterburg, M.S. *et al.* Heterochromatin protein 1 is recruited to various types of DNA damage. *J Cell Biol* 2009; **185**: 577-586.

135. Ziv, Y. *et al.* Chromatin relaxation in response to DNA double-strand breaks is modulated by a novel ATM- and KAP-1 dependent pathway. *Nat Cell Biol* 2006; **8**: 870-876.

136. White, D.E. *et al.* KAP1, a novel substrate for PIKK family members, colocalizes with numerous damage response factors at DNA lesions. *Cancer Res* 2006; **66**: 11594-11599.

137. Sun, Y., Xu, Y., Roy, K. & Price, B.D. DNA damage-induced acetylation of lysine 3016 of ATM activates ATM kinase activity. *Mol Cell Biol* 2007; **27**: 8502-8509.

138. Noon, A.T. *et al.* 53BP1-dependent robust localized KAP-1 phosphorylation is essential for heterochromatic DNA double-strand break repair. *Nat Cell Biol* 2010; **12**: 177-184.

139. Hanahan, D. & Weinberg, R.A. The hallmarks of cancer. *Cell* 2000; **100**: 57-70.

140. Loeb, L.A. Mutator phenotype may be required for multistage carcinogenesis. *Cancer Res* 1991; **51**: 3075-3079.

141. Loeb, L.A., Loeb, K.R. & Anderson, J.P. Multiple mutations and cancer. *Proc Natl Acad Sci U S A* 2003; **100**: 776-781.

142. Nowell, P.C. The clonal evolution of tumor cell populations. *Science* 1976; **194**: 23-28.

143. Lengauer, C., Kinzler, K.W. & Vogelstein, B. Genetic instability in colorectal cancers. *Nature* 1997; **386**: 623-627.

144. van Gent, D.C., Hoeijmakers, J.H. & Kanaar, R. Chromosomal stability and the DNA double-stranded break connection. *Nat Rev Genet* 2001; **2**: 196-206.

145. Shiloh, Y. & Kastan, M.B. ATM: genome stability, neuronal development, and cancer cross paths. *Adv Cancer Res* 2001; **83**: 209-254.

146. O'Donovan, P.J. & Livingston, D.M. BRCA1 and BRCA2: breast/ovarian cancer susceptibility gene products and participants in DNA double-strand break repair. *Carcinogenesis* 2010; **31**: 961-967.

147. Cohen, H.T. & McGovern, F.J. Renal-cell carcinoma. *N Engl J Med* 2005; **353**: 2477-2490.

148. Holthofer, H. *et al.* Cellular origin and differentiation of renal carcinomas. A fluorescence microscopic study with kidney-specific antibodies, antiintermediate filament antibodies, and lectins. *Lab Invest* 1983; **49**: 317-326.

149. Wallace, A.C. & Nairn, R.C. Renal tubular antigens in kidney tumors. *Cancer* 1972; **29**: 977-981.

150. Oberling, C., Riviere, M. & Haguenau, F. Ultrastructure of the clear cells in renal carcinomas and its importance for the demonstration of their renal origin. *Nature* 1960; **186**: 402-403.

151. Costa, L.J. & Drabkin, H.A. Renal cell carcinoma: new developments in molecular biology and potential for targeted therapies. *Oncologist* 2007; **12**: 1404-1415.

152. Yagoda, A., Abi-Rached, B. & Petrylak, D. Chemotherapy for advanced renal-cell carcinoma: 1983-1993. *Semin Oncol* 1995; **22**: 42-60.

153. Arai, E. & Kanai, Y. Genetic and epigenetic alterations during renal carcinogenesis. *Int J Clin Exp Pathol* 2011; **4**: 58-73.

154. Varela, I. *et al.* Exome sequencing identifies frequent mutation of the SWI/SNF complex gene PBRM1 in renal carcinoma. *Nature* 2011; **469**: 539-542.

155. Kaelin, W.G., Jr. The von Hippel-Lindau tumor suppressor protein and clear cell renal carcinoma. *Clin Cancer Res* 2007; **13**: 680s-684s.

156. Kim, W.Y. & Kaelin, W.G. Role of VHL gene mutation in human cancer. *J Clin Oncol* 2004; **22**: 4991-5004.

157. Latif, F. *et al.* Identification of the von Hippel-Lindau disease tumor suppressor gene. *Science* 1993; **260**: 1317-1320.

158. Maher, E.R. *et al.* Clinical features and natural history of von Hippel-Lindau disease. *Q J Med* 1990; **77**: 1151-1163.

159. Maher, E.R. & Kaelin, W.G., Jr. von Hippel-Lindau disease. *Medicine (Baltimore)* 1997; **76**: 381-391.

160. Seizinger, B.R. *et al.* Von Hippel-Lindau disease maps to the region of chromosome 3 associated with renal cell carcinoma. *Nature* 1988; **332**: 268-269.

161. Ohh, M. & Kaelin, W.G., Jr. VHL and kidney cancer. *Methods Mol Biol* 2003; **222**: 167-183.

162. Iliopoulos, O., Kibel, A., Gray, S. & Kaelin, W.G., Jr. Tumour suppression by the human von Hippel-Lindau gene product. *Nat Med* 1995; **1**: 822-826.

163. Schoenfeld, A., Davidowitz, E.J. & Burk, R.D. A second major native von Hippel-Lindau gene product, initiated from an internal translation start site, functions as a tumor suppressor. *Proc Natl Acad Sci U S A* 1998; **95**: 8817-8822.

164. Blankenship, C., Naglich, J.G., Whaley, J.M., Seizinger, B. & Kley, N. Alternate choice of initiation codon produces a biologically active product of the von Hippel Lindau gene with tumor suppressor activity. *Oncogene* 1999; **18**: 1529-1535.

165. van der Harst, E. *et al.* Germline mutations in the vhl gene in patients presenting with phaeochromocytomas. *Int J Cancer* 1998; **77**: 337-340.

166. Crossey, P.A. *et al.* Identification of intragenic mutations in the von Hippel-Lindau disease tumour suppressor gene and correlation with disease phenotype. *Hum Mol Genet* 1994; **3**: 1303-1308.

167. Zbar, B. *et al.* Germline mutations in the Von Hippel-Lindau disease (VHL) gene in families from North America, Europe, and Japan. *Hum Mutat* 1996; **8**: 348-357.

168. Lolkema, M.P. *et al.* Tumor suppression by the von Hippel-Lindau protein requires phosphorylation of the acidic domain. *J Biol Chem* 2005; **280**: 22205-22211.

169. Lee, S. *et al.* Nuclear/cytoplasmic localization of the von Hippel-Lindau tumor suppressor gene product is determined by cell density. *Proc Natl Acad Sci U S A* 1996; **93**: 1770-1775.

170. Lee, S. *et al.* Transcription-dependent nuclear-cytoplasmic trafficking is required for the function of the von Hippel-Lindau tumor suppressor protein. *Mol Cell Biol* 1999; **19**: 1486-1497.

171. Mekhail, K. *et al.* Regulation of ubiquitin ligase dynamics by the nucleolus. *J Cell Biol* 2005; **170**: 733-744.

172. Khacho, M., Mekhail, K., Pilon-Larose, K., Payette, J. & Lee, S. Cancer-causing mutations in a novel transcription-dependent nuclear export motif of VHL abrogate oxygen-dependent degradation of hypoxia-inducible factor. *Mol Cell Biol* 2008; **28**: 302-314.

173. Lewis, M.D. & Roberts, B.J. Role of nuclear and cytoplasmic localization in the tumour-suppressor activity of the von Hippel-Lindau protein. *Oncogene* 2003; **22**: 3992-3997.

174. Lonergan, K.M. *et al.* Regulation of hypoxia-inducible mRNAs by the von Hippel-Lindau tumor suppressor protein requires binding to complexes containing elongins B/C and Cul2. *Mol Cell Biol* 1998; **18**: 732-741.

175. Pause, A. *et al.* The von Hippel-Lindau tumor-suppressor gene product forms a stable complex with human CUL-2, a member of the Cdc53 family of proteins. *Proc Natl Acad Sci U S A* 1997; **94**: 2156-2161.

176. Kamura, T. *et al.* Rbx1, a component of the VHL tumor suppressor complex and SCF ubiquitin ligase. *Science* 1999; **284**: 657-661.

177. Bai, C. *et al.* SKP1 connects cell cycle regulators to the ubiquitin proteolysis machinery through a novel motif, the F-box. *Cell* 1996; **86**: 263-274.

178. Deshaies, R.J. SCF and Cullin/Ring H2-based ubiquitin ligases. *Annu Rev Cell Dev Biol* 1999; **15**: 435-467.

179. Willems, A.R. *et al.* SCF ubiquitin protein ligases and phosphorylation-dependent proteolysis. *Philos Trans R Soc Lond B Biol Sci* 1999; **354**: 1533-1550.

180. Skowyra, D., Craig, K.L., Tyers, M., Elledge, S.J. & Harper, J.W. F-box proteins are receptors that recruit phosphorylated substrates to the SCF ubiquitin-ligase complex. *Cell* 1997; **91**: 209-219.

181. Iwai, K. *et al.* Identification of the von Hippel-lindau tumor-suppressor protein as part of an active E3 ubiquitin ligase complex. *Proc Natl Acad Sci U S A* 1999; **96**: 12436-12441.

182. Lisztwan, J., Imbert, G., Wirbelauer, C., Gstaiger, M. & Krek, W. The von Hippel-Lindau tumor suppressor protein is a component of an E3 ubiquitin-protein ligase activity. *Genes Dev* 1999; **13**: 1822-1833.

183. Stebbins, C.E., Kaelin, W.G., Jr. & Pavletich, N.P. Structure of the VHL-ElonginC-ElonginB complex: implications for VHL tumor suppressor function. *Science* 1999; **284**: 455-461.

184. Wizigmann-Voos, S., Breier, G., Risau, W. & Plate, K.H. Up-regulation of vascular endothelial growth factor and its receptors in von Hippel-Lindau disease-associated and sporadic hemangioblastomas. *Cancer Res* 1995; **55**: 1358-1364.

185. Takahashi, A. *et al.* Markedly increased amounts of messenger RNAs for vascular endothelial growth factor and placenta growth factor in renal cell carcinoma associated with angiogenesis. *Cancer Res* 1994; **54**: 4233-4237.

186. Brown, L.F. *et al.* Increased expression of vascular permeability factor (vascular endothelial growth factor) and its receptors in kidney and bladder carcinomas. *Am J Pathol* 1993; **143**: 1255-1262.

187. Morii, K., Tanaka, R., Washiyama, K., Kumanishi, T. & Kuwano, R. Expression of vascular endothelial growth factor in capillary hemangioblastoma. *Biochem Biophys Res Commun* 1993; **194**: 749-755.

188. Nicol, D. *et al.* Vascular endothelial growth factor expression is increased in renal cell carcinoma. *J Urol* 1997; **157**: 1482-1486.

189. Krieg, M., Marti, H.H. & Plate, K.H. Coexpression of erythropoietin and vascular endothelial growth factor in nervous system tumors associated with von Hippel-Lindau tumor suppressor gene loss of function. *Blood* 1998; **92**: 3388-3393.

190. Flamme, I., Krieg, M. & Plate, K.H. Up-regulation of vascular endothelial growth factor in stromal cells of hemangioblastomas is correlated with up-regulation of the transcription factor HRF/HIF-2alpha. *Am J Pathol* 1998; **153**: 25-29.

191. Golde, D.W., Hocking, W.G., Koeffler, H.P. & Adamson, J.W. Polycythemia: mechanisms and management. *Ann Intern Med* 1981; **95**: 71-87.

192. Semenza, G.L. HIF-1 and human disease: one highly involved factor. *Genes Dev* 2000; **14**: 1983-1991.

193. Freeburg, P.B. & Abrahamson, D.R. Hypoxia-inducible factors and kidney vascular development. *J Am Soc Nephrol* 2003; **14**: 2723-2730.

194. Maxwell, P.H. *et al.* The tumour suppressor protein VHL targets hypoxia-inducible factors for oxygen-dependent proteolysis. *Nature* 1999; **399**: 271-275.

195. Cockman, M.E. *et al.* Hypoxia inducible factor-alpha binding and ubiquitylation by the von Hippel-Lindau tumor suppressor protein. *J Biol Chem* 2000; **275**: 25733-25741.

196. Greer, S.N., Metcalf, J.L., Wang, Y. & Ohh, M. The updated biology of hypoxia-inducible factor. *EMBO J* 2012; **31**: 2448-2460.

197. Maynard, M.A. & Ohh, M. Von Hippel-Lindau tumor suppressor protein and hypoxia-inducible factor in kidney cancer. *Am J Nephrol* 2004; **24**: 1-13.

198. Bruick, R.K. & McKnight, S.L. A conserved family of prolyl-4-hydroxylases that modify HIF. *Science* 2001; **294**: 1337-1340.

199. Ivan, M. *et al.* Biochemical purification and pharmacological inhibition of a mammalian prolyl hydroxylase acting on hypoxia-inducible factor. *Proc Natl Acad Sci U S A* 2002; **99**: 13459-13464.

200. Ivan, M. *et al.* HIFalpha targeted for VHL-mediated destruction by proline hydroxylation: implications for O2 sensing. *Science* 2001; **292**: 464-468.

201. Jaakkola, P. *et al.* Targeting of HIF-alpha to the von Hippel-Lindau ubiquitylation complex by O2-regulated prolyl hydroxylation. *Science* 2001; **292**: 468-472.

202. Ohh, M. *et al.* Ubiquitination of hypoxia-inducible factor requires direct binding to the beta-domain of the von Hippel-Lindau protein. *Nat Cell Biol* 2000; **2**: 423-427.

203. Wang, G.L., Jiang, B.H., Rue, E.A. & Semenza, G.L. Hypoxia-inducible factor 1 is a basic-helix-loop-helix-PAS heterodimer regulated by cellular O2 tension. *Proc Natl Acad Sci U S A* 1995; **92**: 5510-5514.

204. Baba, Y. *et al.* HIF1A overexpression is associated with poor prognosis in a cohort of 731 colorectal cancers. *Am J Pathol* **176**: 2292-2301.

205. Hashimoto, O. *et al.* Hypoxia induces tumor aggressiveness and the expansion of CD133-positive cells in a hypoxia-inducible factor-1alpha-dependent manner in pancreatic cancer cells. *Pathobiology* **78**: 181-192.

206. Birner, P., Schindl, M., Obermair, A., Breitenecker, G. & Oberhuber, G. Expression of hypoxia-inducible factor 1alpha in epithelial ovarian tumors: its impact on prognosis and on response to chemotherapy. *Clin Cancer Res* 2001; **7**: 1661-1668.

207. Zagzag, D. *et al.* Expression of hypoxia-inducible factor 1alpha in brain tumors: association with angiogenesis, invasion, and progression. *Cancer* 2000; **88**: 2606-2618.

208. Bos, R. *et al.* Levels of hypoxia-inducible factor-1alpha independently predict prognosis in patients with lymph node negative breast carcinoma. *Cancer* 2003; **97**: 1573-1581.

209. Kondo, K., Kim, W.Y., Lechpammer, M. & Kaelin, W.G., Jr. Inhibition of HIF2alpha is sufficient to suppress pVHL-defective tumor growth. *PLoS Biol* 2003; **1**: E83.

210. Ohh, M. *et al.* The von Hippel-Lindau tumor suppressor protein is required for proper assembly of an extracellular fibronectin matrix. *Mol Cell* 1998; **1**: 959-968.

211. Russell, R.C. & Ohh, M. NEDD8 acts as a 'molecular switch' defining the functional selectivity of VHL. *EMBO Rep* 2008; **9**: 486-491.

212. Grosfeld, A. *et al.* Interaction of hydroxylated collagen IV with the von hippel-lindau tumor suppressor. *J Biol Chem* 2007; **282**: 13264-13269.

213. Kurban, G. *et al.* Collagen matrix assembly is driven by the interaction of von Hippel-Lindau tumor suppressor protein with hydroxylated collagen IV alpha 2. *Oncogene* 2008; **27**: 1004-1012.

214. Lubensky, I.A. *et al.* Allelic deletions of the VHL gene detected in multiple microscopic clear cell renal lesions in von Hippel-Lindau disease patients. *Am J Pathol* 1996; **149**: 2089-2094.

215. Pazour, G.J. Intraflagellar transport and cilia-dependent renal disease: the ciliary hypothesis of polycystic kidney disease. *J Am Soc Nephrol* 2004; **15**: 2528-2536.

216. Davenport, J.R. & Yoder, B.K. An incredible decade for the primary cilium: a look at a once-forgotten organelle. *Am J Physiol Renal Physiol* 2005; **289**: F1159-1169.

217. Rosenbaum, J.L. & Witman, G.B. Intraflagellar transport. *Nat Rev Mol Cell Biol* 2002; **3**: 813-825.

218. Praetorius, H.A. & Spring, K.R. Bending the MDCK cell primary cilium increases intracellular calcium. *J Membr Biol* 2001; **184**: 71-79.

219. Esteban, M.A., Harten, S.K., Tran, M.G. & Maxwell, P.H. Formation of primary cilia in the renal epithelium is regulated by the von Hippel-Lindau tumor suppressor protein. *J Am Soc Nephrol* 2006; **17**: 1801-1806.

220. Schermer, B. *et al.* The von Hippel-Lindau tumor suppressor protein controls ciliogenesis by orienting microtubule growth. *J Cell Biol* 2006; **175**: 547-554.

221. Lutz, M.S. & Burk, R.D. Primary cilium formation requires von hippel-lindau gene function in renal-derived cells. *Cancer Res* 2006; **66**: 6903-6907.

222. Qi, H. & Ohh, M. The von Hippel-Lindau tumor suppressor protein sensitizes renal cell carcinoma cells to tumor necrosis factor-induced cytotoxicity by suppressing the nuclear factor-kappaB-dependent antiapoptotic pathway. *Cancer Res* 2003; **63**: 7076-7080.

223. An, J. & Rettig, M.B. Mechanism of von Hippel-Lindau protein-mediated suppression of nuclear factor kappa B activity. *Mol Cell Biol* 2005; **25**: 7546-7556.

224. An, J., Fisher, M. & Rettig, M.B. VHL expression in renal cell carcinoma sensitizes to bortezomib (PS-341) through an NF-kappaB-dependent mechanism. *Oncogene* 2005; **24**: 1563-1570.

225. Yang, H. *et al.* pVHL acts as an adaptor to promote the inhibitory phosphorylation of the NF-kappaB agonist Card9 by CK2. *Mol Cell* 2007; **28**: 15-27.

226. Roe, J.S. *et al.* p53 stabilization and transactivation by a von Hippel-Lindau protein. *Mol Cell* 2006; **22**: 395-405.

227. Roe, J.S. *et al.* Phosphorylation of von Hippel-Lindau protein by checkpoint kinase 2 regulates p53 transactivation. *Cell Cycle* **10**: 3920-3928.

228. Russell, R.C. *et al.* Loss of JAK2 regulation via a heterodimeric VHL-SOCS1 E3 ubiquitin ligase underlies Chuvash polycythemia. *Nat Med* 2011; **17**: 845-853.

229. Calabrese, V. *et al.* SOCS1 links cytokine signaling to p53 and senescence. *Mol Cell* 2009; **36**: 754-767.

230. Fernandez-Capetillo, O., Lee, A., Nussenzweig, M. & Nussenzweig, A. H2AX: the histone guardian of the genome. *DNA Repair (Amst)* 2004; **3**: 959-967.

231. Celeste, A. *et al.* Genomic instability in mice lacking histone H2AX. *Science* 2002; **296**: 922-927.

232. Kastan, M.B. & Lim, D.S. The many substrates and functions of ATM. *Nat Rev Mol Cell Biol* 2000; **1**: 179-186.

233. Jaakkola, P. *et al.* Targeting of HIF-alpha to the von Hippel-Lindau ubiquitylation complex by O2-regulated prolyl hydroxylation. *Science* 2001; **292**: 468-472.

234. Wang, Y. *et al.* Regulation of endocytosis via the oxygen-sensing pathway. *Nat Med* 2009; **15**: 319-324.

235. Bluyssen, H.A. *et al.* Fibronectin is a hypoxia-independent target of the tumor suppressor VHL. *FEBS Lett* 2004; **556**: 137-142.

236. Young, A.P. *et al.* VHL loss actuates a HIF-independent senescence programme mediated by Rb and p400. *Nat Cell Biol* 2008; **10**: 361-369.

237. Kamura, T. *et al.* VHL-box and SOCS-box domains determine binding specificity for Cul2-Rbx1 and Cul5-Rbx2 modules of ubiquitin ligases. *Genes Dev* 2004; **18**: 3055-3065.

238. Zhang, J.G. *et al.* The conserved SOCS box motif in suppressors of cytokine signaling binds to elongins B and C and may couple bound proteins to proteasomal degradation. *Proc Natl Acad Sci U S A* 1999; **96**: 2071-2076.

239. Hoffman, M.A. *et al.* von Hippel-Lindau protein mutants linked to type 2C VHL disease preserve the ability to downregulate HIF. *Hum Mol Genet* 2001; **10**: 1019-1027.

240. Stickle, N.H. *et al.* pVHL modification by NEDD8 is required for fibronectin matrix assembly and suppression of tumor development. *Mol Cell Biol* 2004; **24**: 3251-3261.

241. Mendez, J. & Stillman, B. Chromatin association of human origin recognition complex, cdc6, and minichromosome maintenance proteins during the cell cycle: assembly of prereplication complexes in late mitosis. *Mol Cell Biol* 2000; **20**: 8602-8612.

242. Weinstock, D.M., Nakanishi, K., Helgadottir, H.R. & Jasin, M. Assaying double-strand break repair pathway choice in mammalian cells using a targeted endonuclease or the RAG recombinase. *Methods Enzymol* 2006; **409**: 524-540.

243. Ben-Zvi, T., Yayon, A., Gertler, A. & Monsonego-Ornan, E. Suppressors of cytokine signaling (SOCS) 1 and SOCS3 interact with and modulate fibroblast growth factor receptor signaling. *J Cell Sci* 2006; **119**: 380-387.

244. Cai, Q. & Robertson, E.S. Ubiquitin/SUMO modification regulates VHL protein stability and nucleocytoplasmic localization. *PLoS One* 2010; **5**.

245. Ungureanu, D., Saharinen, P., Junttila, I., Hilton, D.J. & Silvennoinen, O. Regulation of Jak2 through the ubiquitin-proteasome pathway involves phosphorylation of Jak2 on Y1007 and interaction with SOCS-1. *Mol Cell Biol* 2002; **22**: 3316-3326.

246. Peng, J. *et al.* A proteomics approach to understanding protein ubiquitination. *Nat Biotechnol* 2003; **21**: 921-926.

247. Zhao, G.Y. *et al.* A critical role for the ubiquitin-conjugating enzyme Ubc13 in initiating homologous recombination. *Mol Cell* 2007; **25**: 663-675.

248. Kim, J.S. *et al.* Independent and sequential recruitment of NHEJ and HR factors to DNA damage sites in mammalian cells. *J Cell Biol* 2005; **170**: 341-347.

249. Plans, V. *et al.* The RING finger protein RNF8 recruits UBC13 for lysine 63-based self polyubiquitylation. *J Cell Biochem* 2006; **97**: 572-582.

250. Christensen, D.E., Brzovic, P.S. & Klevit, R.E. E2-BRCA1 RING interactions dictate synthesis of mono- or specific polyubiquitin chain linkages. *Nat Struct Mol Biol* 2007; **14**: 941-948.

251. Hofmann, R.M. & Pickart, C.M. Noncanonical MMS2-encoded ubiquitin-conjugating enzyme functions in assembly of novel polyubiquitin chains for DNA repair. *Cell* 1999; **96**: 645-653.

252. Roberts, A.M. *et al.* Suppression of hypoxia-inducible factor 2alpha restores p53 activity via Hdm2 and reverses chemoresistance of renal carcinoma cells. *Cancer Res* 2009; **69**: 9056-9064.

253. Lai, Y., Song, M., Hakala, K., Weintraub, S.T. & Shiio, Y. Proteomic dissection of the von Hippel-Lindau (VHL) interactome. *J Proteome Res* **10**: 5175-5182.

254. Metcalf, J.L. *et al.* K63-Ubiquitylation of VHL by SOCS1 mediates DNA double-strand break repair. *Oncogene* 2013.

255. Metcalf, J.L. *et al.* K63-Ubiquitylation of VHL by SOCS1 mediates DNA double-strand break repair. *Oncogene* 2013; **In press**.

256. Iliopoulos, O., Ohh, M. & Kaelin, W.G., Jr. pVHL19 is a biologically active product of the von Hippel-Lindau gene arising from internal translation initiation. *Proc Natl Acad Sci U S A* 1998; **95**: 11661-11666.

257. Gao, J. *et al.* Cloning and characterization of a mouse gene with homology to the human von Hippel-Lindau disease tumor suppressor gene: implications for the potential organization of the human von Hippel-Lindau disease gene. *Cancer Res* 1995; **55**: 743-747.

258. Rankin, E.B., Tomaszewski, J.E. & Haase, V.H. Renal cyst development in mice with conditional inactivation of the von Hippel-Lindau tumor suppressor. *Cancer Res* 2006; **66**: 2576-2583.

259. Beucher, A. *et al.* ATM and Artemis promote homologous recombination of radiation-induced DNA double-strand breaks in G2. *EMBO J* 2009; **28**: 3413-3427.

260. Lai, Y., Song, M., Hakala, K., Weintraub, S.T. & Shiio, Y. The interaction of the von Hippel-Lindau tumor suppressor and heterochromatin protein 1. *Arch Biochem Biophys* 2012; **518**: 103-110.

261. Bannister, A.J. *et al.* Selective recognition of methylated lysine 9 on histone H3 by the HP1 chromo domain. *Nature* 2001; **410**: 120-124.

262. Lachner, M., O'Carroll, D., Rea, S., Mechtler, K. & Jenuwein, T. Methylation of histone H3 lysine 9 creates a binding site for HP1 proteins. *Nature* 2001; **410**: 116-120.

263. Smothers, J.F. & Henikoff, S. The HP1 chromo shadow domain binds a consensus peptide pentamer. *Curr Biol* 2000; **10**: 27-30.

264. Thiru, A. *et al.* Structural basis of HP1/PXVXL motif peptide interactions and HP1 localisation to heterochromatin. *EMBO J* 2004; **23**: 489-499.

265. Smothers, J.F. & Henikoff, S. The hinge and chromo shadow domain impart distinct targeting of HP1-like proteins. *Mol Cell Biol* 2001; **21**: 2555-2569.

266. Badugu, R., Yoo, Y., Singh, P.B. & Kellum, R. Mutations in the heterochromatin protein 1 (HP1) hinge domain affect HP1 protein interactions and chromosomal distribution. *Chromosoma* 2005; **113**: 370-384.

267. Gilbert, N. *et al.* Formation of facultative heterochromatin in the absence of HP1. *EMBO J* 2003; **22**: 5540-5550.

268. Minc, E., Allory, Y., Worman, H.J., Courvalin, J.C. & Buendia, B. Localization and phosphorylation of HP1 proteins during the cell cycle in mammalian cells. *Chromosoma* 1999; **108**: 220-234.

269. Nielsen, A.L. *et al.* Heterochromatin formation in mammalian cells: interaction between histones and HP1 proteins. *Mol Cell* 2001; **7**: 729-739.

270. Larkin, M.A. *et al.* Clustal W and Clustal X version 2.0. *Bioinformatics* 2007; **23**: 2947-2948.

271. Ayoub, N., Jeyasekharan, A.D., Bernal, J.A. & Venkitaraman, A.R. HP1-beta mobilization promotes chromatin changes that initiate the DNA damage response. *Nature* 2008; **453**: 682-686.

272. Baldeyron, C., Soria, G., Roche, D., Cook, A.J. & Almouzni, G. HP1alpha recruitment to DNA damage by p150CAF-1 promotes homologous recombination repair. *J Cell Biol* 2011; **193**: 81-95.

273. Mischo, H.E., Hemmerich, P., Grosse, F. & Zhang, S. Actinomycin D induces histone gamma-H2AX foci and complex formation of gamma-H2AX with Ku70 and nuclear DNA helicase II. *J Biol Chem* 2005; **280**: 9586-9594.

274. Xiao, H., Li, T.K., Yang, J.M. & Liu, L.F. Acidic pH induces topoisomerase II-mediated DNA damage. *Proc Natl Acad Sci U S A* 2003; **100**: 5205-5210.

275. Jung, C.R. *et al.* E2-EPF UCP targets pVHL for degradation and associates with tumor growth and metastasis. *Nat Med* 2006; **12**: 809-816.

276. Hiragami-Hamada, K. *et al.* N-terminal phosphorylation of HP1{alpha} promotes its chromatin binding. *Mol Cell Biol* 2011; **31**: 1186-1200.

277. Davar, D., Beumer, J.H., Hamieh, L. & Tawbi, H. Role of PARP inhibitors in cancer biology and therapy. *Curr Med Chem* **19**: 3907-3921.

278. Dobzhansky, T. Genetics of Natural Populations. Xiii. Recombination and Variability in Populations of Drosophila Pseudoobscura. *Genetics* 1946; **31**: 269-290.

279. Bryant, H.E. *et al.* Specific killing of BRCA2-deficient tumours with inhibitors of poly(ADP-ribose) polymerase. *Nature* 2005; **434**: 913-917.

280. Farmer, H. *et al.* Targeting the DNA repair defect in BRCA mutant cells as a therapeutic strategy. *Nature* 2005; **434**: 917-921.

281. Papeo, G., Casale, E., Montagnoli, A. & Cirla, A. PARP inhibitors in cancer therapy: an update. *Expert Opin Ther Pat* **23**: 503-514.

282. Audeh, M.W. *et al.* Oral poly(ADP-ribose) polymerase inhibitor olaparib in patients with BRCA1 or BRCA2 mutations and recurrent ovarian cancer: a proof-of-concept trial. *Lancet* **376**: 245-251.

283. Tutt, A. *et al.* Oral poly(ADP-ribose) polymerase inhibitor olaparib in patients with BRCA1 or BRCA2 mutations and advanced breast cancer: a proof-of-concept trial. *Lancet* **376**: 235-244.

284. Basu, B., Sandhu, S.K. & de Bono, J.S. PARP inhibitors: mechanism of action and their potential role in the prevention and treatment of cancer. *Drugs* **72**: 1579-1590.

285. Fritzsche, F.R. *et al.* Expression of histone deacetylases 1, 2 and 3 in histological subtypes of testicular germ cell tumours. *Histol Histopathol* **26**: 1555-1561.

286. Fritzsche, F.R. *et al.* Class I histone deacetylases 1, 2 and 3 are highly expressed in renal cell cancer. *BMC Cancer* 2008; **8**: 381.

287. Ozawa, A. *et al.* Inhibition of bladder tumour growth by histone deacetylase inhibitor. *BJU Int* **105**: 1181-1186.

288. Patra, S.K., Patra, A. & Dahiya, R. Histone deacetylase and DNA methyltransferase in human prostate cancer. *Biochem Biophys Res Commun* 2001; **287**: 705-713.

289. Di Micco, R. *et al.* Interplay between oncogene-induced DNA damage response and heterochromatin in senescence and cancer. *Nat Cell Biol* **13**: 292-302.

290. Sharma, N.L., Groselj, B., Hamdy, F.C. & Kiltie, A.E. The emerging role of histone deacetylase (HDAC) inhibitors in urological cancers. *BJU Int* **111**: 537-542.

291. Jones, J. *et al.* Valproic acid blocks adhesion of renal cell carcinoma cells to endothelium and extracellular matrix. *J Cell Mol Med* 2009; **13**: 2342-2352.

292. Jones, J. *et al.* The histone deacetylase inhibitor valproic acid alters growth properties of renal cell carcinoma in vitro and in vivo. *J Cell Mol Med* 2009; **13**: 2376-2385.

293. Mahalingam, D. *et al.* Vorinostat enhances the activity of temsirolimus in renal cell carcinoma through suppression of survivin levels. *Clin Cancer Res* **16**: 141-153.

294. Juengel, E. *et al.* Effects of combined valproic acid and the epidermal growth factor/vascular endothelial growth factor receptor tyrosine kinase inhibitor AEE788 on renal cell carcinoma cell lines in vitro. *BJU Int* **105**: 549-557.

295. Sato, A., Asano, T., Horiguchi, A., Ito, K. & Sumitomo, M. Antitumor effect of suberoylanilide hydroxamic acid and topotecan in renal cancer cells. *Oncol Res* **19**: 217-223.